TÉCNICO LISBOA

Sizing optimization study of a Stand-alone Photovoltaic System in Huambo, Angola

José Gabriel de Castro Bruges Porto

Thesis to obtain the Master of Science Degree in

Electrical and Computer Engineering

Supervisor: Prof. Paulo José da Costa Branco

Examination Committee

Chairperson: Prof. Célia Maria Santos Cardoso de Jesus
Supervisor: Prof. Paulo José da Costa Branco
Member of the Committee: Prof. João Paulo Neto Torres

September 2021

Declaration

I declare that this document is an original work of my own authorship and that it fulfills all the requirements of the Code of Conduct and Good Practices of the Universidade de Lisboa.

Dedicated to my Dear Mother and in memory of my Dear Father.

Acknowledgments

I would like to thank Professor Paulo Branco for his expert advice, encouragement throughout this project and for always finding the time to help me in the development of this work. I would also like to thank, mainly, my family for the patience, strength and financial support they gave me during these years of study and my girlfriend for helping me during this difficult time. And finally, I would like to thank all my friends and colleagues who always supported me and helped me in this stage, which made me stronger and able to face the future knowing that I could always count on them.

Resumo

A electrificação no continente africano continua a ser um grande problema hoje em dia. Em Angola, por exemplo, cerca de 60% das pessoas não têm qualquer ligação à rede eléctrica, e a maioria destas pessoas vive em áreas isoladas/rurais, onde nem existem planos para construir uma rede eléctrica. A fim de alterar esta situação, os sistemas fotovoltaicos, apoiados por baterias ou outros sistemas de geração, já são utilizados para levar a electricidade a muitos destes locais mais remotos. O problema, especialmente com estes sistemas fotovoltaicos autónomos, é que eles acabam sempre por não fornecer toda a energia necessária para as actividades básicas dos consumidores, o que no final conduz sempre a uma perda de abastecimento de carga, e subsequentemente, a um custo extra das outras formas de produção de energia (geradores, biomassa, lâmpadas de querosene). Estes custos adicionais no final podem fazer com que o próprio sistema fotovoltaico demore mais tempo a pagar, ou podem levar a grandes flutuações no preço que os consumidores pagam por kWh no final de cada mês.

Assim, foi desenvolvida e utilizada uma metodologia para dimensionar sistemas fotovoltaicos fora da rede para locais remotos, onde o preço das perdas de energia para os consumidores é acrescentado ao investimento total, juntamente com um algoritmo de optimização para obter o que seria a melhor dimensão para um sistema fotovoltaico a ser construído na área do Huambo. Isto foi conseguido através do cálculo do consumo diário baseado em levantamentos feitos na área, na irradiação, e também, na temperatura da área.

O sistema fotovoltaico fora da rede será composto por painéis fotovoltaicos, baterias $LiFePO_4$, um inversor, um sistema de gestão de baterias e um gerador diesel em combinação com lâmpadas de querosene, como exemplos de fontes de energia mais tradicionais utilizadas nestes países mais subdesenvolvidos. Além disso, o valor final das perdas de energia (VOLL) já será incluído no investimento final do sistema fotovoltaico, de modo que ao longo da vida do sistema, os consumidores terão sempre um fornecimento de energia quase ininterrupto, mesmo que o sistema fotovoltaico não possa fornecer toda a energia necessária para alimentar as cargas. Assim, os nossos estudos provaram que seria possível dimensionar um sistema fotovoltaico sustentável para a área em questão, com um retorno positivo no final de 20 anos, mas com a desvantagem de o preço por kWh ser demasiado elevado para os salários angolanos, como será analisado no final desta tese.

Palavras-chave: Sistemas PV off-grid, baterias de lítio, simulação de sistemas, VOLL, MATLAB

Abstract

Electrification on the African continent remains a major problem today. In Angola, for example, about 60% of the people have no connection to the electricity grid, and most of these people live in isolated/rural areas, where there are no plans to build an electricity grid. In order to change this situation, photovoltaic systems, supported by batteries or other generation systems, are already used to bring electricity to many of these more remote locations. The problem, especially with these stand-alone photovoltaic systems, is that they always end up not providing all the energy needed for the basic activities of the consumers, which in the end always leads to a loss of load supply, and subsequently, to an extra cost from the other forms of energy production (generators, biomass, kerosene lamps). These extra costs in the end can make the photovoltaic system itself take longer to pay back, or can lead to large fluctuations in the price consumers pay per kWh at the end of each month.

Therefore, a methodology to size off-grid photovoltaic systems for remote locations, where the price of energy losses for the consumers is added to the total investment, has been developed and used together with an optimization algorithm to obtain what would be the best dimension for a photovoltaic system to be built in the Huambo area. This was achieved thru the computation of the daily consumption based on surveys done in the area, the irradiance, and also, temperature of the area.

The off-grid photovoltaic system will consist of photovoltaic panels, $LiFePO_4$ batteries, an inverter, a battery management system and a diesel generator in combination with kerosene lamps, as examples of more traditional energy sources used in these more underdeveloped countries. In addition, the final value of the energy losses (VOLL) will already be included in the final investment of the photovoltaic system, so that over the life of the system, consumers will always have almost uninterrupted power supply, even if the photovoltaic system cannot supply all the energy needed to feed the loads. Therefore, our studies proved that it would be possible to scale a sustainable photovoltaic system for the area in question, with a positive return at the end of 20 years, but with the downside that the price per kWh is too high for Angolan wages, as will be analyzed at the end of this thesis.

Keywords: Off-grid PV systems, lithium batteries, system simulation, VOLL, MATLAB

Contents

List of Tables

List of Figures

List of Symbols

$(\frac{P}{E})_R$ Power to energy conversion ratio

$AppName$ Name of the electric app

B_{size} Battery size capacity (kWh)

$C_{B,mobile}$ Battery capacity (Ah)

C_{PV} Capacity of the solar array (kW)

C_{bat} Battery pack capacity (kWh)

C_{other} Other total costs

C_{sys} Cost of System (€)

$ClassType$ Classes of consumers

$E(y)$ Supplied energy to the consumers in year y (kWh)

$E_D(t)$ Demanded energy at instant t (kWh)

$E_{Bat}(t)$ Battery energy level at instant t (kWh)

$E_{PV}(t)$ Produced PV energy at instant t (kWh)

E_{class_day} Consumed energy per user per day

E_{class_year} Consumed energy per class per year

E_{min} Minimum battery energy level (kWh)

E_{user_day} Consumed energy per user per day

G_b Diffused component from the sun

G_b Direct component from the sun

G_g Monthly mean daily global radiation

G_r Reflected component from the sun

$G_{b\_horizontal}$ Radiation component perpendicular to the ground plane

$G_{b\_incident}$ Total direct component from the sun

G_{b_module} Total irradiation on a module

H Daily global solar irradiation

I Hourly global solar irradiation

$Inv(y)$ Cost of investment in year y (€)

Inv_{size} Inverter size capacity (kW)

LT Lifetime of the project

$LT_{inverter}$ Lifetime of inverter

N_{app} Number of apps

$N_{cycles\_80\%}$ Number of charge cycles at a DOD of 80%

$N_{cycles\_DOD\%}$ Number of charge cycles at a specific DOD stated by the manufacturer

N_{houses} Number of houses per residential class

N_{users} Number of users per class

$NumWin$ Number of operating windows

$O\&M(y)$ Cost of operation and maintenance in year y (€)

$P_{Eq,App}$ Appliances equivalent power

P_{app} Nominal power of the applications in watts

P_{el_light} Reference rate power of electric lights or the average power rate

P_{size} Solar panels power capacity (kW)

R_b Ratio of the beam radiation

SOC_{ini} Initial SOC of the batteries at the start of the simulation

SOC_{max} Maximum battery state of charge level

SOC_{min} Minimum battery state of charge level

$T(t)$ Temperature at instant t

T_{cell} Temperature of solar cell (°C)

T_{max} Maximum daily temperature

T_{min} Minimum daily temperature

T_{ref} Reference temperature (°C)

Tot_W Total time of operation of appliances

$VOLL_{class}$ VOLL for each class (h/kWh$_{LL}$)

$VOLL_{diesel}$ VOLL for diesel generator (h/kWh$_{LL}$)

$VOLL_{family\_1}$ VOLL for Family 1 (h/kWh$_{LL}$)

$VOLL_{family\_2}$ VOLL for Family 2 (h/kWh$_{LL}$)

$VOLL_{ker\_lamp}$ VOLL for kerosene lamps (h/kWh$_{LL}$)

$VOLL_{mobile}$ VOLL for mobile charges (h/kWh$_{LL}$)

$VOLL_{total}$ Final total VOLL for each class (h/kWh$_{LL}$)

$V_{B,mobile}$ Charging voltage (V)

V_{noise} Cost of noise and environmental damage (€)

$W_{f,n}$ Operating interval/window of the appliances in hours

$\Delta E(t)$ Difference between energy produced and consumed at instant t (kWh)

α Solar angle or elevation angle

β Tilted angle

β_{opt} Optimal angle

δ Declination angle

η_{BOS} Balance of System efficiency

η_{cables} Efficiency of the cables

η_{ch} Efficiency of charge of the batteries

η_{disch} Efficiency of discharge of the batteries

η_{gen} Efficiency of the generator

η_{inv} Efficiency of inverter

γ Azimuth angle

λ Unit cost of the solar array (€/kW)

ω Hour angle

ω_s Sunrise hour angle

ω_{ss} Sunset hour angle

ϕ Latitude

ψ Unit cost of the battery pack (€/kWh)

ρ_T Temperature coefficients in relation to the power (%/°C)

θ Incident angle

θ_z Zenith angle

υ Diesel specific volume (kg/lit)

ζ Inverter unit cost (€/kW)

c_{diesel} Local cost of diesel (€/lit)

c_{ker_lamp} Cost related to the consumed kerosene during one hour of lamp functioning(€/h)

$c_{recharge\_mobile}$ Price of charging service (€)

h_{funct} Operating schedule of the appliances in hours

$h_{light,LL}$ Associated hours of light related with 1 kWh_{LL}

h_{start} Starting hour of the appliances

h_{stop} Finishing hour of the appliances

r Discount rate

$LiFePO_4$ Lithium Iron Phosphate

Acronyms

AC Alternate Current. 14, 15, 39, 47, 60

AGECC Advisory Group on Energy and Climate Change. 1

AME Absolute Mean Error. 38

ANN Artificial Neural Network. 23

AREP Angola Renewable Energy Program. 11

BiPV Building integrated Photovoltaic Systems. 14

BOS Balance of System. 48

CIGS Copper Indium Gallium Selenide solar cell. 13

CRT Cathode Ray Tube. 41

DC Direct Current. 14, 15, 47, 54, 60

DGPV Distribution Generation Photovoltaic Systems. 14

DOD Deep of Discharge. 19, 57, 58

ENDE Empresa Nacional de Distribuição de Electricidade. 12

ENI Ente Nazionale Idrocarburi. 11

EoT Equation of Time. 29

FiT Feed-in Tariff. 48

GAMEK Gabinete de Aproveitamento do Médio Kwanza. 12

GDP Gross domestic product. 1

GHI Global Horizontal Irradiance. 25

GTI Global Tilted Irradiance. 25

IGBT Insulated-gate bipolar transistor. 60

ISRE Instituto Regulador do Sector Energético. 12

LCoE Levelized Cost of Energy. 3, 19, 49, 61, 66, 69, 77

LCoSLE Levelized Cost of Supplied and Lost Energy. 3, 4, 66, 69, 70, 79, 82–85, 88, 90

LHV Diesel low heating value (kWh/kg). 61

LLP Loss of Load Probability. 18–22

LPS Loss of Power Supply. 3, 4, 69

LPSP Loss Power Supply Probability. 3, 18, 64–67, 69, 70, 75, 77, 80, 82, 85, 86, 88, 90

LST Local Standard Time. 29

LSTM Local Standard Time Meridian. 29

LT Local Time. 29

MOSFET Metal–oxide–semiconductor field-effect transistor. 60

MPPT Maximum Power Point Tracker. 13, 15, 55, 60

NASA National Aeronautics and Space Administration. 23, 34, 35, 38

NPC Net Present Cost. 3, 19, 61, 65, 66, 69, 77, 79, 80, 83, 88, 90

OPEC Organization of the Petroleum Exporting Countries. 9

PCU Power Conditioning Unit. 13

PFC Power Factor Correction. 39

PROPEL Empresa Pública de Produção de Electricidade. 12

PV Photovoltaic. 2, 3, 8, 12–15, 17–27, 36, 48, 49, 51, 53–56, 60, 65, 67, 69, 70, 75–77, 80, 85, 87, 88

RES Residual Sum of Squares. 38

RNT Rede Nacional de Transporte de Electricidade. 12

RSME Root Mean Square Error. 38

SAPVS Stand Alone Photovoltaic System. 13, 14, 38

SEFA Sustainable Energy Fund of Africa. 11

SEITSF Sistemas Eléctricos Integrados de Tecnologia Solar Fotovoltáica. 3

SOC State of Charge. 18, 19, 21, 53, 57, 59, 69

STC Standard Test Conditions. 46

TC Time Correction Factor. 29

UN United Nations. 1, 16

VOLL Volume of Lost Load. 3, 4, 53, 60–66, 75, 80, 86, 90

Chapter 1

Introduction

1.1 Framework

In 2009, around 585 million people in sub-Saharan Africa (about 70% of the population) had no access to electricity solutions, with these numbers expected to rise significantly to about 652 million people by 2030. Besides, 85% of those without access to electricity live in rural areas [1]. Beside this lack of services, the sub-Saharan energy sector is characterized by several other significant challenges, some of which are: low energy access rates, insufficient generation capacity to meet the rising demand, poor reliability of supply and, finally, but most importantly, electricity costs as high as 0,84 €/kWh [2]. For comparison, the average generation capacity of sub-Saharan Africa was about 100 MW per million inhabitants in 2009, ranging from less than 15 MW per million inhabitants in Guinea-Bissau, up to 1080 MW in the Seychelles and about 1680 MW and 3340 MW per million inhabitants in the European Union and U.S, respectively.

The urgent need for a more fast paced electrification rates has been widely identified by regional/economic communities and its largely underpinned by national governments and their policies, although its importance regional and national wise is clearly understood at the policy level. On the reference scenario in the World Energy Outlook, Africa's final electricity consumption is expected to double between 2007 and 2030 from 505 to 1012 TWh. In the meantime, the United Nations (UN) Secretary-General's Advisory Group on Energy and Climate Change (AGECC) has advised that the UN System and Member States commit to ensuring universal access to reliable, affordable and sustainable energy services by 2030 [2].

Even though that extensive vital electrification was reached in the developing world by expanding national grids to rural areas, millions of people in those types of places still have no access to modern energy services or these solutions are not viable. For example, power outages are one of the most common sources of lack of electricity in places with electrification already installed. The estimated economic value of power outages in Africa amounts to as much as 2% of GDP, and 6–16% in lost turnover for enterprises. One important step needed to reducing this electricity gap in rural places is the energy provision based on decentralised systems, like solar, wind, hydro and hybrid systems composed by junction of two totally different systems [3].

In the last couple of years, photovoltaic (PV) systems have greatly increased their presence in the world's energy production. It's a simple form of energy, modular, noiseless, with efficient methods of energy conversion and relatively easy to install on both big solar plants and on the roof of residential and commercial buildings. According to [4], the photovoltaic market grew by 75 GW in the 2016, making a total of 303 GW around the globe, largely due to the fall of the price/W$_p$ ratio between 2009 and 2015.

Renewable systems, like photovoltaic systems, can be deployed not only in areas with electrification but also in rural areas where there is no electricity available, like the most part of Angola, where this work will focus. For example, Angola has only 43% (see Figure 1.1) of its city population with electric energy and less than 10% for rural places, which makes them very dependent in diesel generation [5]. The solar energy potential is immense in this country with 16,3 GW of solar power identified. With the government's announcement to reduce government subsidies for fossil fuels, this will lead to a great increase of electricity prices over the coming years, therefore creating a new demand for alternative energy solutions and encouraging outside investment into the sector.

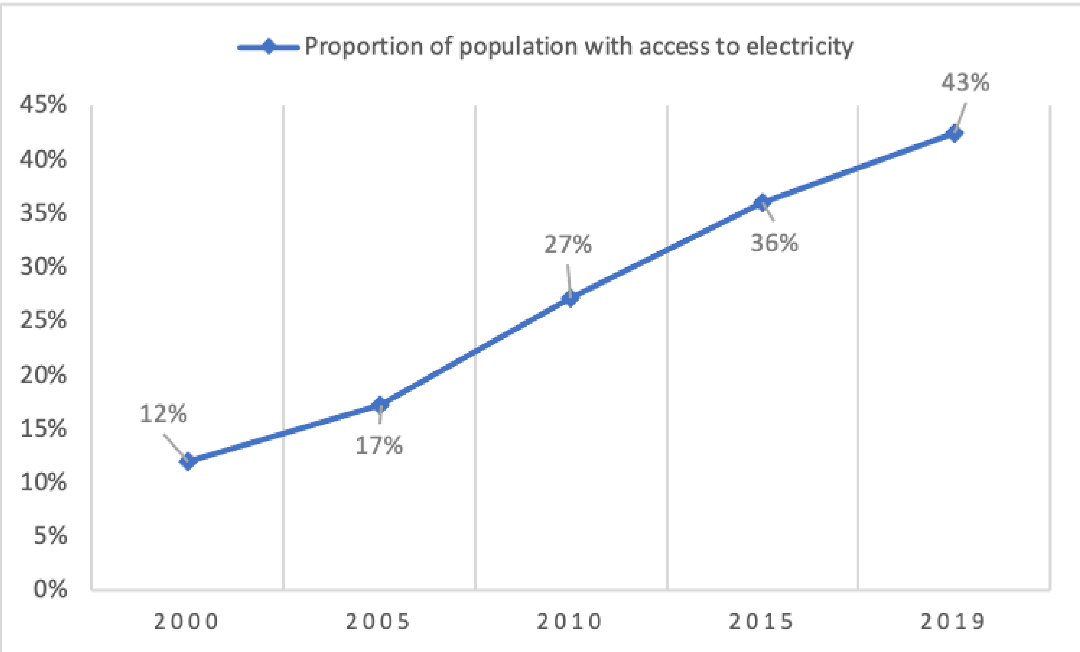

Figure 1.1: Proportion of population with access to electricity, Angola 2000-2019 - adapted from [6]

Much of this solution will be off-grid photovoltaic systems or, in some cases, hybrid ones with PV/wind being the best. In rural cases, electrification has pivotal role in promoting local development, bringing improvement of households welfare, provision of local services and development of new productive activities. The biggest problem with rural electrification utilizing isolated PV systems is in the frame of sustainable development and appropriate technologies [7], which are immensely reviewed in literature [8–12]. For this situation, there is a need of a multi-criteria system sizing method, which embraces the technical, economic and environmental parameters of the context and population.

1.2 Motivation

The idea for this thesis comes from a project done in the course of SEITSF (*Sistemas Elétricos Integrados de Tecnologia Solar Fotovoltaica*) where it was necessary to size a PV system for a small health care unit in Luena, Angola, where no electrification existed. That project was done only using theoretical methods, which lead in the end to an investment without return and a never ending loss in the project lifetime. This was mainly due to the fact that the sum of the investments and the cost of maintenance and operation over the life of the system were much higher than the revenue that could be obtained with a monthly fee paid by the consumers. Even after the initial investment was paid off, the price of maintenance and equipment replacement would make profit impossible. In addition, the project was made without having a notion of the subsidies that could come from the government as a result of the new agreements (*Angola Energy 2025*) and from the private sector.

In this thesis, a new system size optimization technique will be used where the goal is to make the system more reliable and as cost-effective as possible, utilizing a multi-criteria analysis, in addiction to system parameters assumptions and mean daily irradiation data that already have been used in the course's project. Multi-criteria analysis has been employed to support decisions taken in relation to rural energy supply in the developing world in order to replace existing capacity (e.g., wood burning for fuel), or to expand it, whilst also mitigating environmental impacts [3]. The Volume of Lost Load (VOLL), Levelized Cost of Supplied and Lost Energy (LCoSLE, a modified version of the traditional LCoE), Net Present Cost (NPC^*, a modified version of the traditional NPC using the LPS and VOLL data) and Loss Power Supply Probability (LPSP) will be the new parameters for the sizing.

With this new parameters for optimizing the scaling of the PV/battery system, it is possible to propose a micro-grid that is solely estimated and constructed based on the local context, which can be more appropriated than purely theoretical and speculative data. This is possible because of the VOLL methodology which is based on the load demanded that is not produced by the generating plant and its cost to the local people. This situation is very frequent in rural areas because of the shortage of grid electricity and the dependency of other forms of fuel like biomass and diesel generators.

1.3 Objectives

1. Load profile construction based on previous census and thesis informations;
2. VOLL input determination based on local context and energy consumption data;
3. Theoretical review of PV systems technical and economic characteristics and specifications;
4. Elaborate a MATLAB script to:
   (a) Calculate the hourly irradiation and temperature data based on models with mean daily solar irradiations data and minimum/maximum temperature, respectively, to be used has an input for the simulation;

(b) Import the previous constructed load profile, system assumptions and VOLL data;

(c) Simulate data for:

   i. Hourly PV panels production;

   ii. Hourly energy balance based on energy generated and demanded;

   iii. Hourly battery energy balance and State-of-Charge (instantaneous value of the batteries' energy in instant *(t)*);

   iv. Batteries' lifetime prediction;

   v. Number of replacements in project's lifetime for inverter and batteries;

   vi. Lost of Load and Lost of Load probability (day and year);

   vii. Cost of the system;

   viii. Possible Net Present Cost and New Net Present Cost

   ix. Possible Levelized Cost of Energy and Levelized Cost of Supplied and Lost Energy

(d) With this information will be possible to calculate the best PV panel power size and batteries' capacity optimized by:

   i. The required yearly mean Lost of Load value;

   ii. The maximum *Net-Present Cost* (NPC) for the project over its life-time;

   iii. And minimum LCoSLE.

(e) Discussion and comparison of the results with traditional methods (without VOLL and with LPS has an input);

(f) Socioeconomic evaluation of the project.

1.4 Thesis Structure

1. Chapter 1 - Introduction: Brief presentation of the problem and motivation of this work.

2. Chapter 2 - Background work: Presentation of the case studies and state-of-art of optimization methods for sizing of off-grid PV systems.

3. Chapter 3 - Simulation - Inputs, weather and load informations: This chapter will focus on the description of the physical models of PV systems, climate and consumer load information.

4. Chapter 4 - Simulation - Sizing optimization process and MATLAB structure: explanation of the methodology for optimizing the sizing of PV systems.

5. Chapter 5 - Results and socioeconomic evaluation: Full description of the results outputed by the simulation, discussion of the socioeconomic viability of the project and comparison to more traditional methods.

6. Chapter 6 - Conclusion: Final thoughts, comments and future work recommendations.

Chapter 2

Background

In this chapter and as its name implies, the various themes already developed and studied today will be addressed in order to introduce and better understand what will be scaled in the next chapter.

2.1 Angola's case study presentation

This study will focus on Angola, so a brief review on the country's information, energy scenario and solar availability will be made. Angola is a country in Central Africa at the west coast of Southern Africa, staying mostly between latitudes 4° and 18°S, and longitudes 12° and 24°E. It is the second largest Portuguese-speaking country in both total area and population (behind Brazil), and it is the seventh-largest country in Africa. The capital and largest city is Luanda. The country is rich in natural resources such as fish, abundant forests, gold, diamonds, large oil deposits, and it was once praised for its agriculture production, especially in the central highland provinces like Huambo.

After achieving independence in 1975 as a Marxist–Leninist one-party republic, Angola fell in a civil war which lasted about 30 years, where the economic of the country, as well as the energy sector, were practically destroyed. This is why till this day many communities in Angola doesn't have access to electricity, using only diesel generators and other primary ways of energy sourcing, as shown in Figure 2.1. The chronic energy shortage of rural populations, which occurs in many developing countries, has led to the degradation of forests due to the use of their resources as fuel. In addition, the generators are used due to the low cost of oil, but high emissions and noise are down factors.

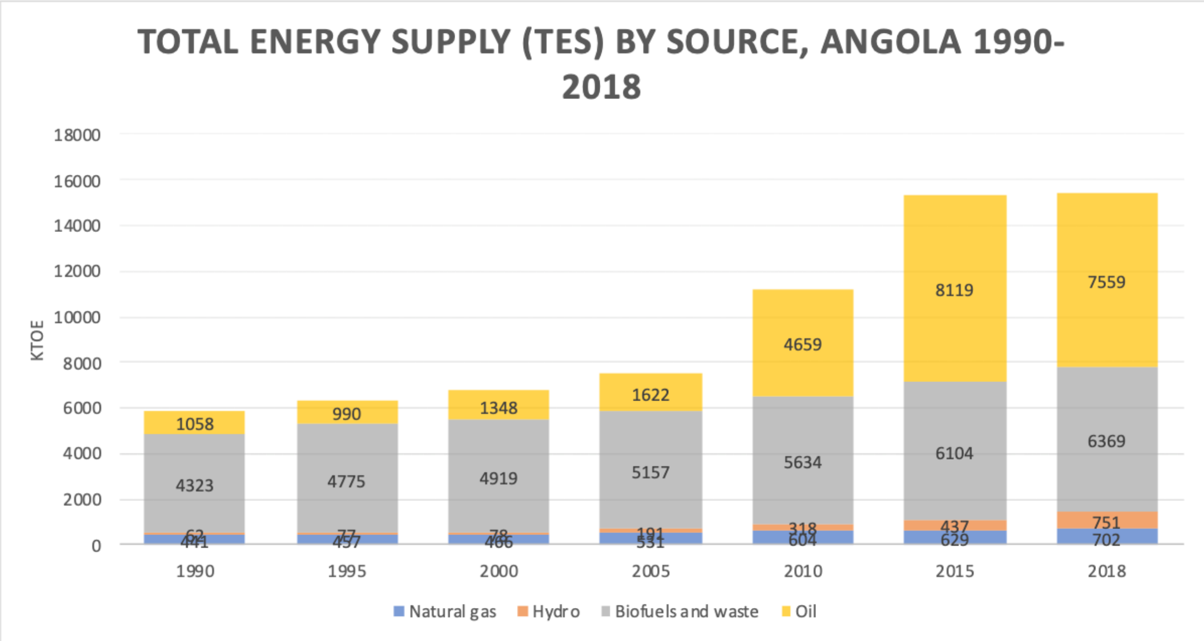

Figure 2.1: Total energy supply by source, in KTOE (Kilotonne of Oil Equivalent), Angola 1990-2018 - adapted [6]

Figure 2.2: Map of Angola

The Angola's energy sector is characterized by a low consumption per capita (250 kWh/per capita) [13] and the electricity is mostly consumed in Luanda, which accounts for 65% of the total demand of the country. Its electrical grid is in very poor conditions to the point where people stop using and prefer a more primary source of energy, as it happens on Huambo, a city in the center-south part of the country (see Figure 2.2) and the location where this work will be focused. The government of Angola's Ministry of Energy and Water reported that the isolated grid that provides energy services for the entire province of Huambo is installed with 15.9 MW, and of that capacity only 24.5% is able to provide delivered energy. In addition, these facts only reflect the situation in the center of Huambo because, if one goes to more peripheral and isolated areas of the province, it can be seen that the situation is even worse. In these areas there is not even a network and the only form of energy is kerosene, biomass and small diesel generators. On a study made by Cornelio, of the 50 households that where questioned, none of them had electricity or piped water services delivered into their residences. In order to counter this situation, take advantage of the great solar resources that the country has and the fall in the prices of photovoltaic panels, the Ministry is intensively working to bring viable photovoltaic technology to these places.

2.1.1 Solar resources and weather conditions

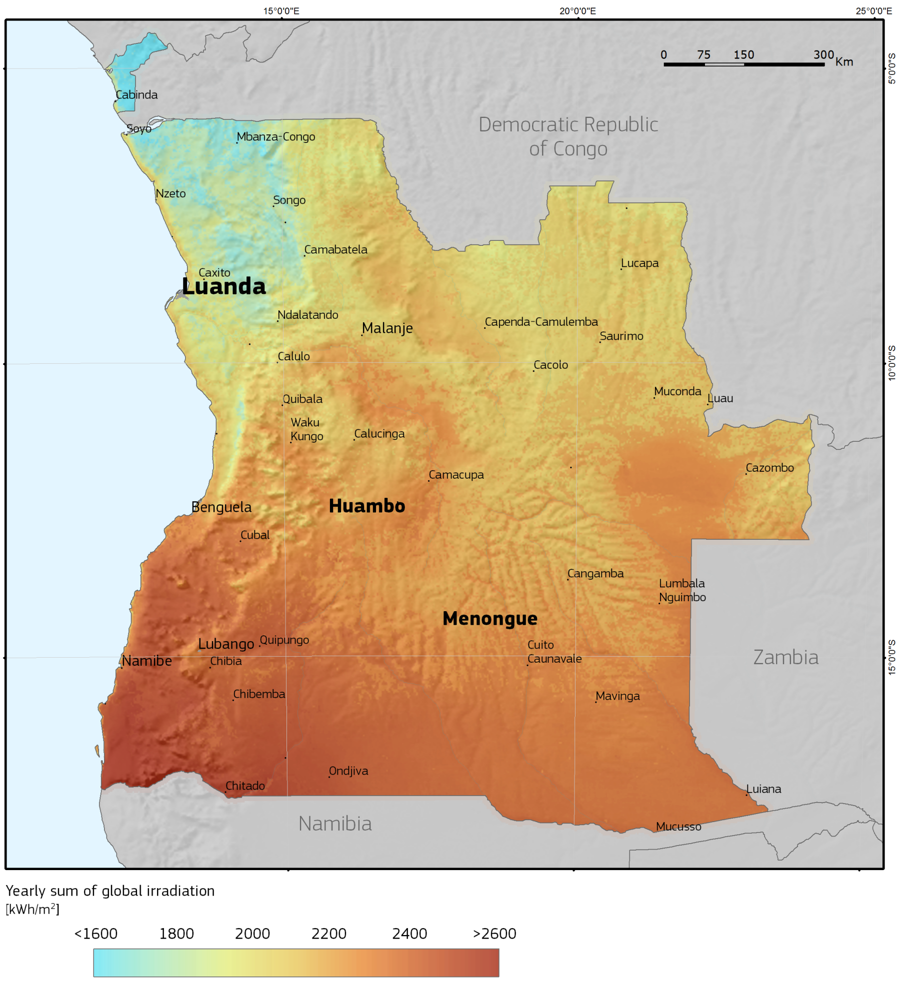

Figure 2.3: Angola's Irradiance Map [15]

Due to its location on the African continent and its proximity to the Atlantic Ocean, its climate is tempered by a cool sea current along the coast and by the altitude on the plateau in the interior, thus making for a sub-tropical climate almost everywhere in the country. Their weather can be divided in two seasons: dry season called Cacimbo (from May to August), hot rainy season, which runs from mid-September to April in the north-east, from mid-October to April in the center, from November to March in the south, while along the coast it only goes from February to April in Luanda, and it's almost non-existent on the southern coast (which is therefore desert). In addition to the absence of rainy days on the southern coast, another circumstance makes the climate even more mild and dry, the Benguela Current, at least in the central and southern part. The dry season corresponds to the austral winter months in which the total time of sunshine hours is higher, thus creating very favorable conditions of irradiation, mainly for PV systems.

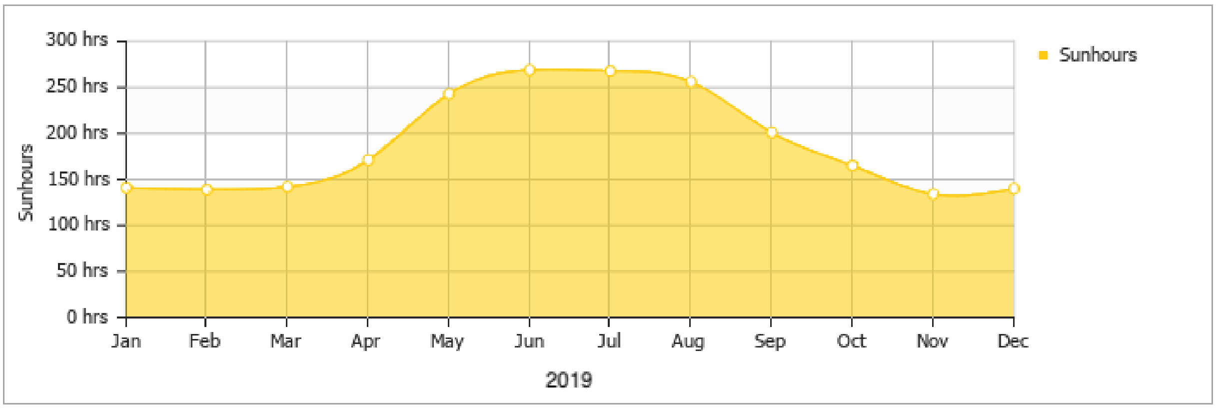

Figure 2.4: Huambo's sunshine hours per month [16]

On the plateau, where Huambo is located (see Figure 2.2), during the coolest season, the sun shines and it never rains, with sunshine hours peaking at 250 per month in 2019, between June and July, as shown in Figure 2.4. However, there are wide variations in temperature between night and day, with minimum temperature values around 7º degrees and maximum temperatures around 25º degrees (as shown in Figure 2.5), thus making the nights very cold, with possible frosts, while making the day really hot. As it can be observed in Figure 2.3, Huambo's irradiance levels stay between 2000 and 2300 kWh/m^2/year, which, with a few simple calculations, can be estimated to produce between 4,9 kWh/m^2/day to 6,2 kWh/m^2/day, with the panel tilted with the optimum angle (β_{opt}).

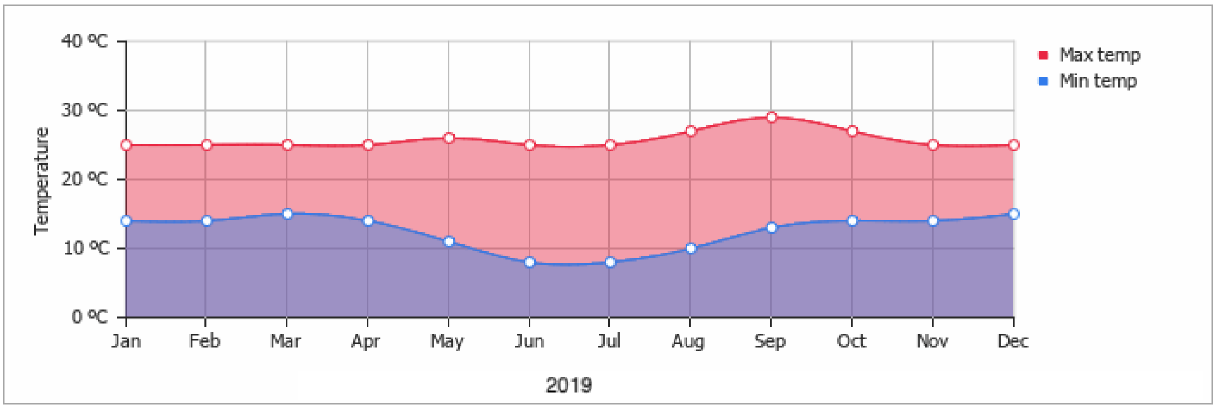

Figure 2.5: Huambo´s average temperature [16]

2.1.2 Electricity in Angola

Angola, an OPEC member, is the third-largest economy in sub-Saharan Africa and one of the biggest oil-producing and exporting countries in the continent. Despite this fact, in 2018, 75% of its generating capacity came from hydro power, with the rest 25% coming from diesel-generators, mainly to support rural countrysides [6]. This is thanks to the the four hydro power plants located across the country, feeding the north center, south and some small isolated areas. These generating systems are Matala Power Station (960 MW), Capanda Dam (520 MW), Cambambe Hydroelectric Power Station (960 MW) and Laúca Hydroelectric Power Station (2069,5 MW), with projects already in development for new ones in the Kwanza River, mainly, Caculo Cabaça Hydroelectric Power Station (2172 MW) and Baynes Hydroelectric Power Station (600 MW), with the latest being a cooperation between Angola and Namibia.

Unfortunately for the country and the people needing electricity in their homes and business, the electrical grid has very little quality and its poorly integrated. It lacks maintenance to the point that outages are a very common situation in everyday life of Angolan people. The high-voltage grid (see Figure 2.6) is composed of the northern grid that runs 400 kV and 220 kV lines and covers Luanda, Uige, Bengo, Zaire, Malange, North Kwanza, and South Kwanza. The central network includes 400 kV lines from Benguela to Bie and Huambo. The southern grid serves Huila and Namibe and uses 220 kV lines. Projects are already in progress to increase and enhance the transmission network to support new production capacity, the link of the grids through a north-central-south backbone and expansion of the grid from 3,354 km to 16,350 km by 2025. However, the three main power production plants Lauca, Capanda and Cambambe are interconnected, while also connected to one or two of the transmission lines, thus creating some inter-connectivity and redundancy of the three grids. In the distribution side, given the high commercial and technical losses, there is an extreme need to develop new distributions infrastructures and to develop a new tariff-based methods given the fact that a lot of people consuming electricity are not even yet metered.

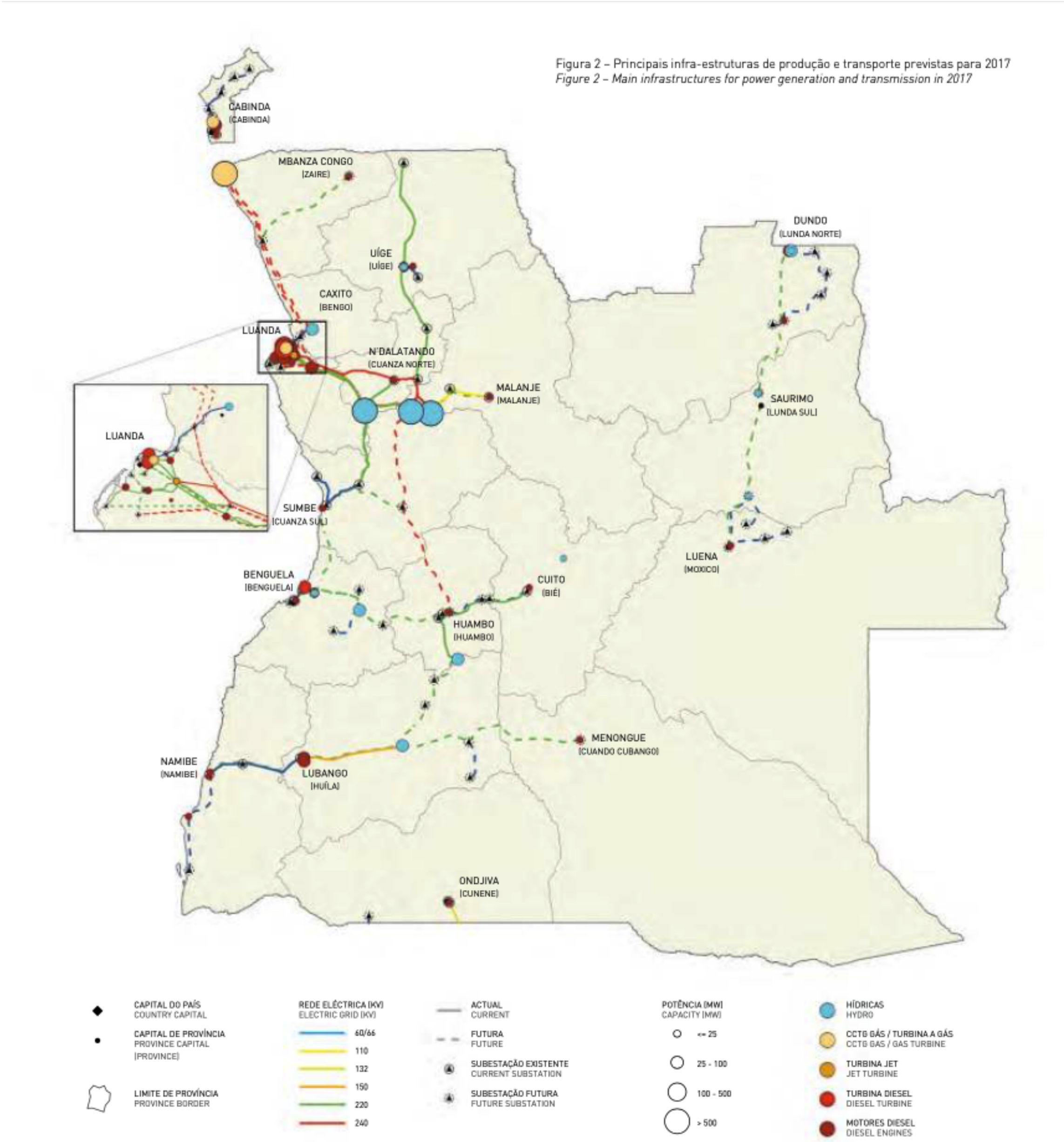

Figure 2.6: Electric network grid Angola 2017 - adapted from [17]

Other important point to make is that government fuel subsidies are ending, those being the number one source of income for poor people to have energy in their lives. Thanks to that electricity cost has risen in a pace that isolated/rural families and enterprises cannot pay, in addition to poor electrification systems or non existing, which drives the prices even higher. Moreover, João Baptista Borges, the Angolan Minister of Energy and Water, announced that the Angolan government was considering increasing the rate of access to electricity, which has set targets of 9.9 gigawatts (GW) of installed generation capacity (current installed capacity is estimated at 5.01 GW) and a 60% electrification rate by 2025, with great focus in rural areas [18], including an increase in low-carbon energy. In this moment, this rate does not exceed 40%, which in this case leaves the government relying on renewable energies sources to supply homes in remote areas. This plan is called Angola Energy 2025.

For that plan, the government has instituted an ambitious infrastructure plan. In 2014, mapping studies identified the potential for 18,3 GW solar power, 3 GW wind power, and 18 GW in hydro-power throughout the country, putting an objective for the generation mix of 64% hydro, 12% natural gas, and 24% diesel powered generation by the end of 2018. To help reach this objective, large-scale projects where implemented in 2017/18 including the Soyo combined cycle natural gas plant (750 MW), and the Laúca hydroelectric project [5]. On the other hand, there is a big downside on this quest for affordable, reliable and sustainable energy: the funding. For projects already in development and future ones, there is a an extreme need for external financing and help in development from private companies. This is directly derived from the current government budget restraints and the economic downturn. The bright side is that lots of independent producers are beginning to take interest in this southern African country, with the recent example of the Italian company *Ente Nazionale Idrocarburi* (ENI) and Sonangol, the Angolan national oil company, joining forces to create Solenova, in June 2019. This new project aims to develop new renewable energy projects developed by the two companies, with Solenova's first project that will be the construction of a 50 MW photovoltaic solar power plant to supply southern Angola. Further more, the AfDB's Sustainable Energy Fund for Africa (SEFA) lent $1 million to the Angolan government, in 2018 to be used to cover the cost of the Angola Renewable Energy Programme (AREP). In addition, the government should also use part of the loan to finance the revision of the regulatory and institutional framework for the renewable energy sector and the operation of the competitive bidding program for electricity supply by independent power producers.

Finally, in the solar field, the Angola Ministry plans to install 30.000 solar off-grid systems that will be able to produce up to 600 MW, with a fixed target date of 2022. Currently, Angola only has an installed solar capacity of 16 MW, which is generated from the Chicapa hydroelectric plant. Of these 30.000 systems, seven of them will be in large scale, with the first of the seven being build in Saurimo, the capital of this province in the north-east of Angola. Work was expected to begin in October 2020, it's predicted to last 17 months and will have a capacity of 26 MWp, with a transmission line and a 220 kV substation also included. The total investment for the seven most important plants is about $550 millions [18], with the government intent to rely on private funding to help. By 2025, the government is expected to make progress toward achieving cost-reflective tariffs, taking the pressure off the sector's reliance on subsidies, improving the financial position of the infrastructures and encouraging outside investment into the sector.

2.1.3 Energy sector overview

In 2014, the Council of Ministers passed the Amendments Proposal to the General Law of Electricity that aims at ensuring a major participation of the private sector, introducing the exploitation of renewable energies and foresees the creation of a National Fund for Rural Electrification [19]. Besides that, this new legislation aims at guarantying a major participation of the private sector in producing, distributing and trading renewable energies, and reflects the government concern regarding the attraction of private capital in this sector, now giving the opportunity for the production of energy to be done by both public and private companies.

One of the most import point of this new proposal is that with this new law the State assumes the rural electrification of the country by creating the Rural Electrification National Fund, which will help swift the development of electrification in isolated areas. Rural electrification is a policy measure, with strategic impact on social inclusion, which aims to promote human development, the well-being of Angolans and it is a key factor for the harmonious development of the national territory. The amendments also raises the opportunities on renewable energy sector motivating private initiative for electricity production and rural electrification projects.

In addition, the program called for the restructuring of the power sector and the creation of three individual companies, which would be fully responsible for each of the three major energy sectors: production, transport and distribution. All three public services would be operated by the Ministry of Energy and Water and these are: PROPEL (Empresa Pública de Produção de Electricidade) the company responsible for national production, RNT (Rede Nacional de Transporte de Electricidade), the responsable for national transmission and ENDE (Empresa Nacional de Distribuição de Electricidade), operating the distribution part of the sector. Furthermore, the company responsible for implementing and managing the hydro projects in the Kwanza river, the GAMEK (Gabinete de Aproveitamento do Médio Kwanza) had its scope increased so that it could oversight the development and construction of most major power projects in the country. Previously, GAMEK was only responsible for the biggest hydroelectric dam in the country - Capanda Central - in the north part of the Angolan territory.

The electric sector restructuring also sought to establish greater autonomy and strengthen the role of the regulator ISRE (Instituto Regulador do Sector Eléctrico) in providing oversight of sector activities and building technical and financial capacity. As stated before, electricity subsidies were cut by 85 percent, in June 2019, leading to retail rate highs of 77%, improving government financial viability and creating a more sustainable business model for the electricity sector, for the purpose of attracting more potential independent power producers. By 2025, the government is expected to make progress toward achieving cost-reflective tariffs, thus lessening the sector's reliance on subsidies, improving the financial position of the utilities, and encouraging outside investment into the sector.

2.2 Photovoltaic systems

2.2.1 Characteristics

Crude oil, coal and gas are currently the main resources for worldwide energetic supply, even so that fossil fuel reserves around the world are rapidly decreasing. This urgent matter must have a significant reflection and serious measures must be taken. With the urge for new, clean and renewable types of energy, one that has gained the most attention of the alternate energies is solar energy. There are two types of solar technology that are used, namely solar thermal and solar cell [20]. A solar cell or PV cell, how it's most commonly known, is a semiconductor device which directly convert the solar radiation into electrical energy, by photovoltaic effect. There are different types of solar PV cells available in market i.e. monocrystalline silicon, polycrystalline silicon, amorphous silicon, cadmium telluride, micromorph, CIGS, and hetero-junction modules [21].

In the beginning of the technology, the PV systems were deployed in satellites, but nowadays it is being used for diversified applications ranging from very low energy consuming appliances such as watches, calculators to megawatt scale grid connected solar PV plant [22]. A single PV cell is used in calculators while a number of PV cells connected in series make a PV module in order to be utilized in harnessing solar energy and produce electricity for small load applications. In addition, several PV modules connected in series and/or parallel make a PV array for large stand-alone and grid-connected generation plants. The solar electricity generated by solar PV systems is one of the most promising options mainly because solar radiation is in abundance, the costs for electricity generation are reducing rapidly, requires negligible maintenance and provides highly reliable energy [23]. Apart from PV modules; the PV systems consists of battery bank and power conditioning unit (PCU) which includes converter, inverter, maximum power point tracking (MPPT), dump load and data logger.

2.2.2 Types of Photovoltaic systems

Nowadays there are three types of PV systems connectivity: stand-alone systems with and without battery packs, grid-tied systems and, the more recent one, hybrid systems that utilize a renewable energy (PV, wind, biomass) with other more conventional form of energy (fossil fuels, coal). Each one has its own particularity, which will be discussed next.

Stand-alone systems

Stand-alone Photovoltaic System (SAPVSS) are widely deployed in isolated areas where there is no access to electricity grid. According to [24], SAPVSSs represent a cost-effective and eco-friendly alternative to conventional high cost diesel-fired generators, particularly in developing countries where most of the population lives in rural and isolated areas, due to the difficulty in accessing the remote areas and the cost of the transportation. Off-grid systems can be used in conjunction with batteries and without batteries. In case of a system without battery packs the consumers utilize immediately the electric energy produced by the modules and in case of no consumption all this energy will be wasted. In night hours all energy must be generated by an extra diesel generator or another technology. In the other hand, SAPVSS can be paired with storage units, such as batteries, which can be integrated in off-grid systems as they represent an alternative capacity source to the conventional generator which has high operational costs due to fuel consumption in addition to CO_2 emissions [25]. Considering solar energy, an interesting statistic described in [26] states that the global average solar radiation, per m^2 and per year, can produce the same amount of energy as a barrel of oil, 200 kg of coal, or 140 m_3 of natural gas [27].

One of the major requirements for a storage system for isolated solar-PV applications are low cost, high energy efficiency, long lifetime, low maintenance, self-discharging and simple operation, although they require high initial investments. Consequently, it is important to manage battery usage because operating conditions and charge-discharge protection have strong influences on battery lifetime and cost

[28]. There are many types of batteries, but the more used are lead-acid batteries because of their cost-effectiveness and longer lifetimes [29]. In order to minimize the size the systems and, consequently, its battery packs, some researchers are concentrating their efforts on the development of low power consumption appliances, which will enable the development of a cost effective system. One of this technologies is the fuel cell, which has a major influence in storage of electric power and thermal energy. However, fuel cells are still not applicable for small scale applications, especially in stand-alone PV systems because of their component costs and operational complexity [30]. Many theories and mathematical methods [31–33] were developed to make stand-alone PV systems more feasible, cost-effective and low maintenance for rural setting. This methods will have a more deep review in the latter sections.

Finally, in terms of major components and characteristics, a SAPVSS consists mainly of the following: a photovoltaic panel, which is responsible for transforming the solar irradiation into electrical energy, that will be delivered to the load or stored in battery packs for further use (the batteries must be preferably a deep charge battery and, as already stated, is non-mandatory); a load management device or regulator has the ability to cut-off the PV and also cut-off the consumers supply accordingly to the battery voltage levels and has the function to regulate the voltage generated either to charge a DC load or to perform a charge cycle to a deep cycle battery; an inverter, which converts Direct-Current (DC) to Alternate-Current (AC) to be used in AC loads (the use of DC loads only may avoid the use of an inverter), and finally, protections systems, which protect both user and the system itself.

Grid-tied systems

Grid-tied photovoltaic systems are, as name name implies, connected to the electric network allowing the sale of electricity to the power distribution companies and the feeding of the loads directly. The biggest advantage of grid interconnection of PV power generation is the more effective utilization of the generated power, even though the technical requirements from both the utility power system grid side and the PV system side need to be satisfied to ensure the safety of the PV installer and the reliability of the utility grid. Clarifying the technical requirements for grid interconnection and solving the problems such as islanding detection, harmonic distortion requirements and electromagnetic interference are therefore very important issues for widespread application of PV systems [34]. In addition, batteries and regulators are not necessary, which makes the system simpler and less maintenance is needed.

Grid connected PV systems can be divided into two parts: building integrated PV systems (BiPV) and distribution generation PV (DGPV) systems. BiPV systems usually supply a specific load and inject the excess energy to the grid. However, the GDPV systems inject the whole produced energy to the grid without feeding any local load. The grid connected systems can be consisted of PV array only as an energy source, or another energy source can be in cooperated with the PV array such as wind turbine, diesel system (as described latter) or a storage unit [35].

Purchase and sell back energy meters are substitute, in some cases, by bi-directional meters and the inverter makes the connection to the grid and the connection of the consumers done at the grid side node possible. Inverter technology is the key technology to have reliable and safety grid interconnection operation of PV system. Low and medium power grid-tied inverters use a Maximum Power Point Tracker

(MPPT) to optimize PV panels performance, constantly adjusting the input of a DC/DC converter, accordingly to the actual irradiance and temperature, which selects the voltage output. With the selection of voltage, the current is limited depending on the I-V curve of the panel.

Hybrid systems

Hybrid systems are typically based on one or more renewable energy sources (e.g. solar photovoltaic or wind) together with a conventional power generator to provide backup when necessary [36] or energy storage systems. This systems need more complex control and protection circuits and are generally used for medium to high power applications.

The two main types of hybrid systems used nowadays is PV-Wind and PV-Diesel. Hybrid PV/diesel systems have greater reliability for electricity production than using PV system alone because diesel engine production is independent of atmospheric conditions, besides that it will provide greater flexibility, higher efficiency and lower costs for the same energy quantity produced. One of the biggest advantages is that PV/diesel as compared to only disel systems provides a reduction in the operation costs and it's more eco-friendly to the environment [37]. This systems can be classified into two types of topology categories: series and parallel. In the series topology, the diesel generator is connected in series with the inverter and therefore it is not able to supply the load directly while the load demand is covered by the storage battery. On the other hand, in the parallel topology whereas the diesel generator is in parallel with the inverter, it can supply the load and the battery at the same time [37].

PV-wind hybrids has taken the advantage of the evolution of the photovoltaic and wind technologies, making possible and reliable to design and build an hybrid PV-wind system. This kind of systems have been a subject of matter, especially over the past few years, mainly regarding its feasibility, modelling, control, optimization techniques and reliability issues [38], despite the fact that these systems are quite recent and the studies continue towards a sustainable growth so that they can be considered reliable enough to be widely used. The two most common types of typologies are: Common AC bus and Common DC bus, where the first one the AC outputs voltage that comes from the PV panels, batteries and the wind turbine, connected to a DC/AC and AC/DC-DC/AC converters, respectively, feed the load directly; in the second case the hybrid the system is connected to a common DC bus, where the DC output voltage that comes from the PV panels, batteries and wind turbine, connected to a DC/DC and AC/DC converters, in parallel, go through a DC/AC inverter to feed the load. The two methods are used worldwide, the more common being the DC bus due to being more efficient and cheaper to install [13].

2.3 Energy sustainability in sizing solar systems

This section discusses the concept of energy sustainability and how it can be used for a good optimization of stand-alone PV systems for rural places. In this context, this thesis has the objective of bringing reliable, clean, affordable and eco-friendly energy to isolated places, helping in a more integrated and fair sizing of the system according to the local context and local weather conditions.

2.3.1 What is Sustainable Energy?

Energy supply to the rural or isolated people in developing countries, like many villages in Angola, is a complex activity that transcends the simple selection of a best technology. The majority of the isolated population lives a socio-economic imbalance between them and the urban areas, which leads to more energy deficient communities in developing countries. Therefore, there is a need to apply the concept of energy sustainability in these communities so that they can enjoy greater development and provide better quality services.

The concept of sustainability requires that the four pillars of the society - economic, political, social and environmental - are considered to be equally important, leading to the fact that sustainable energy resources must be economically viable, politically supported, socially equitable, and environmentally acceptable [39]. Thus, sustainable energy is defined as energy that is reliable, affordable, accessible and that meets economic, social and environmental needs within the overall developmental context of community, but with equitable distribution in meeting those needs [40]. Despite the great need to bring sustainable energy to rural areas, this issue remains one of the greatest challenges for the governments of developing countries, becoming a priority since the UN Conference on Environment and Development held in Rio 1992 and the signature of the United Nations Framework Convention on Climate Change [41].

Every region or nation have different energy requirements due to the fact that each place has its own *environmental, economic, social, and political constraints*, which influence generation capacities and demand profiles. In fact, are these constrains that determine the kind of policy development and implementation that are priority for a *sustainable generation*, which is understood as renewable energy provision; *sustainable energy distribution*, which is understood as equal and secure access to energy resources; and *sustainable energy consumption*, which is understood as energy conservation measures including energy use reduction and energy efficiency. One important point to make is the fact that an energy resource that is defined as renewable does not make it necessarily sustainable, as the palm oil example. Palm oil is a significant component of bio-diesel, is frequently grown on plantations created by clearing rain-forests, displacing indigenous people and wildlife. The CO_2 impact of felling, clearing, and burning alone is more than the CO_2 emissions saved by adding a small percentage of palm oil to road fuels [41].

There is a demand for a balanced composition between energy security, economic development and environmental protection, so that energy sustainability can be achieved [39], where in the future it will be possible to spread energy services to reach disadvantaged populations, to practice rational pricing strategy, and to call actions for structural reform to ensure facilitation and financing of technology transfer. The social component of sustainable energy can be expanded to cover community involvement, affordability, social acceptability, lifestyles, and aesthetics [41]. It encompasses energy systems, which are based on three core dimensions: energy security, social equity, and environmental impact mitigation. A large portion of this would be by incorporating renewable energies into the existing energy mix, even though it will not eliminate the the efficient use of conventional sources to ensure sustainable energy security. The other way, would be by a clear determination to slow down the exploitation of non-renewable resources, to use energy efficiently, and to raise awareness of all energy users that they have to adjust to the new way of doing business and thinking.

The goal of achieving a sustainable energy-based society goes a long way through the policies and decisions taken to this end. These policies are described as sets of decisions toward a long-term approach to a particular problem, which in governmental scopes are usually embodied in legislation and real, driven actions to achieve its objectives [39]. Therefore, sustainable energy policy can be viewed as sets of decisions that leads to investments from private sectors, that present clear business cases to its strategies and are developed in a participatory, transparent, and accountable way, and that are economically viable, environmentally responsible, and socially acceptable for the long term purpose. Due to past and present wars, financial and social constrains, policy formulation, in many developing countries, is often replaced by direct technology implementation without any proper, strategic planning or projection. This happened a lot in sub-Saharan Africa, where electrification and energy systems, one of the major services, are considered to be in very poor quality, with no maintenance and very little integration. This happens giving the fact that exists a big lack of political foresight to support policy making, creating unclear and insufficiently embedded organizational structures, which by then creates energy generation, distribution, and utilization systems that are not thoroughly planned.

2.3.2 PV system sizing and optimization

As stated before, rural electrification is often incorporated in the subject of sustainable development and appropriate technologies. In the development of planning of the energy provisions, assessment methods should emphasise all aspects of the rural problem, mainly in the following areas: technological (maximising supply), economic (reducing costs), social (minimising welfare impacts), and environmental (mitigating damage) [3], so that there is a possibility of reaching sustainability. For this, researchers [42, 43] have taken into account the energy needs and matching such needs without compromising the environment. In their approach, sustainable development is considered, with a concept of designing or selecting technologies, including specific conditions of the targeted areas (people's needs and social/cultural aspects), thus contributing to the concept of appropriate technologies [7].

For the context of rural electrification and renewable technologies, stand-alone solar systems are those expected to contribute the most in the development of new forms of energy in isolated places in the near future. As it is known, solar energy is the most abundant and available renewable resource in developing countries and, thanks to its decreasing components and integration costs, PV systems are becoming more and more popular. However, for a efficient and sustainable system, there is a mandatory requirement of doing an optimized sizing. Scaling an off-grid PV system is not so trivial as it seems, due to the fact that it means matching an unpredictable energy source with an uncertain load demand, while providing the most advantageous conditions in terms of system reliability and cost. The power reliability is directly proportional to the cost of the system, which means the higher power reliability, higher will be the cost, so a balance must be reached. An optimum sizing needs pondering cost with high power reliability [44].

Power reliability

Since this thesis is talking about solar energy, one can say that it is a very intermittent and unpredictable source of energy. Knowing this, the analysis of the reliability of the system is an extremely important step in its design, due to the fact that it is directly linked to the energy production of the system. There are many definitions in literature for what system power reliability truly means, but the one that best fits the context of this thesis is referred to in [45]. Power reliability is defined as the percentage of mean energy demand satisfied by a PV system without interruptions. For quantification purposes, the reliability of a system can be expressed, mainly, through the following concepts [7, 43, 46, 47]:

1. Loss of Load Probability (LLP), which is the share of the electricity demand (E_D) not fulfilled by the power system over a given period of time (generally one year) and is estimated by:

$$LLP = \frac{\sum_{t=1}^{T} LL(t)}{E_D} \tag{2.1}$$

where $LL(t)$ is the Loss of Load or the demand load not fulfilled at a certain time-step (t). When a system LLP is 0 it means the load will always be satisfied and when is 1 it means the load will never be satisfied [48]. The $LL(t)$ can be defined as:

$$LL(t) = \begin{cases} (SOC_{min} - SOC(t)) \cdot \eta_{DISCH} \cdot \eta_{inv} \cdot B_{size} & SOC(t) < SOC_{min} \\ (\Delta E(t) - (\frac{P}{E}_R) \cdot B_{size}) \cdot \eta_{inv} & \Delta E(t) \geq (\frac{P}{E}_R) \cdot B_{size} \end{cases} \tag{2.2}$$

where SOC_{min} is the minimum SOC that the battery can reach, as specified by the manufacturers, $SOC(t)$ is the SOC level at instant (t), η_{DISCH} is the discharge efficiency of the battery pack, η_{inv} is the inverter efficiency, B_{size} is the battery pack total capacity, in kWh, $\Delta E(t)$ is the energy difference between PV generated energy and demanded energy by the consumers, in time instant (t). Finally, $(\frac{P}{E}_R)$ is the power to energy conversion ratio.

2. Loss of Power Supply Probability (LPSP), which can be interpreted as the probability that an insufficient power supply will result when the system is unable to satisfy the load demand. It is calculated using the following formula:

$$LPSP = \frac{\sum_{t=1}^{T} LPS(t)}{\sum_{t=1}^{T} E_D(t)} \tag{2.3}$$

where $LPS(t)$ is the Loss Power Supply on time-step t and can be expressed as:

$$LPS(t) = E_D(t) - (E_{PV}(t) + E_{Bat}(t-1) - E_{Bat\_Min}) \cdot n_{inv} \tag{2.4}$$

with $E_{PV}(t)$ being the output produced by the PV panels at time (t), $E_{Bat}(t-1)$ being the energy balance in the battery pack in the previous time step and E_{Bat_Min} the minimum power level that the battery can reach, as provided by the manufacturer. A LPSP from 0 to 1 means the power cannot fully supply to the load when the solar power is not enough while the battery has been in the allowable maximum DOD or the allowable SOC. Apart from E_D, the rest of the parameters will be discussed in the next chapter.

System cost

The other important aspect in contrast with power reliability is the economic approach. The cost is one of the most inhibiting factors in the growth and development of the system and the most governing factor in its sizing. Inside of cost, the most frequently cited measures have been *investment* and *operational costs*, the cost of reducing greenhouse emissions, the availability of resource costs, battery replacement, fuel costs, and cost per unit of both installation and generation [3]. Many researchers have already used various procedures and techniques to reach the optimal point such as minimizing the Net Present Cost, lifetime and Levelized Cost of Energy of the projects [42, 49].

The Net Present Cost (NPC) used in the optimization of the cost is estimated by:

$$NPC = \sum_{y=1}^{LT} \frac{Inv(y) + O\&M(y)}{(1+r)^y} \tag{2.5}$$

where, for each year (y): $Inv(y)$ considers the investment and replacement costs of the system components, $O\&M(y)$ are the operation and maintenance costs and $(1+r)^y$ is the discount factor. Finally, it represents the total investment costs plus the discounted present values of all future costs during the lifetime of the system. The other way of finding the optimal systems, other than through the lifetime, is by minimizing the Levelized Cost of Energy:

$$LCoE = \frac{r \cdot (1+r)^{LT}}{(1+r)^{LT} - 1} \cdot \frac{NPC}{E(y)} \tag{2.6}$$

where $E(y)$ is the electricity served each year to the consumers by the system; LT is lifetime of the project; and is defined as the total cost of the entire system divided by the energy supplied by the system (in one year period) or defined as the price for the electricity that would equalize the present value of the sum of discounted cost (NPC) and the present value of discounted revenues [7]. In the same way that LCoE is written as a function of NPC, the same can be done for NPC, which in turn can be calculated as a function of LCoE, as the following equation shows:

$$\sum_{y=1}^{LT} \frac{E(y) \cdot LCoE}{(1+r)^y} = \sum_{y=1}^{LT} \frac{Inv(y) + O\&M(y)}{(1+r)^y} = NPC \tag{2.7}$$

Sizing optimization techniques literature review

Techniques for this purpose are based on the solving of the balance between solar radiation and load demand, taking into consideration the different features and lifetimes of the system components. Then, generally speaking, the optimization process generally consists in searching for the combination of the system components sizes (i.e. PV array size and battery bank size), which have the minimum NPC and/or LCoE while fulfilling the LLP condition [46]. Other forms of optimization techniques and technical economic analyses have been widely used in literature in order to investigate smart operational management approaches both in distributed energy systems and islanded systems [36]. In [50], the author reviewed optimization techniques for renewable energy systems in general - wind, solar, hydro, bio and geothermal - giving more focus to thermal solar energy at the expense of photovoltaic energy, how it was also done in [51]. In [52], size optimization techniques based on artificial intelligence techniques for photovoltaic power systems have been reviewed, based on conventional methods. When referring to conventional methods, it is related to empirical, analytical, numerical or hybrid methodologies to reach the exact size of the photovoltaic system through weather data (irradiation, temperature, humidity, clearness index, wind speed, etc.) and the information concerning the site where the PV system will be implemented.

Besides that, there are system sizing techniques that take more influential parameters that are suitable for the system sizing as per availability resources. Some of these are: [53] uses a method based on the worst month scenario; [54] takes the long-term hourly solar irradiation data and peak load demand; typical meteorological year data (daily solar irradiation on horizontal plane, the hourly mean values of ambient temperature and wind speed) and consumer power requirements for an one year time period where used in [55]. Methods based on LLP were adopted in [8–10] with one of the most suited being review in [12]. In [11], optimization of PV systems in Delhi is done defining the daily load, daily solar energy and then curve sizing the LLP curves. The number of PV panels and batteries are based on the minimum cost. Finally in [46], the optimization process is made in three steps:

1. First step - Estimation of PV array output based on one-year solar records;
2. Second step - Calculation of the daily status of the battery storage, which is based on the previous amount of the stored energy, PV array output energy, load energy demand, battery's efficiency and invert's efficiency.
3. Third step - Determination of loss of load probability and cost of the system based on the cost of system components.

All of the above works have used 1 of the 3 main methods or development procedures, which [31] classified in three categories: intuitive, numerical and analytical methods.

Intuitive methods According to [31], intuitive methods are based on an estimation of the dimensions of the system (i.e. PV panels, batteries, inverter) and it is developed without establishing any relationship between the different subsystems nor taking into account the random nature of solar radiation. In fact, the majority of systems sized from these types of methods results in over-sizing and prevents the economic and energetic sustainability. Many of them uses the "worst month" method, which is the use of the month with worst conditions as an input for the calculation.

The arguments for this method is that if it works for this month it will work for the rest of the year, which many of times results in over/under sizing of the systems leading to poor power reliability and high costs. Other problem is the simplified use of mathematical formulas for resolving the system's energy balance, as it was done in [56]. In this work, the optimization process which resolved around finding the cheapest combination of PV array and battery that will meet the load requirement, have not had very good results, leading to economic losses and not being able to supply the required energy, much due to the simplicity of the equations used and the lack of future security it provided for the project. Many other researches were based on intuitive methods: [57] shows that with improved equations the LLP of the system will still be very high, rounding the 8% mark; in [58–60] through the same process as [56], the authors sized systems for 5 sites in Iran, Egypt and Bangladesh. It is already widely known that intuitive methods are running out of capabilities in the field of system sizing optimization due to the fact that new software programs are being built with more efficient and faster methods.

Numerical methods In this case, a system simulation is used to estimate the energy balance of the system and the battery state-of-charge (SOC), for each time period, usually a day or an hour. Besides being more accurate, these techniques can apply the concept of system reliability in a quantitative manner, utilizing the LLP analysis. System reliability is defined as the load percentage satisfied by the photovoltaic system for long periods of time, as stated above [31]. The disadvantage of such methods is the need to have available hourly or daily exposure radiation series for long enough periods of time. Although the reliability is already analyzed, these methods allows to optimise the energy and economic cost of the system.

In turn, this category can still be divided in two ways, namely stochastic and deterministic. The stochastic methods consider the uncertainty in solar irradiation and load demand variation by simulating an hourly solar radiation data and load demand and therefore they are usually more efficient. Meanwhile, the deterministic method is represented by using daily averaged of solar energy and load demand due to the difficulties in finding hourly solar energy available data set. Almost all of major sizing work in literature is based in numerical methods.

An example for stochastic method is presented in [32], where a LLP and related parameters method is review for PV sizing, utilizing hour-by-hour simulation. In [61], another is presented where the criteria is the LLP, once again, and they use 23 years of hourly data to create nomograms that give the array size as a function of average horizontal energy and the storage capacity in function of the LLP. In Corsica [62], an experiment was conducted by performing a simulation of a PV–battery system supplying a 1 kWh load using hourly solar radiation and load demand series. The optimum configuration is selected based on the cost of energy without any definition of the LLP of the selected system, using system sizing curves constructed after the simulation. In [46], an optimal sizing of a stand-alone PV system in Kuala Lumpur, Malaysia has been presented. They use a three step method, as already stated in subsection 2.3.2, but the system cost equation is partially derived and has to be solved graphically. The plot needed for the estimation contains two lines: one represents the loss of load probability, while the other line results from the partial derivative of the system cost equation, being the point of intersection of these two lines being the optimum size of PV. Many researches state that this method has various disadvantages, such as the sizing curve being constructed for each particular load, the use of graphical solution rather than precise formula to calculate the optimum PV size, and it can only be utilized for that specific location and not for other locations in Kuala Lumpur.

For the deterministic part, the authors in [63] talk about an optimum design for a PV system in Sudan based on a clear sky model for global solar prediction. However, to optimize the array and storage sizes, it is assumed that the stored energy in a battery is equal to the difference between the load power and PV array generated power without any consideration of battery charging/discharging efficiencies, which may cause some serious errors in the sizing estimation. Besides that, the authors chosen the optimum configuration based on the LLP only, while the cost of the energy was not considered, while they used a monthly solar radiation series which means that the uncertainty of the solar energy is not considered at all.

Analytical methods The third and final method is the analytical one that it is done by the use of equations that would describe the size of the system according to its power reliability [31]. This process allows for the calculation of the PV system to be very very simple but, on the other hand, it can be very hard to find the coefficients of these equations making it a very inaccurate technique. The best example for the implementation of this method is in [64], which is an improvement of [46]. In a way of contradicting the disadvantages of that last work, researchers proposed a model where the LLP lines where modelled in formulas through MATLAB FitTool Box. With these new formulas is easier to find the intersection/optimal point, since it is only necessary to minimize them. In addition, after calculating the fit coefficients for each region, it is possible to calculate an average of that value and use it for bigger places, like whole countries.

All of the others works presented in literature have basically the same process as the above. In [9], the LLP curves are used to analyze a PV system, creating reliability maps that represent each LLP considered for three Spanish locations namely Madrid, Murcia and Santander. A more deterministic method is reviewed in [65] where an optimization of PV system is presented based on a long term solar radiation series for the UK. The author used daily load demand and solar radiation data which indicates that the uncertainties of solar radiation and the variation of the energy demanded were not considered. The climate data was divided in two categories, one with values equal or above the overall solar radiation, while the other category contains the days which have average solar radiation lower than the calculated overall solar radiation average. For final sizing, it's only necessary to scale the PV generator and storage battery based on the constructed general sizing curve.

2.3.3 Challenges for PV system size optimization

Although there are already many methods for optimizing the design of PV systems, these, however, bring with them some challenges that will need to be overcome to ensure a good result. The main struggles in achieving good effectiveness in this process are related with input utilized for the models and the models themselves. These constrains are:

Availability of weather data

For both PV and wind systems, it can be said that climate data are perhaps the most important information in a sizing process. However, in rural areas, the process of acquisition of this data is not so easy, since there are not many weather stations. In addition to this problem, it is also difficult to get this same information, but with shorter time intervals in order to make hourly simulations, in such a way that makes the whole procedure more effective. As a way to overcome this situation, researchers have started to design techniques so that these data can be predicted by computer or models to estimate hourly information through daily average data, many of which are based on stochastic methods. In the current times, daily average irradiance data can be easily extracted from NASA's Surface Meteorology and Solar Energy website [66] and even new techniques with ANN have already been created for the purpose of predicting data where there is not even the possibility to extract information.

Load forecasting

In the same way that hourly radiation data are vital for the design of the project, load data in a more detailed way from the location are equally important. A complete year profile in hourly time intervals would be the best way to extract an optimal size for the system, although this information is very difficult to obtain, especially in less developed areas. That said, researchers usually use only the hourly profile information of the load in order to be able to make their predictions or by ANN programs, due to the high development of technology for solar systems based on artificial intelligence.

Models accuracy and simplicity of the methods

For the optimization process of the system sizing to be effective and precise, the physical model of the photovoltaic system needs to incorporate all possible variables and needs to be as simple as possible. These variables have to do with: the production capacity of the panels, such as the temperature of the solar cells; the batteries, such as the battery life and its minimum State-of-Charge; the location and orientation of the system, such as latitude, longitude and location characteristics specifications, and finally, the efficiency of the system in general and its components. The best optimization techniques use the simplest models with the most accurate results. However, for that it will be necessary to mix technologies or find a method with a multi-criteria for optimization. A multi-criteria analysis is useful as the prioritisation of electricity generation options is a multi-faceted problem, requiring consideration of both qualitative and quantitative factors. Given the need to incorporate environmental considerations into energy planning, this accelerated the use of multi-criteria approaches. Action A may be better than Action B according to one criterion but worse according to another, hence compromise solutions must be found [3].

System components variety

The last of the challenges is perhaps the most time consuming for researchers in this area. Choosing the right components for the specific system is an extremely difficult task due to the wide variety of components that the market presents. It is very easy to find two panels with the same power, but after further observations of their specifications one can discover that their efficiencies and internal characteristics will hardly be the same. Furthermore, a battery that is good in a warmer place may not be so good in a cold place due to its temperature dependent characteristics. A good choice of components is essential in order to achieve the necessary optimization and for that a prior analysis of the location and its details is indispensable, just as a numerical simulation of the system is fundamental.

2.4 Solar radiation review

Due to the great importance that solar radiation has in the development of PV systems and in human life in general, it will be necessary to dissect this subject a little more. One part of the sun's electromagnetic radiation is the sunlight and consists of infrared light, visible and ultraviolet. The solar luminosity is related to the solar irradiance, which is defined as the electromagnetic energy per unit area and time (kWh) or power per unit area (W/m^2). In physical terms the solar irradiance is defined as the flux density. The flux density of solar irradiance decreases with increasing distance from the Sun in the power of $1/r^2$. The total irradiance reaching the surface of the earth, global irradiance, consists of direct and diffuse components [67].

2.4.1 Direct and diffuse radiation

Due to the interaction of solar photons and the atmosphere in their way to the Earth's surface, solar radiation can exist in two different forms: direct, or "beam", which is radiation that is directly emanating from the sun and diffuse radiation, which in this case, is emanating from the rest of the sky hemisphere and results from the interaction of incident global irradiance and the constituents of the earth's atmosphere [67]. Under overcast cloudiness, direct radiation disappears if the cloud is dense enough, and is then transformed into diffuse radiation, which is therefore normally more intense than under clear conditions. When talking about the development of solar systems, there is a need to determine not two but three radiation components: the direct component from the sun (G_b), the diffuse component from the sky (G_d) and the diffuse component from surface reflections (G_r); since radiation is the most important parameter for evaluation of solar energy potential of a particular region and the most basic value for PV simulations. The last component is not widely used, except in the case of a highly reflective ground (snow or white sand).

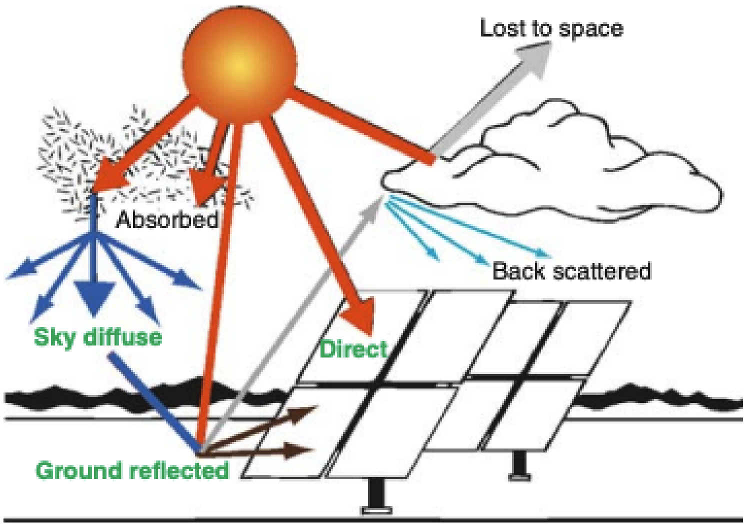

Figure 2.7: Example for direct, diffuse and reflected radiation [67]

2.4.2 Solar Radiation on a tilted surface

In PV panels, whenever it is necessary to develop a new system, the type of surface that is studied is always the tilted surface (in respect to the horizontal). It is necessary to make this difference, since the power incident on a PV module depends not only on the power contained in the sunlight, but also on the angle between the module and the sun. In addition, if the panel is not tilted then all the components spoken above will not be necessary for the calculation of the global radiation, since there is no radiation reflected on the ground or other materials. The radiation reflected or Albedo effect is a particular case of the diffuse radiation if the focusing surface is tilted relatively to the horizontal plane and if is the radiation reflected in any non-atmospheric element. The global and diffuse components of solar irradiance are usually measured at meteorological or radiometric stations on a horizontal plane which means that a way to calculate this data for the inclined plane will be needed since the data on inclined surfaces is not available [68]. This occurs because, in horizontal planes is the Global Horizontal Irradiation (GHI) is the one used for calculations, which is the sum of the solar radiation energy (direct and diffuse) that hits one square meter in a horizontal plane in one day. In the other hand, in tilted planes (facing the north in the south hemisphere) it is utilized the Global Tilted Irradiation (GTI) which is the same as GHI but with β_{opt} included in the calculation, that is the optimum angle for the maximum performance of the panel across the year. The solar radiation intensity received by a PV module at a site depends on its orientation as well as weather conditions [21].

There are many ways and models for the calculation of the monthly average daily total radiation on a tilted surface (GTI). Due to their distinctive natures and its different ways of interacting with a tilted surface, the beam and diffuse components need to be assessed separately, with direct and reflective being almost trivial utilizing algorithms and computer power available these days. With the diffuse radiation, it is different, because it needs a more complex process evolving various models and the information of global and direct radiation incident on a horizontal surface. One way is described in [69–71] and it is based on the models by Liu and Jordan [72], Badescu [73] and Tian [74], which all consider that diffuse radiation is isotropic (distributed uniformly all over the sky). It is obtained using the variables above and it's described as:

$$GTI = G_B + G_D + G_R \tag{2.8}$$

where G_D is the global daily diffuse radiation, G_R is the reflected solar irradiation and G_B is the daily direct radiation received on a tilted surface and it can be expressed as:

$$G_B = (G_g - G_d)R_b \tag{2.9}$$

where G_g and G_d are the monthly mean daily global and the monthly mean daily diffuse radiation on a horizontal surface, respectively. R_b is the ratio of the beam radiation on a tilted surface to that on a horizontal surface and is expressed as:

$$R_b = \frac{cos(\theta)}{cos(\theta_z)} \tag{2.10}$$

with θ being the incident angle or the angle between the sun rays and the normal to the PV panel surface and θ_z being the zenith angle. More information on those angles will be below.

However, in many works, the diffuse irradiance is not considered, once it usually corresponds to less than 10% of the total irradiance in clear sky days and its component decreases with the tilt angle. That said, the most important component for the calculation of total irradiation on a module (G_{b_module}) is the direct or beam incident component and can be calculated by [75, 76]:

$$G_{b\_incident} = \frac{G_{b\_horizontal}}{sin(\alpha)} \tag{2.11}$$

where $G_{b\_incident}$ represents the maximum direct irradiance from the sun. On the other hand, $G_{b\_horizontal}$ is the radiation component perpendicular to the ground horizontal plane, which is the ones usually measured in the radiometric stations. Lastly, α represents the solar angle or the elevation angle.

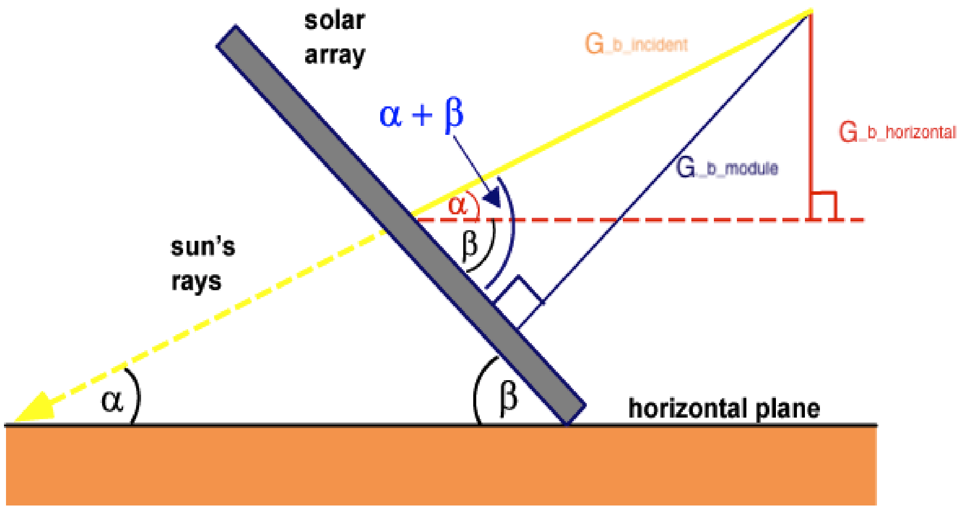

Figure 2.8: Horizontal, incident and module radiation angles - adapted [76]

From the above figure, G_{b_module} can be derived as:

$$G_{b\_module} = G_{b\_incident} sin(\alpha + \beta) \tag{2.12}$$

Finally, substituting equation 2.11 in equation 2.12 gives the the radiation incident on a tilted surface utilizing only the values that are easily known ($G_{b\_horizontal}$):

$$G_{b\_module} = G_{b\_horizontal} \frac{sin(\alpha + \beta)}{sin(\alpha)} \tag{2.13}$$

Angles on tilted panels

All the angles related to PV panel power production are important given that only the continuous change of angle between the sun and the fixed surface is enough for the power density in a fixed photovoltaic module to be lower than that of the incident sunlight. It is because of this that a subsection will be dedicated to this subject.

Incident angle The incidence angle, θ, is the angle between the sun vector and the normal to any tilted surface and is given by the following relation [70]:

$$\begin{aligned} cos(\theta) = {} & sin(\delta)sin(\phi)cos(\beta) - sin(\delta)cos(\phi)sin(\beta)cos(\gamma) + cos(\delta)cos(\phi)cos(\beta)cos(\omega) \\ & + cos(\delta)sin(\phi)sin(\beta)cos(\gamma)cos(\omega) + cos(\delta)sin(\beta)sin(\gamma)sin(\omega) \end{aligned} \tag{2.14}$$

where δ is the declination angle, β is the tilted angle, γ the azimuth angle, ω the hour angle and, finally,the latitude angle (ϕ), which is the angle forming according to the equator center. The north of the equator is positive and the south of the equator is negative and it varies between $-90° \leq \phi \leq 90°$ [27].

Solar angle The solar angle or elevation angle [°] is the angular height of the sun in the sky measured from the horizontal and is 0° at sunrise and 90° when the sun is directly overhead, which occurs for example at the equator on the spring and fall equinoxes. It is defined by:

$$\alpha = sin^{-1}(sin(\delta)sin(\phi) + cos(\delta)cos(\omega)cos(\phi))) \tag{2.15}$$

where ϕ is the latitude [°] and ω the hour angle [°]. On solar noon can be estimated by:

$$\alpha = 90 + \phi - \delta \tag{2.16}$$

Azimuth angle The azimuth angle (γ) is the compass direction from which the sunlight is coming. At solar noon, the sun is always directly south in the northern hemisphere and directly north in the southern hemisphere. At the equinoxes, the sun rises directly east and sets directly west regardless of the latitude, thus making the azimuth angles 90° at sunrise and 270° at sunset. In general however, the azimuth angle varies with the latitude and time of year and the full equations to calculate the sun's position throughout the day are given by:

$$\gamma = cos^{-1}[\frac{sin(\delta)cos(\phi) - cos(\delta)sin(\phi)cos(\omega)}{cos(\alpha)}] \tag{2.17}$$

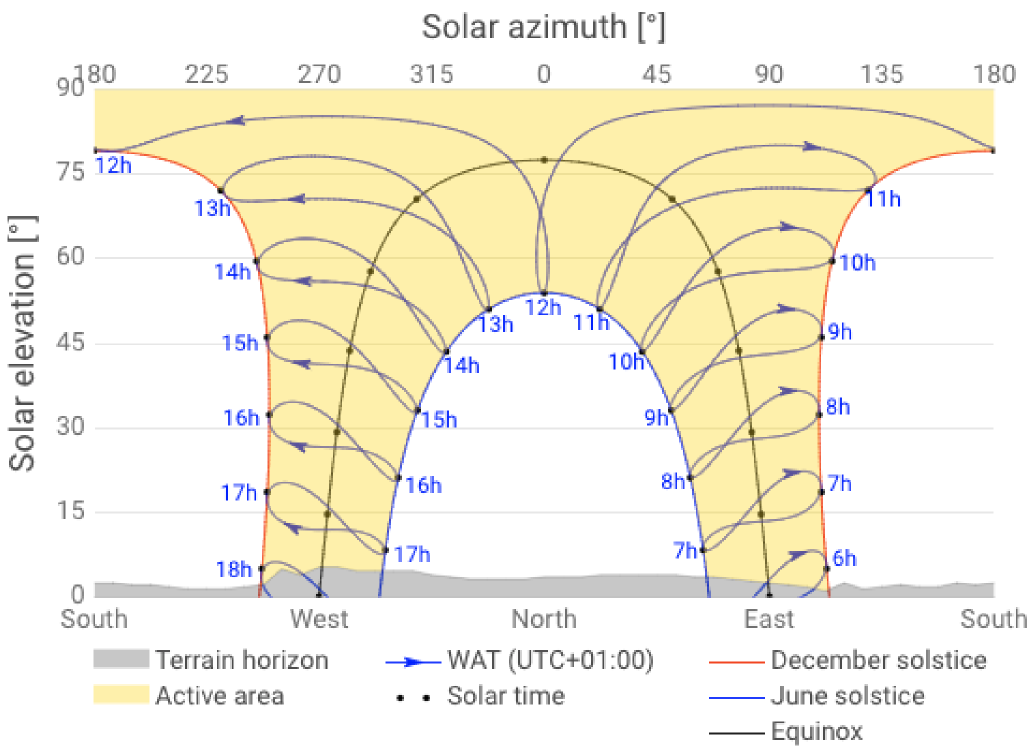

Figure 2.9: Relation between azimuth and elevation angles in Huambo [15]

Hour angle The hour angle is one of the coordinates used in the equatorial coordinate system to give the position of a point on the celestial sphere. The angle may be measured in degrees or in time, with 24 hours equalling 360 degrees exactly. By definition, the Hour Angle (ω) is 0° at solar noon, negative in the morning and positive in the afternoon. Since the Earth rotates 15° per hour, each hour away from solar noon corresponds to an angular motion of the sun in the sky of 15° or as an example, if an object has an hour angle of 2,5 hours, it crossed the local meridian 2,5 sidereal hours ago (i.e. hours measured using sidereal time), and is currently 37,5 degrees west of the meridian. It it described by:

$$\omega = 15°(LST - 12) \tag{2.18}$$

where LST is the Local Standart Time. LST in turn is calculated by:

$$LST = \phi + \frac{TC}{60} \tag{2.19}$$

with TC being the Time Correction Factor (in minutes) that accounts for the variation of the Local Solar Time (LST) within a given time zone due to the longitude variations within the time zone and also incorporates the EoT.

$$TC = 4(\phi - LSTM) + EoT \tag{2.20}$$

The EoT is the equation of time, in minutes, and is an empirical equation that corrects time for the eccentricity of the Earth's orbit and the Earth's axial tilt. It's given by:

$$EoT = 9,87sin[2\frac{360}{365}(d-81)] - 7,53cos(\frac{360}{365}(d-81)) - 1,5sin(\frac{360}{365}(d-81)) \tag{2.21}$$

with d being a Julian day. The LSTM is the Local Standard Time Meridian and it is a reference meridian used for a particular time zone and is similar to the Prime Meridian, which is used for Greenwich Mean Time. Its equation is:

$$LSTM = 15°\Delta T_{GMT} \tag{2.22}$$

where ΔT_{GMT} is the difference of the Local Time (LT) from Greenwich Mean Time (LST) in hours. Finally, and only for the specific cases of sunrise (ω_s) and sunset (ω_{ss}), one can rewrite equation (2.18) as follows:

$$\omega_{sun} = cos^{-1}(-tan(\phi)tan(\delta)) \tag{2.23}$$

For latitudes above 66,5° N, there is the possibility of a day or a night longer than 24 hours, so that the above equation can only be applied when $|\phi| < \frac{\pi}{2} - \delta$, since $cos^{-1}|tan(\phi)tan(\delta)| > 1$ is indefinite [77]. Since the solar hour angle is symmetrical about solar noon, the two values can be calculated by the following system:

$$\omega_s = TT - \omega_{sun} \quad (2.24)$$

$$\omega_{ss} = TT + \omega_{sun} \quad (2.25)$$

where (ω_s) and (ω_{ss}) are the sunrise and sunset hour, respectively and TT is the transition time, which is the time of day when the ω is equal to 0º (solar noon).

Optimal angle The optimal angle (β_{opt}) is the angle between the panels and the horizontal plane and varies throughout the year, with a possible gain up to 12% when the panels are tilted this angle [68]. It is south oriented in the Northern Hemisphere and north oriented in the Southern Hemisphere and varies between $0° \leq \beta \leq 180°$. In literature, only the latitude (ϕ) is used as a reference for the estimation of the optimal angle, especially when local and weather and climatic conditions are not considered. On the contrary, when these conditions are included in the determination of the angle and when it is possible to have a tilted panel with an optimal angle update every day, its calculation should be calculated by:

$$\beta = |\phi - \delta| \quad (2.26)$$

where δ is the declination angle. Of course, the most accurate way to determine this angle is to make measurements on site once it depends on the local conditions (buildings, trees), weather and climate conditions. Other methodologies for obtaining the optimum angle are proposed in [72] and [78].

Declination angle One of the most important angle needed for an optimal panel inclination is the declination angle (δ). It is the angle between the sunlight and the equator plane and occurs due to the 23,45° angle between Earth´s rotational angle and the orbital plane. It is positive in the north and varies between $-23,45° \leq \delta \leq 23,45°$ and its highest point on the summer solstice (21st of June) while its lowest is on the winter solstice (22nd of December) on the Northern Hemisphere and vice-verse on the Southern Hemisphere. Since it is in the solstices that this value reaches its maximum or minimum, it makes sense that it is in the equinoxes that this angle has a value of 0° . This happens since sunlight falls on the equator with a steep angle at these two times of the year. The vernal equinox is on the 20th of March and the autumnal equinox is on the 23rd of September, with daytime and night-time durations being equal on these dates. The declination angle is calculated by [27]:

$$\delta = 23,45 sin[360 \cdot \frac{(284+d)}{365}] \quad (2.27)$$

where *d* represents a Julian day.

Zenith angle The zenith angle is the angle between the sun and the vertical and is similar to the elevation angle but it is measured from the vertical rather than from the horizontal, thus making the zenith angle:

$$\theta_z = 90^\circ - \alpha \tag{2.28}$$

2.4.3 Models for estimation of hourly weather data

Estimation of Solar information

Normally, in less developed countries and in rural areas, there are not many weather stations available, thus causing a huge shortage of data regarding solar radiation and temperature. Precise information, mainly about Global Solar Irradiation is essential to achieve the objective of a reliable system, because its production is directly linked to the irradiance that the system receives. Many of the available data are averages of months and maybe even days, but for the purpose of a sizing project, may lead to several forecast errors in the long term, much due to the irregular nature of solar energy. Because of this, many mathematical models have been created and modified in order to make access to this type of information as easy as possible. According to [79], this models can be divided in three categories, conform to what they consider, being these:

1. The effect of time, which means only the time of the day is included in the estimation [80–82];
2. The random variation of weather conditions and the axis symmetric distribution between hourly global radiation of morning and afternoon times, which results in a normal distribution [83, 84];
3. Neither the hours of the day nor the weather variations [85].

The most used model would be from [80], as it is the simplest and requires the least possible input information. On the other hand, it was analyzed in [81] that numerical inaccuracies of the original correlations are found to arise based on the following factors:

1. reliance on uncorrected measurements of diffuse insolation with pyranometer;
2. the use of a single value of extraterrestrial insolation for a whole month;
3. and the negligence of seasonal variations in the diffuse/hemispherical ratio.

The new information concluded that the diffuse component is significantly larger than that predicted by the original formulas of Liu and Jordan. With the new analytical expressions presented in their research and with the parameters obtained by a least squares fit to the data, resultes in formulas that provide a complete description of the long term average insolation incident on surfaces. The only meteorological input is the long term average daily total of hemispherical insolation on the horizontal surface. Finally, Gueymardt introduced the concept of tilted surfaces on the models thus making the relationship between Global Solar Irradiation daily and hourly the following:

$$\frac{I}{H} = \frac{[a + bcos(\omega)]r_o}{f_c} \tag{2.29}$$

where

$$a = 0,4090 + 0,5016 sin(\omega_s - 60°) \tag{2.30}$$

$$b = 0,6609 - 0,4767 sin(\omega_s - 60°) \tag{2.31}$$

$$f_c = a + 0,5b \frac{\frac{\pi\omega_s}{180} - sin(\omega_s)cos(\omega_s)}{sin(\omega_s) - \frac{\pi\omega_s}{180}cos(\omega_s)} \tag{2.32}$$

$$r_o = \frac{\pi}{24} \frac{cos(\omega) - cos(\omega_s)}{sin(\omega_s) - \frac{\pi\omega_s}{180}cos(\omega_s)} \tag{2.33}$$

(2.34)

with ω_s being the sunrise hour angle and ω the local sun hour, both in degrees.

Temperature estimation model

In the same way that it will be necessary to modify the irradiance values so that the simulation result is as precise and accurate as possible, the temperature values will also have to be worked on. Due to the impossibility of extracting hourly information about the temperature, it will be necessary to use a stochastic method in order to solve this problem. The model used for this purpose is the one presented in [86] and was created for the purpose of crop growth. Many other models based on sine function curve fitting or through complex energy models have already been used, but they are difficult to represent [87]. The model used here will be based on the minimum and maximum temperatures of the respective day, the longitude and latitude of the location and the sunrise and sunset.

The algorithm divides the day into two segments, from sunrise to 14 h and from 14 h to sunrise of the next day. The method assumes T_{max} at 14 h and T_{min} at sunrise, and the intervening temperatures are calculated from the following equations:

- For $0 \leq t < \omega_s$ and $14h \leq t \leq 24h$

$$T(t) = \frac{T_{max} - T_{min}}{2} + \frac{T_{max} - T_{min}}{2} \cdot [cos(\frac{\pi \cdot t'}{10 + \omega_s})] \tag{2.35}$$

- and for $\omega_s \leq t \leq 14h$

$$T(t) = \frac{T_{max} - T_{min}}{2} - \frac{T_{max} - T_{min}}{2} \cdot [cos(\frac{\pi(t - \omega_s)}{14 - \omega_s})] \tag{2.36}$$

where ω_s is the time of sunrise in hours, $T(t)$ is the temperature at any hour and t is time in hours, with $t' = t + 10$ if $t < \omega_s$, $t' = 14$ if $t > 14h$.

Chapter 3

Simulation - Inputs, weather and load informations

In this chapter, a description of all the elements that will be used has an input for the simulation will be presented and described. These elements correspond to a description of the data used for the creation of the hourly data for the irradiance and temperature values; the creation of the load profile and its argumentation and, finally, the photovoltaic system initial technical and economic considerations/assumptions needed for the simulation.

3.1 Weather data

3.1.1 Solar resources

For the first step of the simulation, it will be necessary to calculate the hourly irradiance values. This is due to the fact that hourly data is difficult to find, especially for isolated sites like the one under study. Therefore, for this calculation one will need daily average irradiance data in kWh/m^2/day to be processed by the mathematical model explained in section 2.4.3. Another important point to note is that for a more accurate simulation, the smaller the time-step, the more accurate the results will be [83]. The first idea was to use 20 years of average daily data for the simulations, but unfortunately, due to the computational power and time required to process for all hours of the last 20 years (that would be around 175000 variables), this will not be possible. Having said that, it was decided to use a method widely used in solar system simulations, the worst year method, which uses the irradiance data from the worst year in history so that the system is oversized in order to operate on very low radiance days and still be able to provide energy to consumers.

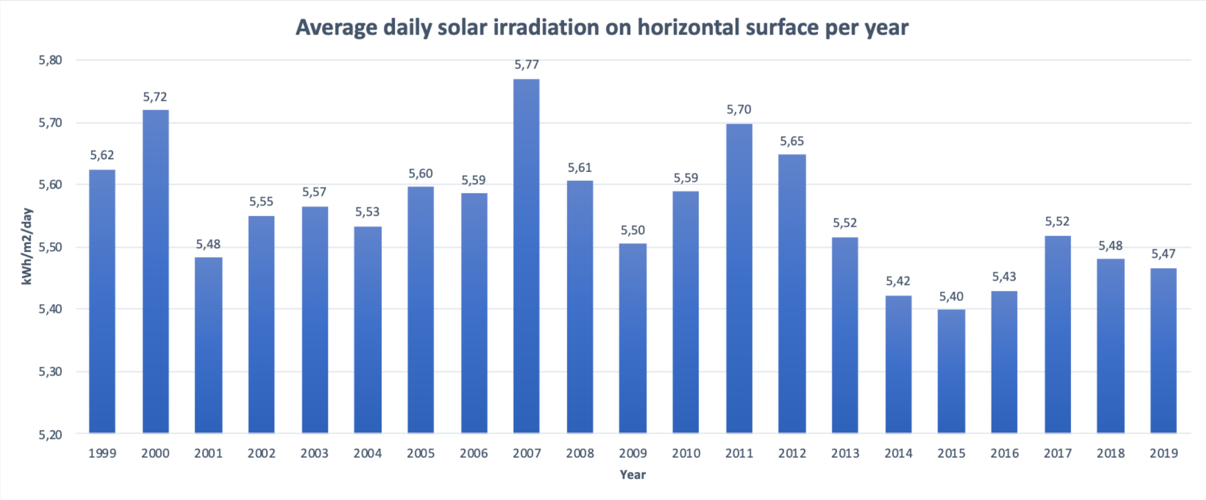

Figure 3.1: Graph of daily irradiance averages over a year for 20 years of data adapted from [66]

From NASA's website it was possible to find more than 40 years of mean daily irradiance values, where the last 20 were chosen because they are the most accurate. This information was then processed in order to understand which of these 20 years was the worst year for insolation. An average of all the daily averages for each year was calculated, as shown in Figure 3.1, and it can be seen that the year with the worst daily average is 2015. After the year is chosen, the average daily irradiance data for that year is fed into the simulation in order to be processed by the model. For the calculation of the hourly irradiance, in addition to the Gueymardt model, all the equations in 2.4.2 will be needed for the estimation.

Month	**Mean daily irradiation [kWh/m^2/day]**			
	NASA website	Model prediction	Difference between predicted model and NASA data in [kWh/m^2/day]	Difference between predicted model and NASA data in percentage (%)
Jan	4,89	4,89	-5,82E-04	-0,01%
Feb	4,92	4,92	-1,87E-03	-0,04%
Mar	5,43	5,43	-8,58E-03	-0,16%
Apr	5,65	5,64	-1,03E-02	-0,18%
May	5,97	5,97	-3,27E-03	-0,05%
Jun	5,53	5,54	7,73E-03	0,14%
Jul	5,51	5,52	1,02E-02	0,18%
Aug	5,55	5,55	4,55E-04	0,01%
Sept	5,40	5,39	-7,11E-03	-0,13%
Oct	5,84	5,84	-1,45E-03	-0,02%
Nov	5,31	5,31	-8,62E-04	-0,02%
Dec	4,74	4,74	5,61E-03	0,12%

Table 3.1: Comparison between mean irradiation data from NASA website and Gueymardt model for Huambo in 2015

The equations stated above will be used to give the algorithm more tools to make the final results more precise and accurate. Using the calculation of sunrise and sunset times, and other time correction equations, one can get different values for each day, month and even different seasons. Once the hourly irradiance value on a horizontal surface has been calculated, these values are then transformed into hourly irradiance values on an tilted surface with the help of an average value of β_{opt}, calculated by equation (2.26). Table 3.1 shows the comparison between the monthly average daily irradiation data from the NASA website and the data calculated after been processed by the algorithm. As can be seen, the data provided by the model can have an insignificant difference to the real data, thus making the prediction of hourly irradiance levels very accurate.

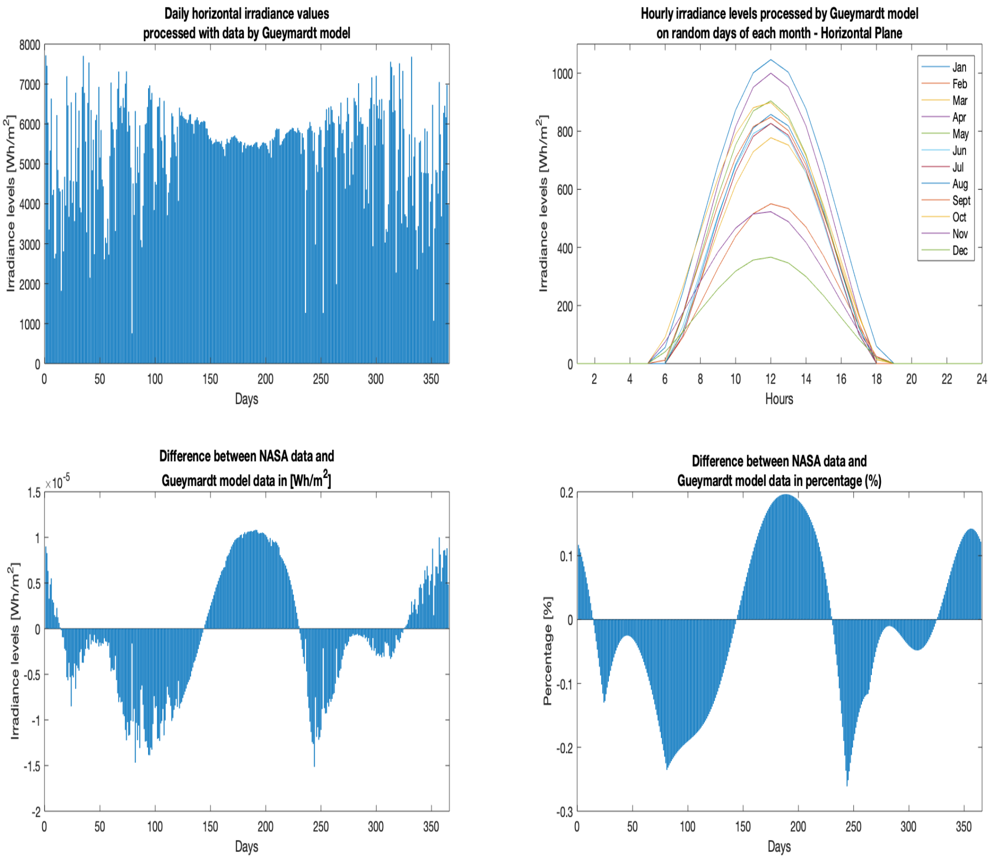

Figure 3.2: Hourly irradiance levels processed by Gueymardt model on random days of each month - Horizontal Plane

Finally, for the purpose of analyzing the irradiance levels on inclined surfaces and to observe the influence of the angle β_{opt}, figures 3.2 and 3.3 are presented, where the first figure shows: a) the total irradiance on one day on a horizontal plane predicted by the model; b) the hourly irradiance level on a random day of each month of the year; c) the difference in kWh/m^2 between the data provided by NASA and the data created by the Gueymardt model, and finally, d) the same difference but in percentage form. In the same way, figure 3.3 shows the same 4 plots but for a tilted plane, with a fixed angle of

21,88°. This angle was calculated from an average of all β_{opt} values during the year, estimated using the equation 2.26. It was not possible to use the equation to update the inclination value of the panels all year, since this change would have been made either by man's hand or by an automatic system, both of which would have made the project even more expensive. It can be clearly seen the advantages that an update of the optimal angle can bring to the production of solar panels.

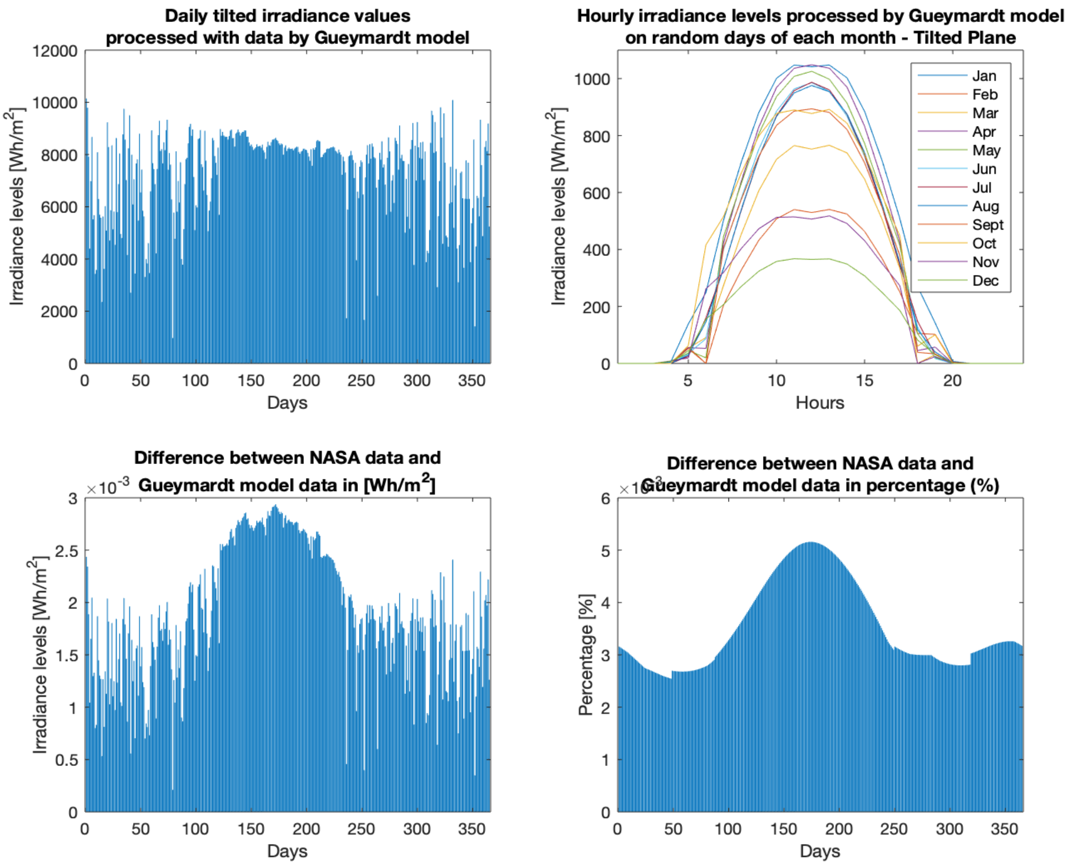

Figure 3.3: Hourly irradiance levels processed by Gueymardt model on random days of each month - Tilted Plane with β_{opt} = 21,88°

3.1.2 Temperature

After entering the insolation data, it is also necessary to enter the temperature data into the simulation. The ambient temperature values are highly important, since the output of the PV system is directly linked to both insolation and temperature, due to their effect on the PV cells. This effect will be explained in a little more detail in the part referring to the characteristics of the PV system and its physical model.

Having said this, the method of creating temperature data is very similar to the insolation data, since for these isolated sites it will be impossible to have hourly data of the average ambient temperature. Therefore, it will be necessary to use a mathematical model in order to synthetically create the temperature data, which was explain in subsection 2.4.3. Among the climate data, insolation is the most important of the two weather groups. Therefore the temperature values were chosen after the worst year of irradiation levels had been selected.

Month	Average daily temperature [ºC]			
	NASA website	Model prediction	Difference between predicted model and NASA data in [ºC]	Difference between predicted model and NASA data in percentage (%)
Jan	19,50	20,55	1,06	5,42%
Feb	20,08	21,20	1,12	5,58%
Mar	20,50	21,73	1,24	6,05%
Apr	20,47	21,71	1,24	6,07%
May	19,22	21,10	1,88	9,79%
Jun	17,89	20,21	2,32	12,97%
Jul	18,73	20,81	2,08	11,13%
Aug	19,82	22,04	2,22	11,22%
Sept	23,36	24,94	1,58	6,76%
Oct	24,65	25,90	1,25	5,06%
Nov	22,54	23,96	1,41	6,27%
Dec	20,94	22,17	1,22	5,84%

Table 3.2: Difference between predicted model and NASA data values

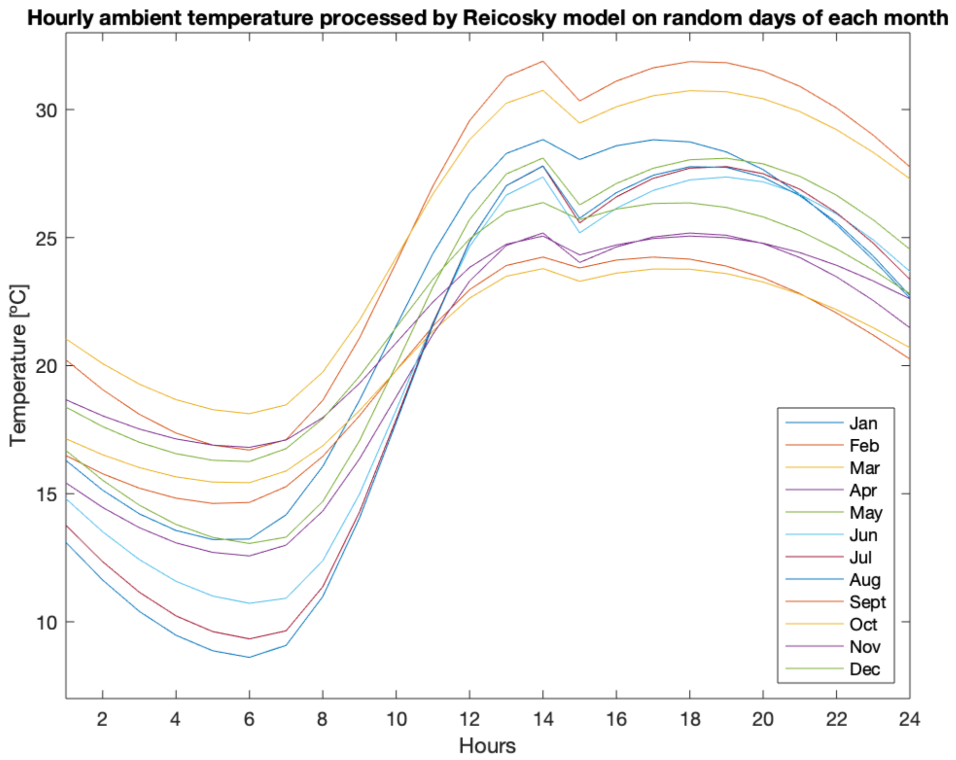

Figure 3.4: Hourly ambient temperature processed by Reicosky et al. model on random days of each month

Table 3.2 shows the average values for air temperature taken from NASA's website and the average values calculated from the predicted hourly temperatures. From the observed data it is possible to conclude that the model does not present the same accuracy as the model used for irradiance, managing to exceed 10% error in one month. This value, however, will not be the best for comparisons since the values that one really needs for the simulation are the hourly values. Therefore, according to [87] the method used in this thesis is the one that presents the lowest Absolute Mean Error (AME), Root Mean Square Error (RSME) and Residual Sum of Squares (RES) in a 24 hour period. Finally, figure 3.4 represents the ambient temperature on a random day in each month outputted by the model.

3.2 Load profile

For a successful optimization process, one of the most important sources of information about the location and its community will be the demanded load data. Through these, it is possible to have a theoretical idea of what a possible size for SAPVS will be. For the creation of the load curve, it was used the energy consumption information presented in [14], all from Huambo area. This survey was done to 50 houses in the rural and peri-rural areas of Huambo, although only the rural area will be used for this work. Furthermore, in all of these areas, at the time of the questionnaire, there was no electricity grid installed and the houses had no electrical installations. For the construction of the daily load, a 5 step methodology will be used [7]:

1. The first step will be to separate people/companies into classes ($ClassType$), each class will have its number of elements identified (N_{users}) and each group of users will be separated in households, if they are part of any of the residential classes (N_{houses});

2. Next, all electrical applications will be identified ($AppName$) and described according to their nominal power (P_{app}) and equipment number per user or house (N_{app});

3. After collecting information about users and their equipment, it will be necessary to assume an operating schedule, in hours (h_{funct}), for each application and its respective number of operating intervals ($NumWin$) and operating interval in hours ($W_{f,n}$), as described in the following equations:

$$Tot_W = \sum_{n=1}^{NumWin} W_{f,n}$$
$$h_{funct} \leq Tot_W \tag{3.1}$$

4. In order to calculate the power of each application over the operating hours, the following expression is used (kWh):

$$P_{eq,App} \cdot Tot_W = P_{app} \cdot h_{funct} \cdot N_{app} \tag{3.2}$$

5. Finally, the complete daily curve is built based on each application, its contribution and user within each class.

3.2.1 Types of loads

Since the purpose of this project would be to supply electricity to remote places, the intention would only be to feed the loads necessary for people's basic living conditions, which are mainly AC loads. From the survey done in [14], it is possible to determine that, in the rural district, the most important service that needs energy would be the lighting, followed by television and finally the conservation of food and its confection. In other words, one can say that the most important applications for then lower class would be:

- Illumination, for quality life purposes;
- Refrigerator, for conservation of food;
- Television, for entertainment.

This only describes what would be the most important electrical equipment in so-called "normal" houses in Angola. For people with a few more incomes or for companies, the equipment will be different as exemplified in Table 3.4.

3.2.2 Electrical appliances

Illumination

There are two main types of lighting used in the houses and companies of Angola: incandescent lights and traditional fluorescent lights with iron-core ballast and starter.

For this project, the incandescent light used will be a 60 W light to simulate the types of lighting that may exist in the houses of Huambo. An incandescent light is a type of lamp with a wire filament heated, through a current supplied by the terminals connected to the filament or incorporated in the glass, until it glows. The filament is enclosed in a glass bulb with a vacuum or inert gas to protect the filament from oxidation.

The other types of lamps most commonly used will be the traditional fluorescent lamps, which is a low-pressure vapor of mercury gas-discharging lamp that uses fluorescence to produce visible light. An electric current in the gas excites mercury vapor, which produces short-wave ultraviolet light that then causes a phosphor coating on the inside of the lamp to glow. This current can reach up to 30 A due to the negative differential resistance nature of this type of lamps, which means as more current flows through them, the electrical resistance of the fluorescent lamp drops, allowing for even more current to flow. Connected directly to a constant-voltage power supply, a fluorescent lamp would rapidly self-destruct because of the uncontrolled current flow. Because of this, fluorescent lamps require a ballast (iron based core mostly) to stabilize the current through the lamp, and to provide the initial striking voltage required to start the arc discharge. A ballast is an inductor placed in series, consisting of a winding on a laminated magnetic core. The inductance of this winding limits the flow of AC current. In addition, many of these lamps are aided by Power Factor Correction (PFC) capacitors, which are used in parallel with the lamps, especially those used for industrial purposes, due to the reactive nature of the lights.

A fluorescent lamp converts electrical energy into useful light much more efficiently than incandescent lamps, despite its higher price. Since this type of lamp is the most used for commercial and industrial sites, it will be used in other buildings with exception of the residences.

Nowadays there are other types of more efficient and durable lamps, being the compact fluorescent and LED ones the most used. Despite their advantageous properties, they will not be used in this project, since the focus is on impoverished areas, that is, one has already assumed in this sense that the most recent model of lamps for lighting did not exist.

Refrigerator

The refrigerator chosen for the simulation was a Kentt 201E, previously used in previous thesis in the Energy Scientific Area [13, 68]. This refrigerator has specifications very similar to those found in this type of equipment, in these more remote places, due to the weak evolution of technology. It has a 1886 A compressor, which makes it easily one of the most consuming appliances in the home. For a better data treatment efficiency and better approach to reality, the load diagram of the active power of the refrigerator was obtained for one hour with the refrigerator almost full in the 3^th level, since the refrigerator has 7 levels, as can be observed in Figure 3.5.

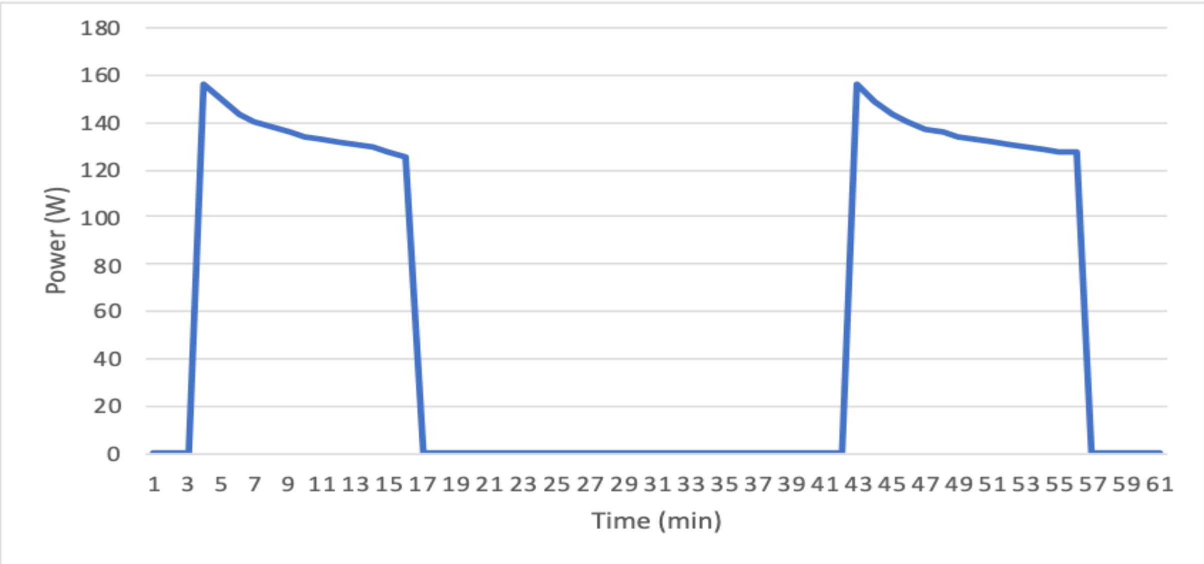

Figure 3.5: Refrigerator consumption in 1 hour

Thus it is possible to determine that the refrigerator, for the above conditions works twice an hour, in periods of 15 min each. Therefore, it consumes an average power of 61 W per hour.

Television

For television, and since this thesis focuses on isolated locations with few possibilities, it was necessary to come up with a device with technology similar to that found in these locations. Having said this, it is used the same television present in the works of the Scientific Area of Energy, because it has the best characteristics for this project. The television in question is a cathode ray tube television, one that almost nobody uses nowadays, due to the large passage for LCD, LED and the newer ones, OLED. But as in developed countries, unfortunately, the technology costs to get there, so one will use this equipment for data removal. The CRT TVs also need a large current at the beginning of use in order to heat the metal plate behind the electron gun. The television used for the project was the Sony KV-14LT1E 13” Colour TV, which according to its technical information, has a power consumption of 41 W.

Mobile charger

It is assumed that some people may already have telephones and therefore a charging station should be assumed for each house from a certain class. The worldwide nominal power for a mobile charger is about 5 to 10 W.

3.2.3 Functioning assumptions

In order to make this micro-network more complex and real, some extra elements have been added in order to truly simulate a small community. Each new building will feature some equipments not presented in normal homes. The assumptions for these equipments and for its operating hours are the following:

1. Residential consumers:
    - The refrigerators, as usually, are always on during the day, meaning it will work for 12h/day, in two periods of 15 min.
    - CRT TV have a operating window between 18h and 24h, functioning only 4h in that period.
    - The light is switched on at the end of the afternoon, around 18 h, and switched off at the end of the night, around 24 h. Due to the different hours of sunshine during the year, this value represents the average of power consumption in that year.
    - Mobile charging will have an operating window of 14 h, which means it can be operated in that time but it will only have a 8 h run time.
    - Finally, in the residential consumer type, there will be 4 types of classes and the wealthier classes may have more equipment than others, and therefore an other type of equipment is added here that can range from a radio, to a standing fan or other small and low consumption devices. It will have 4 h of operation, within a 9 h interval.
2. Primary school:
    - The fluorescent light tubes are assumed to have an operating window of 8 hours, operating 4 of these hours, to assist the classes.
    - A mobile charging station will be present too, with a 4 hour possible functioning time in and 8 hour interval.

- An old TV is available too, with the same 8 hours operating window but only 3 hours of proper functioning.

3. Health Care Unit

- Light tubes will have a wider window of operation with 24 hours of proper functioning. Of this interval, in the minimum 12 hours will be utilized.
- The vitals monitors are the equipment with the highest window of operating, with 24 h. This is because it is an equipment that may have to be used at any time. Its hours of functioning however are estimated to be 16 h, because it is believed that there won't always be patients in need of one.
- A refrigerator will be available too, for the conservation of medicines and other products needed of refrigeration for health. The model of the refrigerator will be the same as the one found in the residences, for greater easiness in the treatment of data. Its operating windows and hours of operation will be the same as the device in the above point.
- A mobile charger with a larger operating window will be used in order to simulate an emergency communication medium that will have to be constantly charged. So its window will be 24 hours, with approximately 8 to 12 hours in full load.
- Other health equipment will be added, such as a sterilization machine. It is a machine that does not need a lot of time of operation and therefore will have only 2 hours of operation in a window of 24 hours, since it may be necessary to use it at any time.

4. Market/Kiosk

- The lights of the market are supposedly switch on in the morning, when there is still not much sunlight, or in the late afternoon when it is about to dusk. Given that, it was chosen an operating interval of 6 hours, with an average of 4 of those hours being used.
- When it comes to food conservation, here this study has found some problems. As there is no industrial refrigerator in the laboratory in order to withdraw the data regarding its consumption, it was decided to make an estimate and use the power of about 20 refrigerators (divided in too sets) used for residential consumers as a reference. Its operating times and respective windows will also be the same as those used above.
- A station for charging phones will used too, because its usual in this types of rural places to have a unique spot for people that don´t have electricity at home to charge their equipments. A 12-hour operation window will be used, with 10 of these hours truly used for its operation.
- Due to the warm climate that is usually lived in these places, a fan is used in this profile, working all day (at least while the market is open). Having said that, it has a 10-hour running time in a 10-hour window as well.

5. Local Council

- Since it is an assistance point for the whole community, some more technological elements have been added, such as a small computer that will have an 8-hour window but only 2 hour of operation since it is only for very specific situations.

- This was the same thought for the internet router. It needs to be on all day long but with very low power consumption, thus making it have a 24-hour operating window. Nevertheless, since its consumption is extremely low throughout the day, only 1 hour at full power will be used in the daily load.

- A mobile charger is present too, with a 14 h functioning window and 10 of those hours used.

- A standing fan with the same operation characteristics of the market will be considered.

- The lights are assumed to be turned on in the morning and at the end of the afternoon, making a total of 9 hours of operating interval for 6 hours actually used.

6. Street lights

- Used only at end of the afternoon or at night. Operating window of 12 hours with 8 of them functioning.

All the above mentioned assumptions and associated buildings will be arranged in Table 3.4, together with their user class (*Class Type*), how many devices will be used (N_{App}), their nominal power (P_{App}) and, finally, their equivalent power ($P_{Eq,App}$), according to Equations 3.1 and 3.2. Furthermore, with all this information it is also possible to calculate the energy needed for each residence/company or for each user per day or per year, as can be seen in the Table 3.3.

Class Type	**Nº houses**	**Nº users**	E_{user_day} kWh/day	E_{class_day} kWh/day	E_{class_year} kWh/year
Residential I	10	4	1,48	14,80	5402,00
Residential II	7		3,1	21,7	7920,5
Residential III	5		4,31	21,55	7865,75
Residential IV	4		5,76	23,04	8409,6
Street lights	-	1	23,2	23,2	8468
Primary School		1	2,388	2,388	871,62
Health Care Unit		1	7,692	7,692	2807,58
Market		1	17,5	17,5	6387,5
Local Council		1	4,71	4,71	1719,15
Total Load	-	-	70,14	136,58	49851,70

Table 3.3: Energy consumptions for Huambo's micro-grid

Consumer Type	Nº users	Nº households	Class User	Applications	P_{app} [W]	N_{app}	h_{funct} [h]	$W_{(f,1)}$ h_{start}	$W_{(f,1)}$ h_{stop}	$W_{(f,2)}$ h_{start}	$W_{(f,2)}$ h_{stop}	Tot_W	$P_{eq,app}$
Residencial	4	10	I	Lights	60	4	6	18	24			6	240,00
				Mobile charger	5	1	8	0	8	18	24	14	2,86
		7	II	Lights	60	6	6	18	24			6	360,00
				Mobile charger	5	1	8	0	8	18	24	14	2,86
				TV	42	1	4	18	24			6	28,00
				Fridge	61	1	12	0	24			24	30,50
		5	III	Lights	60	8	6	18	24			6	480,00
				Mobile charger	5	2	8	0	8	18	24	14	5,71
				TV	42	1	4	18	24			6	28,00
				Fridge	61	1	12	0	24			24	30,50
				Standing fan	45	1	10	8	24			16	28,13
		4	IV	Lights	60	10	6	18	24			6	600,00
				Mobile charger	5	4	8	0	8	18	24	14	11,43
				TV	42	1	4	18	24			6	28,00
				Fridge	61	1	12	0	24			24	30,50
				Radio	50	1	4	6	9	18	24	9	22,22
				Standing fan	45	2	10	8	24			16	56,25
Street lights	-	1	-	Lights	50	50	8	0	6	18	24	12	1666,67
				LED	8	50	8	0	6	18	24	12	266,67
Primary school		1	-	Lights (tubes)	36	15	4	8	16			8	270,00
				Mobile charger	5	2	6	8	16			8	7,50
				TV	42	1	4	8	16			8	21,00
Health care Unit	-	1	-	Lights (tubes)	36	10	14	0	24			24	210,00
				Vitals Monitor	50	2	16	0	24			24	66,67
				Fridge	61	1	12	0	24			24	30,50
				Mobile charger	5	2	12	0	24			24	5,00
				Sterilising machine	100	1	2	0	24			24	8,33
Market	-	1	-	Lights (tubes)	36	15	4	6	8	17	21	6	360,00
				Conservation of food	610	2	12	0	24			24	610,00
				Mobile charger	5	5	10	8	20			12	20,83
				Standing fan	45	1	10	8	13	15	20	10	45,00
Local Concil	-	1	-	Internet router	10	1	12	0	24			24	5,00
				Lights (tubes)	36	15	6	6	8	18	24	8	405,00
				PC	100	1	2	8	12	14	18	8	25,00
				Mobile charger	5	5	10	0	7	17	24	14	17,86
				Standing fan	45	2	10	8	13	15	20	10	90,00

Table 3.4: Load assumptions for Huambo's micro-grid

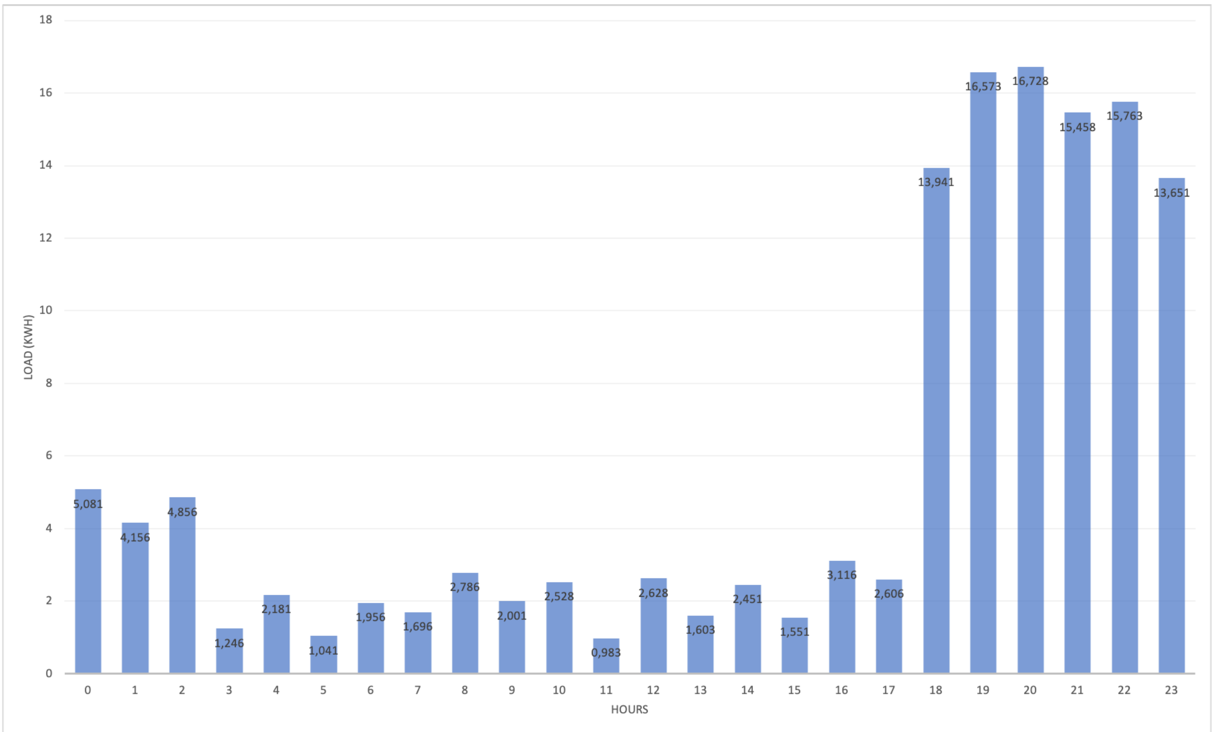

Figure 3.6: Diagram for the load profile of Huambo's micro-network project

As can be observed in Figure 3.6, peak hours are at night when people are already at home after their work. The high load value experienced at night is due, in particular, to the street lights and home entertainment equipment. Although the refrigerators' loads were all distributed equally throughout the day so as not to overload the network, it is possible to see several peaks during the day due to the entry into operation of the refrigerators on the market.

3.3 Techno-economic assumptions and specifications of the system

Finally, and as a last step before starting the system simulation and the consequent search for the optimal system, it is necessary to introduce some characteristics of the solar panels, batteries, inverter. In addition, it is necessary to have a notion of the state of the photovoltaic market on the African continent, since one of the main tools in the optimization process is the economic evaluation of the installation. These values are not only compulsory but also very important in order to proceed to the beginning of the simulation.

3.3.1 Technical characteristics of the system

After all the information regarding climate and load is entered, some physical characteristics of the system should be known before proceeding with the simulation. Some of these specifications are the following:

- PV panels:

  1. ρ_T - temperature coefficient of power in relation to the temperature of the solar cell;
  2. T_{ref} reference temperature, i.e. the temperature at which the panel cells were tested;
  3. η_{BOS} - balance system efficiency which embraces all losses not directly related to the sun energy conversion process.

- Batteries:

  1. SOC_{ini} - initial SOC of the batteries, which has to do with their balance before the first charge;
  2. SOC_{min} - minimum value that limits the State-of-Charge of a battery so that its life cycle is not damaged and the battery does not need to be replaced sooner;
  3. SOC_{max} - maximum value that limits the State-of-Charge of a battery so that its life cycle will not be damaged;
  4. η_{ch} - battery charge efficiency, provided by the manufacturer;
  5. η_{DISCH} - discharge efficiency of a battery, provided by the manufacturer;
  6. $N_{cycles\_80\%}$ or $N_{cycles\_DOD\%}$ - number of charge cycles at a DOD of 80% or at a specific DOD stated by the manufacturer.

- Inverter:

  1. Inv_{size} - since the maximum power of the inverter will only be modelled by the maximum value of the daily load curve, this value can be specified already. Since the peak load in one day, according to Figure 3.6, is 16,7 kW, one can model the inverter to have a 15 to 25% higher conversion capacity in order to cope with more loads that will be added in the future.
  2. Finally, its life expectancy ($LT_inverter$) should also be introduced, something that can be easily found in manufacturers' manuals.

In terms of assumptions about the characteristics of solar panels, the values used will be based on various data from different studies. From [88], it is possible to analyze the values described in Table 3.5, which are part of a study made with several types of solar panels, where the objective was to visualize the various temperature coefficients in relation to the power (ρ_T [%/℃]). Of the various panels studied (Modules in Survey), not all reported a conclusive value, and the number of those that did is described in the column Modules Reporting ρ_T. Finally, of those that did report a valid number, an average is calculated and then presented in the last column of the table. Using this information, it is possible to see that the value most reported for monocrystalline panels was -0,46 %/°C. In terms of reference temperature (T_{ref}), the most used value is the one referring to the Standard Test Conditions (STC) that has a value of 25 °C. Finally, one have to calculate the efficiency of the system without counting the radiation/electric energy conversion components (solar panels), i.e. the efficiency of charging and discharging the batteries, the efficiency of the DC to AC conversion in the inverter, and the losses in the cables. For this, the following equation will be used:

$$\eta_{BOS} = \eta_{inv} \cdot \eta_{Bat} \cdot \eta_{cable} \tag{3.3}$$

This equation describes that the Balance of System efficiency (η_{BOS}) is calculated by the product of the efficiency of the inverter, the efficiency of the batteries, and finally the efficiency of the power cables. Since the objective of this work is to understand if this methodology is a good option for sizing solar systems for isolated areas, there is no exact cable length to calculate the voltage drop and efficiency. Having said this, and using [89, 90] as an example, an efficiency of 95% will be used.

For the batteries, as a way of having a more recent example, their characteristics were based on the new solar batteries available on the market. One of the examples are the Power batteries [91], which are $LiFePO_4$ solar batteries, that have an efficiency of 95% to 99% and a discharge efficiency of 95% to 99%, besides being able to use almost 100% of their Depth-of-Discharge. Regarding the initial balance of the batteries (SOC_{ini}), this value will be based on the information provided in the datasheet of the batteries, where the battery manufacturer states that although all their batteries are delivered to the consumer with a charge of around 75%, it is expected that the consumer before the first charge will let the batteries drop to 50%, in order to extend the life of the battery further. This will only happen for the first post-factory charge, since after this charge, the battery will be limited to a SOC_min of 10% and a SOC_max of 90% in order to prolong its life. In relation to the inverter, since one already have the value of its power and since its efficiency is modulated by the equation presented in [92], which will be explained in Chapter 4, it will only be necessary to have a notion of its expected lifetime, something that can be done through the Table 3.6. Looking at this table, the value chosen and that best fits with this project will be 10 years and will give the possibility of being chosen either a central inverter or a string inverter.

PV Module Type	**Modules In Survey**	**Modules Reporting ρ_T**	**Average Value of ρ_T [%/℃]**
Polycrystalline silicon	10	7	-0,48
Monocrystalline silicon	8	4	-0,46
Monocrystalline/amorphous silicon hybrid	1	1	-0,30
Thin film amorphous silicon	4	4	-0,20
Thin film CIS	1	1	-0,60

Table 3.5: Average Value of ρ_T [%/℃] for multiple types of PV modules - adapted from [88]

Inverter Type	**Standard Warranties**	**Extended Warranty**
String Inverter	5-10	20
Micro Inverter	20-25	NA
DC Optimizers	20-25	NA
Central Inverters	5-10	20
Battery Based Inverters	2-5	10

Table 3.6: Average warranty values for inverters - adapted from [93]

3.3.2 Economics and markets

In the last decade, a high drop in the prices of solar system components has been observed and a clear increase in investment, not only in this same technology, but also in all other clean energies have been observed as well. This was due a lot to the improvements in the efficiency of the panels and their manufacture, which depending on the solar characteristics of their installation, could reduce the payback time by up to 5 years. More optimizations and cost reductions will be possible in the PV panels components, due to the great speed that the technologies are growing and their proper implementation. Some methods used by researchers are the following [94]:

- higher conversion efficiency;
- less material consumption;
- application of cheaper materials;
- innovations in manufacture;
- mass production;
- and optimised system technology.

Along with the cost reduction in solar panels, one will also see a reduction in system components in general, or as it is known in the Balance of System (BOS) cost and their installation. The BOS includes all the components of the PV system besides the modules, like wirings, inverter, batteries and so on. In addition, due to a very strong increase in the demand for PV systems, the industry have reacted and, in the coming three to four years, new factories will bring more silicon to the market, produced by more cost-effective methods. Or, on the other hand, the amount of silicon needed for producing cells can decrease due to some technological improvements.

This production cost breakdown that the world is experiencing turned out to be decisive to the tremendous growth in the solar market and this has made countries invest even more in solar energy. If one excludes China from the Asian market, Europe maintains the leadership regarding the cumulative installed capacity, being Germany the main investor with over 47 GWh of installed electricity generation capacity by 2019 [1]. In the other hand, China has made many investments in this area in the past years, managing to gain the status of largest solar electricity producer in the world, growing from a capacity of about 700 GWh to about 220 TWh. This was largely due to the introduction of a new Feed-in Tariff (FiT) that was developed to accelerate investment in the implementation of renewable technologies in many locations in the country. This was achieved by offering long-term contracts to power generation companies, which guaranteed an investor buy back price at which the power purchaser (distribution utility in most cases) will buy power that is being fed to the grid directly. This tariff or buy back price is calculated considering the overall investments in the solar projects along with regulated return on the investment [13].

In addition to the above, costs in developed countries are falling more rapidly due to grid parity [95], while new markets for the solar industry are emerging and developing nations. Grid parity occurs when an alternative energy source can generate power at a Levelized Cost of Energy (LCoE) that is less than or equal to the price of power from the electricity grid. This reduction in cost is caused by policy and regulatory incentives, oversupply of installation components and advancements in technology. The world is increasingly recognising the potential of solar energy to provide sustainable energy and this is reflected in the growth in the number of targets and support policies enacted by governments. By 2015, 164 countries had renewable energy targets in place, with around 45 of them had targets specific to solar energy. Developing and emerging economies have led the expansion in policy targets and in the development of sustainable energy in recent years [26].

PV system costs in Africa

Just as the cost of components for solar systems has fallen across the world in general, Africa is no exception. As mentioned earlier, Africa is a continent with huge access to renewable resources and more and more of its countries are taking advantage of these less polluting forms of energy. The African continent can be said to already have several hydroelectric power generation infrastructures and are now turning their attention to PV systems. Thanks to this, since 2009 until 2015, the prices of solar panels on the continent had decreased by 80%. Motivated by this revolution in PV system prices, a study done by the International Renewable Energy Agency [96], in 2015, revealed some costs associated with the various types of PV system component installation, such as the following:

- Solar home system ($<$ 1 kW);
- Solar home system ($>$ 1 kW);
- Solar PV mini-grid ($>$ 50 kW);
- Utility-scale solar PV ($>$ 1 MW).

These installations were studied in both off-grid and on-grid, with and without batteries and for various sizes so as to be able to have a wider scope of comparison. For this thesis, it is the off-grid systems with batteries that are in focus. Therefore in Table 3.7, the various market values for the different components of a PV system are presented.

Types of installation	PV panels €/kW	Batteries €/kWh	Inverter €/kW	Charge controller €/kW	Soft costs €/kW	Other hardware €/kW
Solar home system ($<$ 1 kW)	1850	2250	-	580	1670	1670
Solar home system (1 kW to 5 kW)	1750	1670	183	850	1780	1590
Solar PV mini-grid (100 kW to 1 MW)	1300	750	500	-	1670	1450
Utility-scale solar PV ($>$ 1 MW)				2000		

Table 3.7: Every component market value for the African continent, 2015 - adapted from [96]

It is important to note that although the battery values for systems up to 10 kW are too high for any project in current times, this thesis will adopt the monetary value referring to the Solar PV mini-grid class

($>$ 50 kW). This is because since this report was made in 2015, both the prices of solar panels and battery prices have fallen exponentially, as can be seen in the examples of batteries used in [68] and [91], which are both $LiFePO_4$ type batteries, where they have a value of 307 €/kWh and 460 €/kWh, respectively.

From Table 3.7, the main values necessary to later deduce the investment/cost of the system are the values relative to the market price, in €/kW, of the panels, batteries and inverters. Regarding the soft costs and the price of other hardware, these will have a weight of 25% in relation to the sum of the investments in the three main components of the system. With this information, and using the system cost (C_{sys}) equation of [46], the investment in a system can be deduced by:

$$C_{sys} = \lambda \cdot C_{PV} + \psi \cdot C_{bat} + C_{other} \tag{3.4}$$

where C_{PV} is the capacity of the solar array (kW); C_{bat} is the battery pack capacity (kWh); λ is the unit cost of the solar array (€/kW); ψ is the unit cost of the battery pack (€/kWh) and C_{other} is the other total costs, except the solar array and battery and including the inverter, soft costs and other hardware. It can still be explained as follows:

$$C_{other} = \zeta \cdot Inv_{size} + 0,25 \cdot (\lambda \cdot C_{PV} + \psi \cdot C_{bat}) \tag{3.5}$$

with ζ being the inverter unit cost (€/kW); Inv_{size} being the inverter size, in kW and 0,25 refers to the 25% related to the soft costs and the price of other hardware.

3.3.3 Table of techno-economic values

Finally, and using all the information described above, it is possible to conclude the following values for the techno-economic characteristics of the photovoltaic system, presented in the Table 3.8, which will be later introduced to start the simulation.

Component	Variable	Value for simulation purposes	Unit
PV Panels	ρ_T	-0,46	%/°C
	T_{ref}	25	°C
	λ	1250	€/kW
Batteries	SOC_{ini}	50	%
	SOC_{min}	10	
	SOC_{max}	90	
	η_{CH}	95	
	η_{DISCH}	96	
	$N_{cycles\_100\%}$	2000	cycles
	ψ	400	€/kWh
Inverter	Inv_{size}	20	kW
	$LT_{inverter}$	10	years
	ζ	500	€/kW
Cables	η_{cables}	95	%
Project lifetime	LT	20	years
Maintenance fee	-	50	€/kW
Discount rate	r	6	%

Table 3.8: All techno-economic assumptions used for the system simulation

The discount rate (r), project lifetime (LT) and maintenance fee variables have not been described above as they are neither in the economics of the system nor in the technical part. Therefore, their values were based on several works on PV system sizing. The discount rate (r) is used in discounted cash flow analysis to calculate the present value of future cash flows. The discount rate reflects opportunity costs, inflation, and the risks that accompany the passage of time, and always has values around 6% to 8%. Here, the higher the perception of risk, the higher the discount rate and vice versa. For the project lifetime, given the fact that solar panels have a lifespan of 20 to 25 years [11], 20 years is the most common number to be used for this variable as [97] refereed in their work. The maintenance fee was the most difficult information to find, and not even in the report of the Agency is there any reference to anything related to this subject. Because of this, the value of 50€/kW used in [7] will be used, as it is a very similar context and system.

Chapter 4

Simulation - Physical components simulation and system sizing optimization process

This chapter will describe the sizing optimization method used for the simulation of the optimal size for the photovoltaic system and its tools, including the new indices, VOLL and the physical models of the components itself for a better accuracy of the data used for the optimization. Furthermore, a brief analysis of the structure of the algorithm made in MATLAB will be done, using the code itself and an informative flowchart.

4.1 System constitution and physical model

Stand-alone PV Systems (SAPVS), as shown in Figure 4.1, are the focus of this work and that is why it is necessary to dissect the way this system will be simulated in order to reach the desired optimization. A system simulation consists in solving the energy balance of the system and the change in the battery state of charge (SOC) for each time-step considered, usually an hour [7]. In addition, it will be assumed from the beginning that this community in question already had some forms of energy such as kerosene and diesel generators, so the focus can be only on the constitution of the PV system without mixing with other forms of energy production. However, whenever it is necessary to activate one of these secondary sources of energy (i.e. when the energy provided by the PV system cannot cover what is required by the location), the economic value will be added to the final value of the PV system, as will be described later in the optimization process.

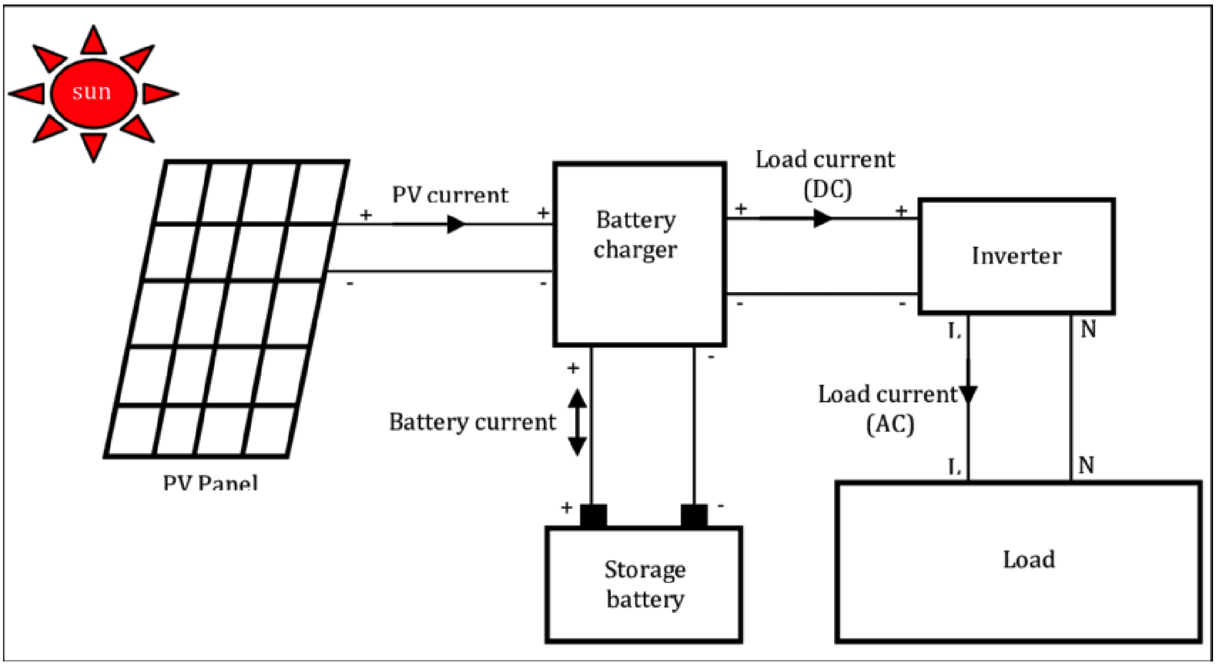

Figure 4.1: Stand-alone PV system general diagram - adapted from [98]

4.1.1 PV panels

The first step for the simulation of the system itself consists in the estimation of the PV energy output for each time-step of the simulation (t). The photovoltaic module presented in every solar energy system represents the fundamental power conversion unit. As stated above, a PV module typically comprises of a number of solar cells in series, that are a P-N junction semi-conductor acting as a DC current source. When photon energy comes on to the surface of the PV cell, they start agitating the electrons [99]. Thanks to its semi-conductor architecture, PV cells have a non-linear voltage-current (V-I) characteristic.

The performance of a PV module depends strongly on the irradiation that it is receiving. Standard sunlight conditions on a clear day are assumed to be 1000 W of solar energy per square meter and it is sometimes called "one sun" or a "peak sun". Less than one sun will reduce the current output of a PV module by a proportional amount [100]. Besides that, cell temperature (T_{cell}), is an important factor in determining the performance of PV cells, giving the fact that an increase in cell temperature is a decrease in voltage (0,085-0,123 V) and an increase in current (0,0026-0,0032 A), leading to the conclusion that an increase in 1 °C decreases PV module's power by 0,5 to 0,6% [101].

For modelling purposes, in many works one will find that solar cells current/voltage output relation can be calculated by [20]:

$$I = I_L - I_D = I_L - I_0[\exp(\frac{V + IR_s}{\alpha}) - 1] \tag{4.1}$$

Where:

- I_L = light current (A);

- I_0 = saturation current (A);
- V = output voltage (V);
- R_S = series resistance (Ω);
- α = thermal voltage timing completion factor (V).

But since the interest of this thesis is in solving the energy balance problem of the system, a mathematical model that considers not only the flow of energy generated by the PVs in kWh, but also includes the losses in cables and in all the equipment that is not responsible for energy conversion will be used in this work. This due to the fact that solar cell temperature affects the output power of a solar array significantly, the model also considers the effect of the temperature on a solar cell (T_{cell}). Assuming that the system will already have an MPPT included, one already knows that the panels will always work at the maximum operating point, so that they will always maintain their maximum production regardless of the variation in solar radiation. The following equation will output the results for each (t):

$$E_{PV}(t) = PV_{size} \cdot (1 - \rho_T \cdot (T_{cell}(t) - T_{ref})) \cdot H_\beta(t) \cdot \eta_{BOS} \tag{4.2}$$

where:

- $H_\beta(t)$ is the specific solar irradiation on tilted surface for the chosen instant;
- PV_{size} is the rated power of the panels under simulation at the irradiance of 1 kWh/m^2, an ambient temperature of 25 ºC and an air mass value of 1,5;
- ρ_T is the temperature coefficient of power respect to solar cell temperature provided by the manufacturer (usually 0,35÷0,45%/ºC);
- η_{BOS} is the balance of system efficiency which are all the losses not directly related to the sun energy conversion process;
- T_{ref} is the reference temperature at which the panels are usually tested, usually 25 ºC.
- and $T_{cell}(t)$ is the solar cell temperature in each time-step, which can be estimated by means of the following equation, presented in [70]:

$$T_{cell}(t) = T_{amb}(t) \cdot (1 + 1,25 \cdot H_\beta(t)) \tag{4.3}$$

where $T_{amb}(t)$ represents the average ambient temperature on the instant (t).

4.1.2 Batteries

The second step consists in estimating the amount of energy that flows through the battery and the change in the battery State of Charge. Batteries perform several important tasks such as reducing intermittence of the renewable resources, extending the electrical service hours to night time periods, and allowing the system to run for extended periods without any power generation. Some important aspects must be considered when sizing and choosing batteries for PV system projects, like: battery banks types, service life, autonomy days, input and output charge voltage, efficiency and deep cycle discharge. The life cycle, deep discharge and efficiency parameters depend of the load demand, model and type of battery as well as the temperature where the battery bank is operated [27]. Today, there are two main types of batteries for solar purposes: lithium-ion and lead-acid. Each type has its advantages and disadvantages, the main ones being represented in the Table 4.1.

	Lithium-ion	Lead-acid
Advantages	Longer lifespan (>4000 cycles) Higher efficiency (>96%) Constant power delivery	Costs less More reliable
Disadvantages	More expensive	Higher maintenance Low lifetime

Table 4.1: Main advantages and disadvantages between lithium-iron and lead-acid batteries

Due to the big price drops in the battery business, especially in those made of lithium-ion, there is now a strong focus on these types of batteries due to their great advantages. These batteries can be further divided into 4 different types of cell chemistries with their respective specific characteristics, which are: $LiMn_2O_4$/graphite cell chemistry, that uses low-cost materials that are naturally abundant; $LiNi_{1-X-Y2}Co_XAl_YO_2$/graphite cell, which has high specific energy and long life; $Li_4Ti_5O_{12}$ is used as the negative electrode material in Li-ion batteries with long life and good safety features and, finally, $LiFePO_4$/graphite (or carbon) cell chemistry that is a type of lithium battery that has the best number of cycles performance and best chemical and thermal stability. The union of these last conditions makes the $LiFePO_4$ battery the perfect candidate for this project, largely due to the fact that it has a long life without much maintenance. For this simulation, the batteries will work in such a way that when the difference between the panels' production and the energy demanded by the consumers (ΔE) is positive, the system will charge the batteries, but when this difference is negative it should always supply the consumers first, as will be the case during the night hours. The following equation will be used to find this difference:

$$\Delta E(t) = E_{PV}(t) - \frac{E_D(t)}{\eta_{inv}} \tag{4.4}$$

where $E_{PV}(t)$ and η_{inv} is the PV output production on instant (t) and inverter efficiency, respectively. Knowing these data it is now possible to calculate the energy that will pass through the batteries E_{Bat}, updating it with the value they have at the previous instant, as the following formula indicates:

$$E_{Bat}(t) = \begin{cases} E_{Bat}(t-1) + \Delta E(t) \cdot \eta_{CH} & \Delta E > 0 \\ E_{Bat}(t-1) + \frac{\Delta E(t)}{\eta_{DISCH}} & \Delta E < 0 \end{cases} \tag{4.5}$$

where $E_{Bat}(t-1)$ is the value of energy balance of the battery at the previous time instant, η_{CH} is the charge efficiency of the battery pack and η_{DISCH} is the discharge efficiency of the battery pack.

Here the first assumptions need to be made, due to the fact that it is already necessary to at least know what type of battery will be used in the project. This is due to the need to know the charge and discharge efficiency of the batteries and its minimum and maximum SOC levels. As stated above, the batteries on the rise in the market are the lithium-iron phosphate batteries ($LiFePO_4$), and these are the ones that will be used in the project, or at least the ones that are presumed to be best sized for the character of the load and the situation. These batteries have large charge cycles and can go up to 100% of its DOD, with the respective charging (η_{CH}) and discharge (η_{DISCH}) efficiencies presumably being above 90% and approximately 98%, respectively. After the power value in the batteries is updated, another important aspect to estimate will be the SOC of the battery (or the DOD depending on the project or situation for which one will use this value). The state of charge (SOC) is the level of charge of an electric battery relative to its capacity. The units of SOC are percentage points, in which 0% is equal to an empty battery and 100% refers to a fully charged battery. An alternative form of the same measure is the depth of discharge (DOD), the inverse of SOC ($DOD = 1 - SOC$), where the 100% is equivalent to a fully discharged battery and 0% is equivalent to a fully charged battery. SOC is normally used when discussing the current state of a battery in use, while DOD is most often seen when discussing the lifetime of the battery after repeated use. The SOC will be updated based on the following model:

$$SOC(t) = \begin{cases} SOC(t-1) + \frac{\Delta E_{Bat}(t)}{B_{size}} & \Delta E > 0 \\ SOC(t-1) - \frac{\Delta E_{Bat}(t)}{B_{size}} & \Delta E < 0 \end{cases} \tag{4.6}$$

The last point for calculating the battery specifications will be its lifetime. In literature, there are many methods for the simulation of the battery pack lifetime as it cannot be estimated directly since it depends mainly on the energy cycled by the batteries, with the most used being the one in the *rainflow* cycles counting method, based on Downing's algorithm [102] and the analytical methods as the one used in [103]. The first method is based on counting the charge/discharge cycles Z_i corresponding to each range of the Depth of Discharge, split in m intervals, for a year and for each of these intervals there is a number of Cycles to Failure (CF_i), which is provided by the battery manufacturer's datasheets, often in the form of a graph relating the DOD to the CF_i.

Often this type of information is not available and so approximations are necessary. These approximations can be made from generalized graphs, as shown in Figure 4.2, which are available to anyone, or through studies specific to the batteries that will be used in these situations. The problem with the latter process is that it can increase the budget of the system even more and delay its development, and using generalized graphs can lead to errors not in the short term but in the long term.

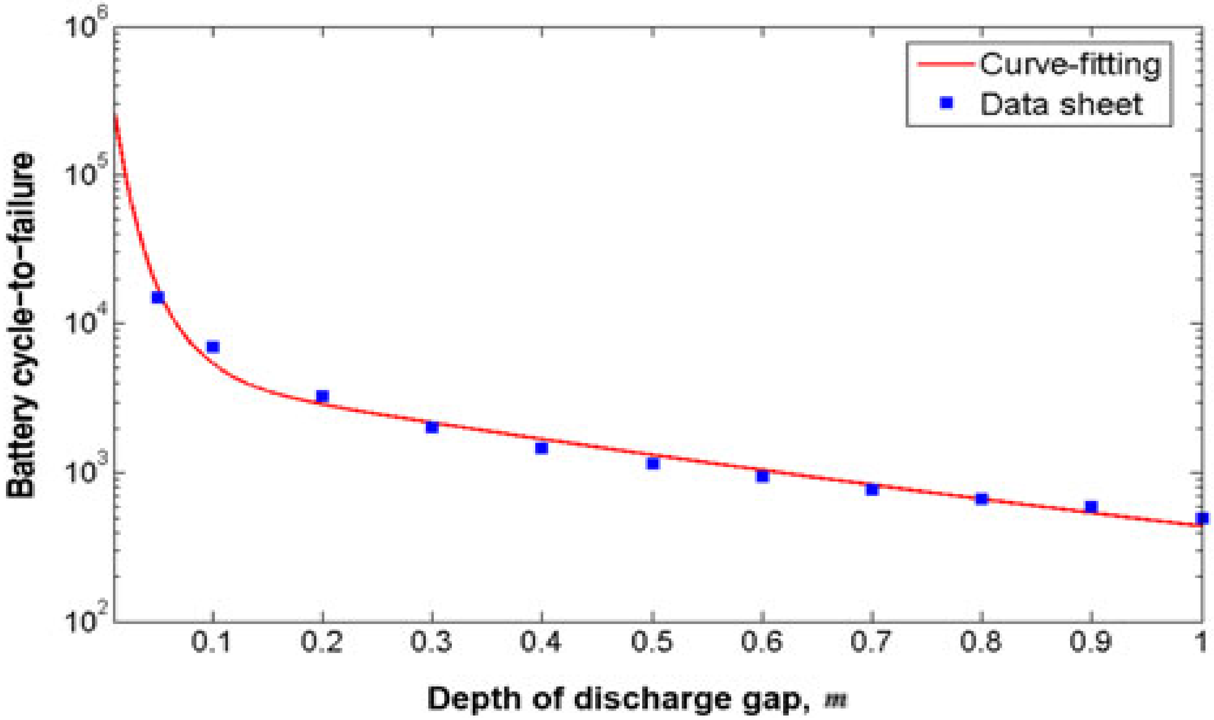

Figure 4.2: Cycles of Failure (CF_i) vs Depth of Discharge (DOD)

The second process, using analytical methods, is to model the life of the battery using a mathematical equation that can then be solved. These models take into account degradation, corrosion, effect of the temperature, and more and can be calculated as the energy that can be cycled during its life (capacity · number of equivalent full cycles) divided by the annual energy discharged from the battery:

$$Life_{Bat} = \frac{\text{Energy cycled during battery life}}{\text{Annual energy disch. from battery}} = \frac{C_{Bat} \cdot N_{cycles}}{\frac{E_{Bat\_year}}{\eta_{DISCH} \cdot \eta_{inv}}} \tag{4.7}$$

with N_{cycles} being the number of equivalent full cycles until battery failure. In some cases, battery manufacturers usually only show in their datasheets the information for the number of cycles the battery can perform at 80% depth of discharge (DOD), $N_{cycles\_80\%}$ or they only show the curve of number of cycles to failure versus the depth of discharge, $N_{cycles\_DOD\%}$ (usually from 20% to 80% DOD). In the first case, it will be calculated by equation (4.8) and in the second case by equation (4.9).

$$N_{cycles} = 0,8 \cdot N_{cycles\_80\%} \tag{4.8}$$

$$N_{cycles} = \frac{DOD}{100} \cdot N_{cycles\_DOD\%} \tag{4.9}$$

Management system

For good control and prevention of damage to the battery pack, it will be necessary to add a Battery Management System (BMS) to the design and simulation. This device will be responsible for protecting the battery pack, maximizing efficiency, controlling the temperature of the cells and cell operation since during the cell operation period there are situations where the battery can over-charge or even over-discharge, which exponentially affects the useful life of the batteries. For this there is a constant monitoring by the BMS, mainly, of the following indicators:

- The voltage of the total battery pack or of the individual cells;
- The current during the charge and discharge process;
- The average temperature of each cell and the pack;
- And finally, the SOC also of each battery and the total battery bank

Of these indicators the most important for this simulation will be the SOC, since this simulation is only working with raw energy values and not system voltages and currents. In addition, control by estimating the SOC is already a technique widely used by the various BMSs on the market. To simulate this type of control the following steps will be taken:

1. At the beginning of the algorithm, when the battery details are being entered, the initial SOC (SOC_{ini}) value should also be established (this value being related to initial pack balancing);
2. The SOC_{min} and SOC_{max}, battery state-of-charge minimum and maximum values, respectively, should also be entered according to the manufacturer's specifications (this will help with the lifetime of the batteries), which in the case of the newer $LiFePO_4$ ones, may have a SOC_{min} and SOC_{max} of 5% to 10% and 95% to 100% respectively, as the example found in [91];
3. The following condition needs to be set:

$$SOC_{min} \leq SOC(t) \leq SOC_{max} \tag{4.10}$$

   which means:

   - If at the instant following the initial (t) there is a discharge cycle, the BMS will let the batteries reach the SOC_{min} level. When this value is reached, the program will prevent any more power from being supplied through the batteries;
   - At the next (t) that there is a positive ΔE, the BMS will cause all this energy to be used to charge the batteries to the SOC_{max} level, stopping the charging cycle as soon as $SOC(t)$ equals SOC_{max};

In addition to this control through SOC, another condition will be placed on this simulation and that is employed in the methodology that was used as an example in this paper, which is the battery power to energy ratio ($(\frac{P}{E})_R$). What this threshold does is limit the amount of power flow that a battery pack can provide in an instant, i.e. if a battery pack has a B_{size} of 100 kWh and a ($(\frac{P}{E})_R$) of 0.5 then it means that the battery pack can only provide a maximum of 50 kW in an hour. In mathematical form the above condition is written as:

$$\Delta E \leq ((\frac{P}{E})_R) \cdot B_{size} \tag{4.11}$$

4.1.3 Inverter

Usually in the world, the loads at alternative current are used for homes and in order to convert DC to AC, an inverter becomes necessary. Currently, there are exclusive models for isolated systems which already have an integrated battery charger and controller. Depending on the AC voltage and power consumption, the voltage of the charger and the same voltage of the inverter vary from 12, 24 or 48 V. There are also inverters for isolated systems with voltages that exceed 48 V [27]. The inverter energetic performance is not constant and an important point to note here is that the energy performance of the inverter is never constant, since it is highly dependent on its output power [20]. Almost all inverters today come with devices already pre-installed that control the point of maximum power (MPPT). There are two types of inverters available in market i.e. thyristor based line-commutated inverter and IGBT or MOSFET based self-commuted inverter. The self-comuted inverter is prominent for grid connected PV systems as it regulate power factor, reduce harmonics distortion and maintain quality of AC waveform [35]. Throughout the years, power electronics converters have been modeled according to their efficiency as a function of the input normalized power, where losses are assumed to be a quadratic function. In this case, the performance model used is an polynomial function carried out from a quadratic interpolation of an experimental curve generated at the INES - Institute of Energy Systems Technology [92]:

$$\eta_{inv}(t) = 1 - \frac{1}{\varphi_{inv}(t)} \cdot (0,0094 + 0,043 \cdot \varphi_{inv}(t) + 0.04 \cdot \varphi_{inv}(t)^2) \tag{4.12}$$

where

$$\varphi_{inv}(t) = \frac{P_{in}(t)}{P_{rated\_conv}} \tag{4.13}$$

with $P_{in}(t)$ being the input power in instant (t) and P_{rated_conv} the inverter output rated power. The output rated is chosen according to the peak load values that will need to be supplied at certain times.

4.2 Value of Lost Load

4.2.1 Definition and assumptions

In the literature there are various meanings for what the VOLL is, from [104] mentioning that it may be the value of unserved energy to [105] where they argue that it is an average of what consumers are willing to pay to avoid without running out of their primary source of electricity. At the end of the day, it ends up being a monetary expression for the costs associated with interrupting power supply [7]. This index or value ended up being created due to certain innovations that needed to be made in the context of sizing photovoltaic projects and from their studies some conclusions were drawn, namely:

- that this method arose in the context of countries of, where the electrical systems presentation was at its peak technology;
- that it comes from the need of analysing the security of the system, which needs a source that is always available;
- it is directly linked to the local energy market and its characteristics;
- its estimated value is directly proportional to the causes and consequences of the supply interruption;
- and there are several ways to calculate this value, from proxy methods to case studies [105].

Despite these benefits, looking at them closely one can see that they do not really relate to the off-grid, isolated site situation on which this case study is based. On the other hand, this is exactly what the researchers of [7] had in mind when creating this new methodology, with the modifications made to NPC and LCoE through VOLL. First of all, two primary assumptions were made by these scientists which have also already been used in this paper, which are:

- when there is a break in the supply of power generated by the solar system, consumers will always revert to more traditional forms of energy;
- and, that the VOLL will be associated with the inherent costs of this outage, and will count for the use of traditional energy systems.

In order to estimate the total value of VOLL in relation to the off-grid and sustainable energy context, five steps were proposed:

1. estimating the daily consumption associated with each application on the grid and of its respective consumer class so that it can then be calculated its value in case of loss of load;
2. identify the most traditional forms of energy to replace electrical applications, such as the kerosene lamps that will replace the normal ones, the portable battery chargers or the trip to the kiosk in case of electricity shortage to charge the mobile phone and the diesel generator for the rest;
3. for each traditional energy, calculate its respective value in VOLL [€$/kWh/_{LL}$]], considering that for:
   (a) the case of the generator, the VOLL can be estimated as follows:

$$VOLL_{diesel} = \frac{c_{diesel}}{\eta_{gen} \cdot LHV \cdot \upsilon} \tag{4.14}$$

   where c_{diesel} [€$/lit$] is the local cost of diesel, η_{gen} is the efficiency of the generator, LHV $[kWh/kg]$ is diesel low heating value, and υ is the diesel specific volume $[kg/lit]$. Furthermore, a modification to this equation was made in order to compensate for the strong noise, bad odor and nuisance that diesel generators, especially the older ones used in these areas, can generate to the local population. Therefore, the variable V_{noise} is created and will represent 25% of the $VOLL_{diesel}$, a value that later is added to the equation as a compensation mode. The final equation for $VOLL_{diesel}$ is the following:

$$VOLL_{diesel_1} = \frac{c_{diesel}}{\eta_{gen} \cdot LHV \cdot \upsilon} + V_{noise} \tag{4.15}$$

with V_{noise} being:

$$V_{noise} = 0,25 \cdot (\frac{c_{diesel}}{\eta_{gen} \cdot LHV \cdot \upsilon}) \tag{4.16}$$

(b) for lightning purposes, an equivalence between electricity and traditional systems in terms of time the light is needed its done by means of $[h/kWh_{LL}]$:

$$h_{light,LL} = \frac{1}{P_{el\_light}} \tag{4.17}$$

which relates the associated hours of light related with 1 kWh$_{LL}$, with P_{el_light} being the reference rate power of electric lights or the average power rate available if more than one light is available, resulting on the $VOLL_{ker\_lamp}$ being calculated by:

$$VOLL_{ker\_lamp} = c_{ker\_lamp} \cdot h_{light,LL} \tag{4.18}$$

where c_{ker_lamp}[€$/h$ is the cost related to the consumed kerosene during one hour of lamp functioning and can be computed by means of average data among households.

(c) For the final case, the VOLL related with the mobile charging at the markets or with portable charging devices is given by:

$$VOLL_{mobile} = \frac{c_{recharge\_mobile}}{C_{B,mobile} \cdot V_{B,mobile}} \tag{4.19}$$

where $C_{B,mobile}$ is the battery capacity, $V_{B,mobile}$ the charging voltage and $c_{recharge\_mobile}$ the price of charging service.

4. For people with different traditional forms of energy, a VOLL will be required for each of these classes ($VOLL_{class}$);

5. finally, the total VOLL ($VOLL_{total}$) will be calculated by adding up the weighted $VOLL_{class}$ values.

4.2.2 Estimation of values

To calculate the VOLL values, as already mentioned, it will be considered that there were already people with diesel generators and, in spite of this, there are still people using more traditional means like coal and kerosene, in order to reduce the consumption costs. Therefore, to calculate the total VOLL it will be necessary to estimate the percentage of users that still use these more traditional fuels, the value that these fuels will add to the final VOLL value and also to add the part of the cost of consumers with diesel generators. For these calculations and looking at the formulas presented above, there is some information that will need to be assumed or found. All this techno-economic information related to the project can be found in Table 4.2.

Techo-economic data for VOLL computation

Diesel generator efficiency	n_{diesel}	35	%
Diesel Low Heating Value	LHV	11,83	kWh/kg
Diesel specific volume	υ	0,846	kg/l
Diesel cost	c_{diesel}	135	Kz/l
Mobile battery capacity	C_{B_mobile}	2000	mAh
Mobile battery voltage	V_{B_mobile}	5	V
Recharging phone cost	c_{rech_mobile}	50	Kz/charge
Kerosene cost	-	123	Kz/l
Household lighting expenditure in kerosene/month	-	4920	Kz/month
Household lighting expenditure in kerosene/hour	c_{ker_lamp}	6,61	Kz/hour
Minimum salary	-	21454,10	Kz/month
Kz-€ Exchange	-	743,84	Kz/€

Table 4.2: Tecno-ecnomic data for VOLL estimation

The diesel data is widely spread on the internet and can be easily accessed, for example, by the following reference [106]. The generator efficiency is bought between the original article of this methodology and the thesis of Wheeler and Southward. In terms of information regarding kerosene, its price was taken [108], from the government's energy section reorganisation plan (see 2.1.3) and its consumption per dwelling was estimated using the values from the article of this methodology. Finally, for the VOLL regarding charging mobile phones by portable batteries or at kiosks, the averages that were used for mobile phone voltage (V_{mobile}) are the same as in the original article, since the characteristics of this one have not changed and only an update of the battery capacity of mobile phones (c_{mobile}) was done. The cost price per charge ($c_{recharge\_mobile}$) was also lowered a little to give contrast to the difference of electricity price between Angola and Uganda (place where Mandelli et al. study was done).

Knowing the information in the table above, the equations 4.14 to 4.19 and the information contained in the table 3.4 regarding the various values of the user loads, one may already be able to conclude the results regarding $VOLL_{diesel}$, $VOLL_{ker\_lamp}$ and $VOLL_{mobile}$, as presented in the table 4.3.

Resulting VOLL values

$VOLL_{diesel}$	0,065	
$VOLL_{ker\_lamp}$	0,148	€$/kWh_{LL}$
$VOLL_{mobile}$	6,722	

Table 4.3: Estimated values of VOLL for the different classes

To calculate the VOLL of the various household classes, first it is necessary to have an idea of which ones use a mix of electricity and which ones use only diesel generators, before the installation of the photovoltaic system. Here, it will be assumed that class *Family_1* and *Family_2* are using the generator only when possible for food preservation, rechargeable batteries or kiosk charging for cell phones, and kerosene lamps for lighting. In other words, if one calculates the weight that these various energy applications have in the total load of *Family_1* class of users, one can get a value of 97% for lighting and 3% for the mobile phones. For *Family_2* the results are 70% for lighting, 1% for charging mobile phones, 24% for the refrigerator and 5% for the television. With these weights the VOLL referring to *Family_1* and *Family_2* are, respectively:

$$VOLL_{family\_1} = 0,97 \cdot VOLL_{ker\_lamp} + 0,03 \cdot VOLL_{mobile} = 0,326€/kWh \quad (4.20)$$

$$\begin{aligned} &VOLL_{family\_2} = \\ &0,70 \cdot VOLL_{ker\_lamp} + 0,01 \cdot VOLL_{mobile} + (0,24 + 0,05) \cdot VOLL_{diesel} \\ &= 0,209€/kWh \end{aligned} \quad (4.21)$$

Knowing now the results of the families where there is still more than one energy source, one can calculate the weights of these two families and the remaining families and businesses to the total load, since they only use generators,one can calculate their total weight. Looking at the Table 3.4 it can calculated that the *Family_1* and *Family_2* have a weight, respectively, of 15,4% and 15,1% of the total daily load, and that the remaining classes have a weight of 69,5%. These values will cause the result of $VOLL_{Total}$ to be as given by the following equation:

$$\begin{aligned} &VOLL_{Total} = \\ &0,108 \cdot VOLL_{Family\_1} + 0,159 \cdot VOLL_{Family\_2} + 0,733 \cdot VOLL_{diesel} \\ &= 0,116€/kWh_{LL} \end{aligned} \quad (4.22)$$

4.3 Sizing optimization methodology and context

As mentioned at the beginning of this thesis, the main objective of this simulation is to arrive at a size of panels and batteries that is completely thought out and designed according not only to the needs of the population where this system will be installed, but also to the climatic conditions of this same location. This system should be completely autonomous, only requiring maintenance when necessary, according to the manufacturers' information, and should supply enough energy for the size of the community load already analyzed in section 3.2.

For this to be possible, a thorough analysis of the power reliability and cost of the system must be done, using their respective indices for this purpose. This is where the real importance of the LPSP comes in, since it is one of the primary input data in system sizing simulations and it's necessary to put a limit on the load that is not supplied and that can be tolerated by the consumers. Unfortunately, due to the fact that this thesis is studying an isolated site, with no previous information, there is no possibility of already having a notion of this value, contrary to what would happen in more developed countries, since people would already have other experience with electrical applications and electricity. With this knowledge, it is then possible to define the target LPSP and create the conditions to achieve it.

Like some isolated places of Huambo, the locals and the PV system designers themselves have no reference for the reliability of the system that they will set up, so much so that the concept of Lost of Load can even reach the point of being insignificant in this situation. This happens because people in these places have no connection to the grid, and therefore their experience with electricity and other applications becomes a barrier to the creation of the tolerance of the loss of load provided. In addition, people who have access to electricity through traditional sources or through diesel generators end up using these energy sources only in case of extreme necessity and not for their daily lives [44, 46].

Several researchers have tried to study other ways to reach this Lost of Load target, and one of them would be through the analysis of consumer loads, something that was already done in [16] and that will be used as one of the criteria in the optimization process of the simulation of this thesis. However, some more criteria were created as a way to change the way of predicting these values for isolated sites, like the methodology that is used in this work, making use of two modifications [7] to the already known indicators of system cost, namely (2.5) and (2.6). These modifications were made, mainly, due to the following three conditions:

- Both the process and the results should be directly linked to the local context, making the conditions and assumptions for the design cannot be defined externally;
- Being an off-grid system, priority will be given to more reliable systems over less reliable ones, thus putting much emphasis on LPSP;
- and finally, the cost of electricity should be as low as possible, much due to the impoverished population of these locations.

To achieve the first two points, it was proposed to change the traditional NPC formula so that it now includes an economic value referring to the energy that was not supplied. Knowing that previously these people already possessed more primitive forms of electricity generation, it will always be assumed that when there is a lack/breakdown of the energy supply generated by the solar system, these people will always return to these more traditional forms of energy (portable batteries, kerosene lamps and diesel generators) in order to satisfy their basic energy needs, so that in the end there is a symbolic value for the loss of load, which is expressed by the indicator Value of Lost Load (VOLL). Therefore, the new equation referring to the Net Present Cost (NPC) of the system will be:

$$NPC^{*} = \sum_{y=1}^{LT} \frac{Inv(y) + O\&M(y) + \sum_{t=1}^{T} LPS(t) \cdot VOLL}{(1+r)^{y}} \tag{4.23}$$

where $LPS(t)$ is the Lost of Power Supply in instant (t) and VOLL the total value of Lost Load. With this amendment, this definition contributes to favor the most reliable systems because it internalizes into the NPC a cost associated with the Loss of Load which contributes with higher values for less reliable and cheaper systems, and with smaller values for more reliable and more expensive systems. With this change and knowing that the LCoE comes from the NPC by the equation 2.7 it is possible to rewrite equation 2.6, now taking the name of *Levelized Cost of Supply and Lost Energy* (LCoSLE) as follows:

$$LCoSLE = f(PV_{size}, B_{size}) = \frac{r \cdot (1+r)^{LT}}{(1+r)^{LT} - 1} \cdot \frac{NPC^{*}}{E(y)} \tag{4.24}$$

Using the convenient LCoE value, it may be possible to compare the cost of various technologies over their economic period. Furthermore, since the Angolan energy market is almost entirely monopolistic, this index becomes even more important here, as it is referenced in [1] and is a perfect way to analyse systems in isolated markets with little information, thus becoming a benchmark for the cost of electricity that can be paid by the community. As the new LCoSLE already incorporates all the system information, including load demand, climate values, physical model characteristics and VOLL, it can be used to arrive at the identification of the perfect size of solar panels (in KW) and batteries (in kWh), mainly because:

- it is based on the estimation of the VOLL, which is directly linked to the local context;
- it does not require LPSP to be a primary input value, so that the optimization does not suffer from the disadvantages mentioned above;
- it identifies the optimal system as soon as VOLL is set;
- and finally, it identifies an optimal system completely designed for local conditions.

This identification is reached by minimising the LCoSLE value of all simulated systems. By minimizing these values it is possible, not only to conclude an optimal panel and battery size, as described above, but also this value will lead to an optimal NPC* and an optimal LPSP, thus making its input problem non-existent and making this variable just another output of the system optimization process.

4.3.1 MATLAB algorithm exemplification

In order to arrive at the optimal system, a MATLAB algorithm was built based on the equations used by [7] and [47]. This algorithm, as can be seen in Figure 4.4, is started in three main input blocks: the first block receives the geographic location and respective climatic data of the site; the second block is composed by receiving the hourly value of the local consumers' loads and respective pre-assessment of the Value of Lost Load (VOLL); and finally, the third block is composed by inputting the physical system and all the techno-economic data of the solar panels and batteries, which could possibly be used in the installation of the system, for the calculation of the solar energy production and storage used in the optimization process. From this data, only the information regarding the local irradiance and temperature levels have a procedure before entering the first phase of the optimization, this being the process of estimating the hourly values from the daily values, using the models mentioned in Subsection 2.4.3. All the steps described above and their respective data used can be found in Chapter 3.

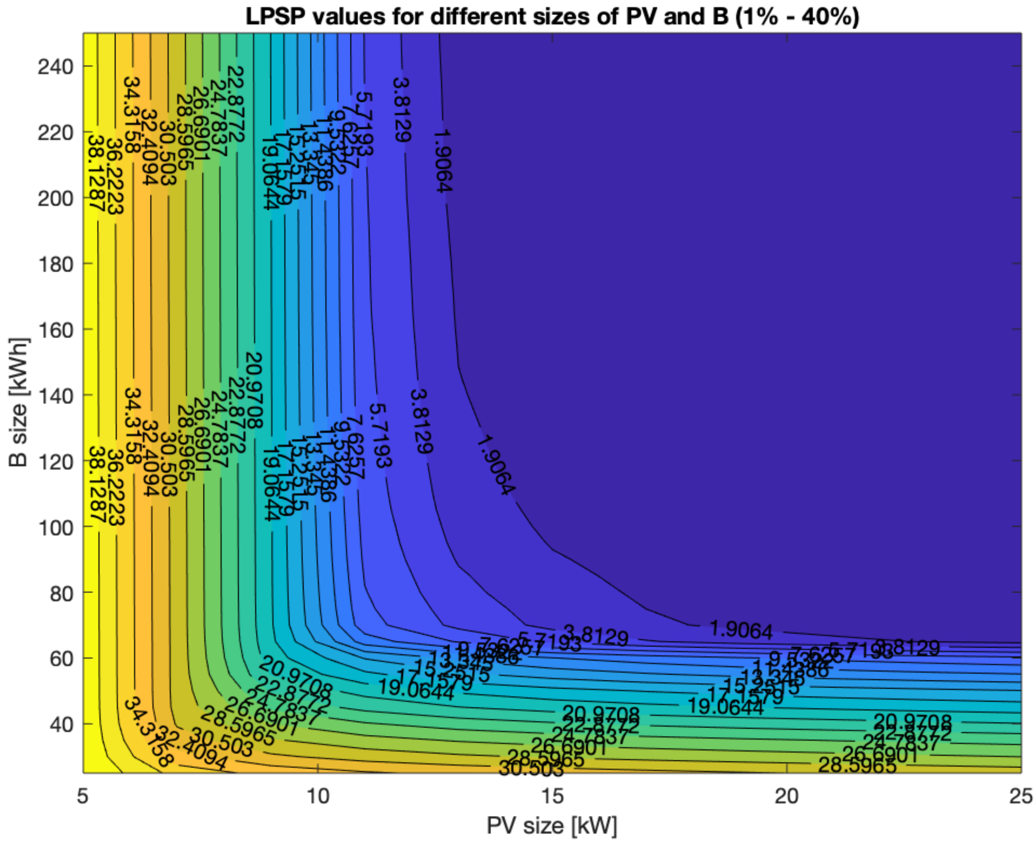

Figure 4.3: LPSP values for different sizes of PV and B (1% - 40%)

Following the input data entry it will be necessary to limit a window size for both the solar panels and the battery bank. The values chosen for this simulation for the PVs were from 20 KW to 50 kW with a step of 0,3 kW and for the batteries from 125 kWh to 250 kWh with a step of 0,5 kWh. This window was chosen based on a first simulation, with a larger window where it was observed that it would not be necessary to have such large values, as it would make the LPSP (now an optimization output) too large (see Figure 4.3), thus making the amount of energy lost and not supplied too great. In order to try to get the system to converge to a value between 1% and 20% of LPSP, the window was then set to the values above.

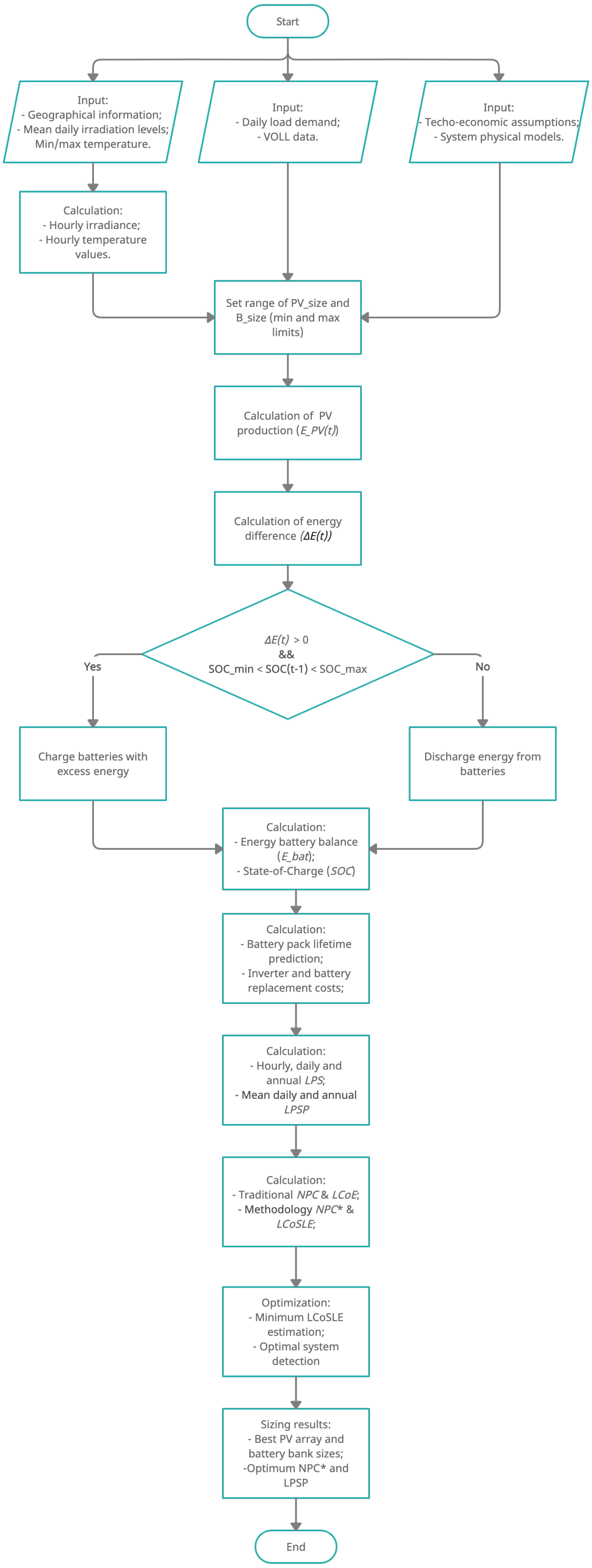

Figure 4.4: MATLAB algorithm process flowchart

With the simulation window chosen, the first part of the optimization process and search for the optimal system can begin, with the calculation of the solar energy production for each value of the PV and battery size window chosen above, using the equation 4.2. This value will be needed in order to understand the production capacity of the PV under the referenced weather and load conditions, and will then be used to calculate how much the batteries will be charged or how much will need to be discharged from the batteries to compensate for the lack of solar energy production. This value comes from the energy difference (ΔE - see equation 4.4), which is part of a new process, which is between the energy produced and the energy demanded by the consumers, where, if this difference is positive ($\Delta E > 0$) then the production of solar energy can supply the consumers in its totality and the rest of the production is used to charge the batteries, and when this difference is negative ($\Delta E < 0$) then it means that the production cannot satisfy the demand of the load and therefore it will be necessary to discharge this energy from the batteries, if possible. This possibility is referred to because the batteries will have a BMS or Battery Management System that controls the charging and discharging of the batteries, that is, although the difference can be positive at a certain instant (t), the batteries may not be charged, since they are already at the maximum SOC limit (SOC_{max}) required by the manufacturers to control the life cycles of the battery. This situation can also occur, although in an inverse way, at night, since it may be necessary to supply energy to consumers due to the lack of photovoltaic energy production and the batteries can no longer supply it since they are at their minimum SOC limit (SOC_{min}). The SOC value used for this control is calculated in the same step as the batteries' energy value, using the equations 4.5 and 4.6 for the batteries' energy and their State-of-Charge, respectively. To finish the first part of the optimization process, which is the simulation of the physical components of the system, it is necessary to calculate how many battery and inverter replacements will be needed. For the inverters, this information is something entered in the first part of the program, so it will only be necessary to predict the useful life of the batteries. For this, the equation 4.7 is used, which estimates the forecast in years of battery life according to its capacity, cycles and energy discharged over 1 year. With this value the amount of battery replacements can already be calculated and a list of the years in which these replacements will be needed will be created.

Knowing the values for production, consumption and energy storage for the various simulated systems, the first part of the optimization is closed and the system can now be economically evaluated. For this, the next process is to calculate the system's lost and undelivered energy (LPS) and its respective percentage relative to the demanded load (LPSP). This value represents all the energy that was demanded by the consumers at instant (t) and could not be supplied due to lack of production or energy in storage. For the calculation of these values, both the equation 2.1 and 2.3 could be used, and the second one was chosen for its better results. The second part of the economic evaluation of the systems, is now to calculate the values referring to the traditional NPC and LCoE and referring to the NPC* and LCoSLE of the new methodology. The values of both methodologies will be calculated in order to have a more detailed comparison, with the necessary equations for the traditional method being found in Section 2.3.2, while for the method based on the methodology under study, they can be found in Section 4.3.

With all the information calculated above, it is finally possible to take the last and most important step in the search for the optimal system: the minimization of the LCoSLE value. With this procedure, it is possible to arrive at a single value for which the system is optimal for the load and climatic conditions introduced. Furthermore, by knowing this value, one automatically knows what size PVs are needed and what storage capacity is required for the batteries. In addition, as already stated above, here the LPSP comes out as an output making this value the optimum for the lowest price of electricity (LCoSLE). All the steps described above can also be followed through the flowchart created for this purpose (see Figure 4.4), with the results presented in the next chapter.

Chapter 5

Simulation - Results, observations and discussion

This chapter will present all the technical, economic and social results of the simulation of the optimal system for Huambo and its specific characteristics, described in the previous chapters. In addition, an analysis of the graphs referring to the economic values will be made, relating these values to the economic capacities of the consumers and to the characteristics of the system itself.

5.1 Technical evaluation of the system

In order to arrive at the optimal system, it is necessary to analyze very well every technical part of the production and storage of the system. The first result to analyse is Figure 5.1, which presents the total daily energy produced by the solar panels during one of the 20 years of the project's life time. In order to help the analysis of the next graphics, of the 365 days used to simulate the 20 years of the project, 3 samples of days will be made, which will be divided into two groups of 120 days (approximately 4 months) for the first 240 days and 125 days for the last days of the year, thus dividing the year into 3 quarters. The first and third quarters comprise the days of the rainy season, while the second quarters comprises the Angolan dry season or Angolan winter.

Using the first image of Figure 3.3 as a comparison, it can be observed that it is during the dry season (Angolan winter) that the production of solar energy is more concrete and stable, despite presenting lower values than the rest of the year. It is in this quarter that the production per day shows the highest average, this value being 170 kW per day. In the other two quarters, comprising the rainy season, the inconsistency in production is greater, averaging 138,4 kW and 144 kW per day for the first and third quarters of the year, respectively. Nevertheless, it is in the winter season that it presents the best average production values, due to its stable production and it can also be observed that the daily production value is also lower than many of the good production days of the other two quarters. This is due to the fact that this is the time of year when the days have fewer hours of sunshine.

Although the production can be higher than during the dry season, the inconsistencies in production can lead to little energy being stored in the batteries, leading to loss of power and supply problems later on. Despite this, with the average values taken from the figure and using these values and comparing them to those in Chapter 3, one can conclude that on average, this value is able to cover the 136 kWh per day of the consumers and the 49,85 MW annually. In addition, there are two other ways in which the solar system can be made more efficient in the first and third quarters of the year. Firstly, one could manually change the optimal angle of the panels (β_{opt}) at the different times of the year so that the efficiency in receiving the solar irradiance is higher, since in this project this value is fixed at 21,88° for the whole year. Still, the best way would be to have the panels automated so that their optimal angle is updated every day without the need for human intervention. Unfortunately, any of these ways would be too costly, so they were not used.

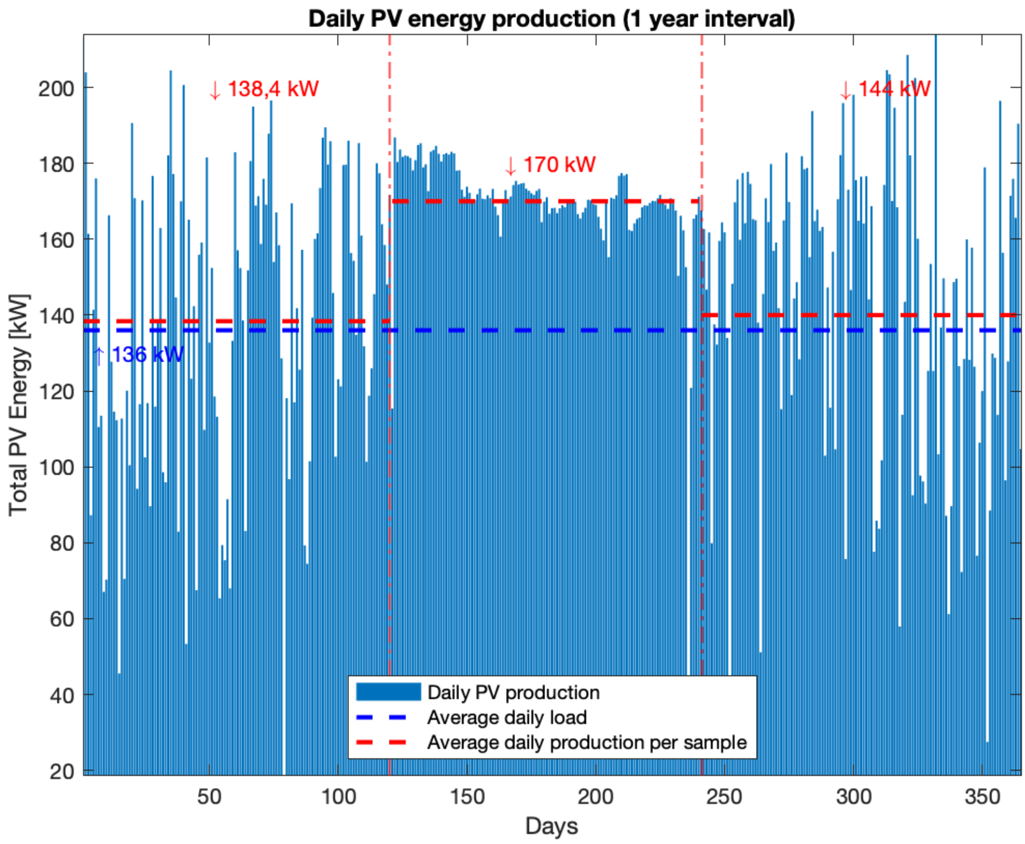

Figure 5.1: Simulation result for the total daily PV production (1 year time interval)

Although the average values seem to cover the daily load, this generally does not happen. On the rainy season, the irradiance levels are not high enough for the solar system to produce enough energy for consumers. This is where the battery system has its main function: to store the energy produced during the day that has not been used, so that it can be used in hours without sun or in days with bad weather conditions. For charging the batteries, the difference between production and consumption will be used, as already discussed in Chapter 3. The profile of the difference between the energy generated and consumed can be observed in Figure 5.2, where it can be seen in fact that there are days when consumption far exceeds production. Here, using the same system of dividing the days of the year used to analyze the graph above, one can confirm what has already been referenced. That is, even though the average production of electricity through solar panels in the three quarters is above the average load consumption of the location, due to the large inconsistencies in production, in the first and third quarters of the year there will be a large deficit between production and demand. This average deficit will present a value of -13,8 kW for the first four months of the year and -7,8 kW for the last four months. Due to the extremely stable production in the second four months of the year, the difference between production and consumption already shows a positive value of 18,1 kW, meaning that at this time of the year, the production of energy through the panels is completely secure and therefore storage will be possible.

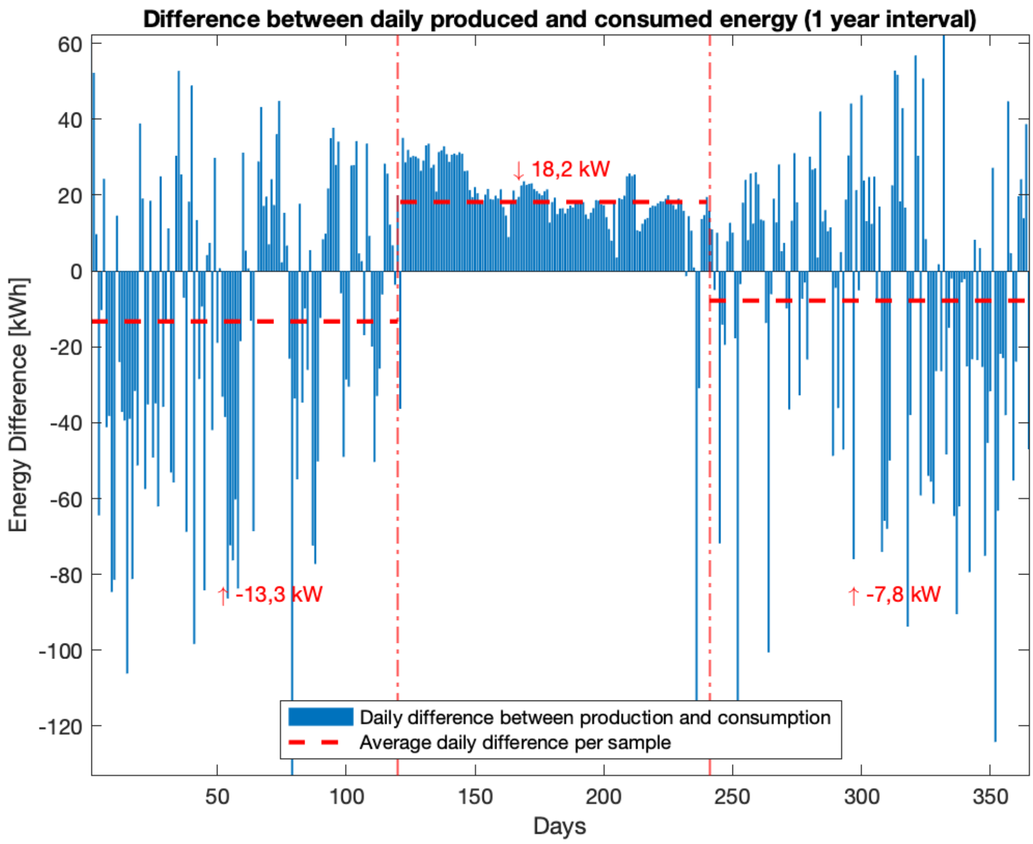

Figure 5.2: Simulation result for the difference between produced energy and consumed in 1 year time period

Since this work is using a fixed daily load, the main reason for the inconsistencies in production is only due to the irradiance levels presented on those days. Seeing this difference, one can immediately conclude that this will have a tremendous impact on the charge of the batteries, something that can be confirmed by Figure 5.3, which shows the charge level (SOC level) of the batteries at midnight each day in one year interval. It can be observed that at the beginning of the year, towards the end and on the days with the worst irradiance, the batteries already arrive at night at their minimum charge level almost every day. This minimum level was fixed when it was introduced in the simulation that the SOC_{min} would be 10% of the total SOC of the battery, in order to save more in the useful time of the batteries.

Using the same sample days used to analyze Figure 5.1, it can be noted that in the first 120 days of the year, in the first part of inconsistency in production, the batteries finish these days with 17% of their capacity or less, making only 7% of their capacity available to be able to supply consumers in times of lack of production of solar energy. Now doing some calculations, the energy expenses from midnight to 6h are about 22,2 kWh and 7% of the capacity of the batteries equals 11,5 kWh, which means that most days during this season there will not be enough solar energy stored to satisfy the basic needs of consumers at night. At this time of the year, in order for there to be no power outages and for there to be no return to other more traditional forms of energy, the batteries would have to reach midnight with an average value of 23,7% (38,5 kWh) on most days so that the power shortage at night would not be so great. With this value, the 16,25 kWh of minimum battery energy level and the 22,2 kWh of energy supplied to the load would be completely safe. Nevertheless, in this first quarter, only on 18% of these days do the batteries reach midnight with more than 23,7% of charge.

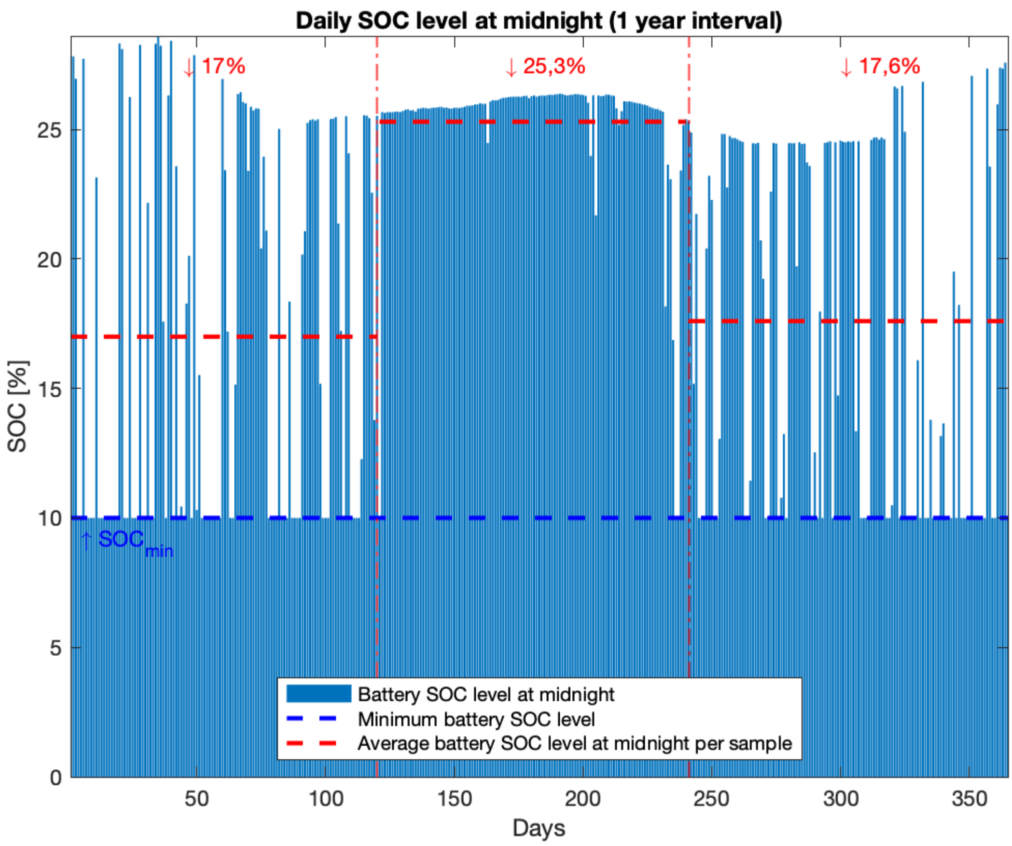

Figure 5.3: Simulation result for the battery levels at midnight in 1 year time period

In the last 125 days of the year, the situation is very similar with the average SOC being around 17,6%

those days, and using the data from the first quarter, one can see that most of these days, again, the solar production and respective energy storage will not be sufficient to meet the demand. Furthermore, the average load needed in this season would be the same 23,7%, since the daily load does not change, making a 6,1% energy deficit, with batteries having their minimum charge at midnight on only 24% of the days.

As for the second quarter of the year, which in this case is equivalent to the Angolan winter, although some absolute values of irradiances are lower than in the other two quarters of the year, here the production presents a greater consistency, making the batteries reach midnight with an average charge level of 25,3%. With this value, the 23,7% minimum load is completely safe, still leaving some energy in reserve. Moreover, only on 10% of winter days do the batteries reach midnight with the level below 23,7%. Knowing that from 6 in the morning there will always be electrical production, it means that the consumption for the winter season in Angola is basically autonomous. As a way to confirm this, if one calculates the average LPSP of this quarter, ones reaches a very low value of 1,12%, corresponding to that only 183,6 kW of the total energy needed in this season was not supplied, which corresponds to less than one and half day, approximately, of consumption in a 120 day sample. On the other hand, by way of contrast in the first quarter the LPSP takes a value of 16,72% and 13,31% for the third quarter.

In order for the batteries to be able to charge to a level that would always provide uninterrupted power for several days, the size of the batteries and solar panels would need to be much more oversized for this project. This is because, in order to be able to cover the days of high inconsistency in production, it would be necessary to have a system with a LPSP value very close or even equal to 0. But for this to happen, the purpose of this thesis would not be achieved, and for this very reason the VOLL methodology is used here. This is because from the beginning there was a notion that a system for the social and economic conditions required could never have such a low LPSP or survive with just the solar panel system, since the goal is for consumers to always have some kind of energy supply, either from PV systems or from more traditional energy sources, and that all these associated costs are already included in the final price of electricity in order to simplify people's lives. The purpose of this thesis is to show which system is the most reliable and at the same time which system is the cheapest for people's economic conditions, which in this case would never have an LPSP of 0. In this case, there has to be a management of the solar system with the diesel generation system and other forms of energy, so that there is never a shortage of electricity. Although, as was analyzed in the paragraph above, the shortages that there will be during the year due to insufficient battery capacity, one has to keep in mind that people need energy for their lives, so even if there is no stored energy, they will find another way to sustain themselves energetically. Looking at Figure 5.4 and using the quarter days, as done above, one can observe that in the first period the daily level of the batteries present an average level of 58,3 kW, in the second quarter an average of 76,2 kW and 62,1 kW in the last quarter, thus reinforcing the idea that it is in the Angolan winter that production can be more stable.

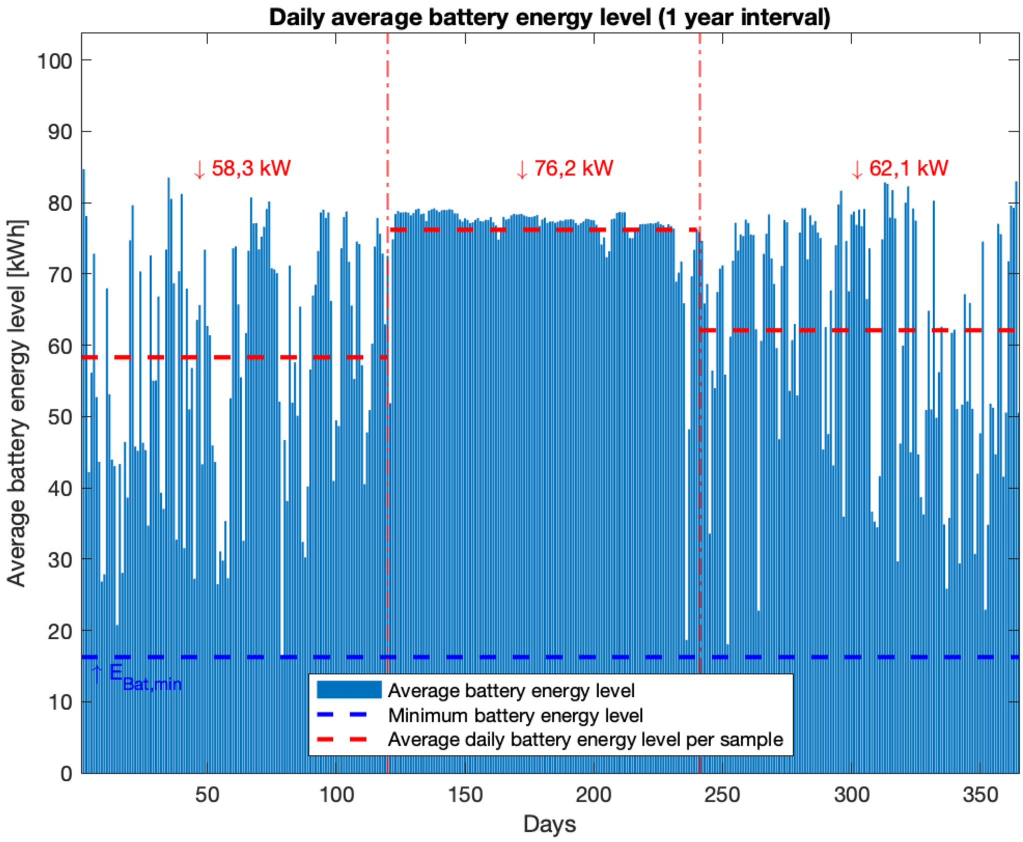

Figure 5.4: Simulation result for the difference between produced energy and consumed in 1 year time period

Additionally, one can observe, using Figure 5.4, that despite the rainy days presenting less irradiance, the system throughout the year manages to maintain a level of batteries well above the minimum limit, ending up having a value close only on the days that the daily irradiance reaches levels below 2000 W/m^2. It was very much because of this that $LiFePO_4$ batteries were chosen for this project, as it was seen in the very first simulations that this project would bring very high cyclic wear to the batteries. With this in mind, in the first simulations made with lead-acid batteries, it was observed that these would only have 3/4 years of life in this project, making a total of 5 or 6 replacements required in the 20 year life of the PV system. With all these replacements, the cost would increase significantly which led to the use of $LiFePO_4$, since its capacity and its life cycle can be more than double that of the lead-acid batteries and its price has been decreasing for years [109]. With these lithium batteries it is possible to increase the useful life of the batteries to 7 years, as can be seen in Figure 5.5, thus making it necessary to replace the batteries only twice in the 20 years of the project's useful life.

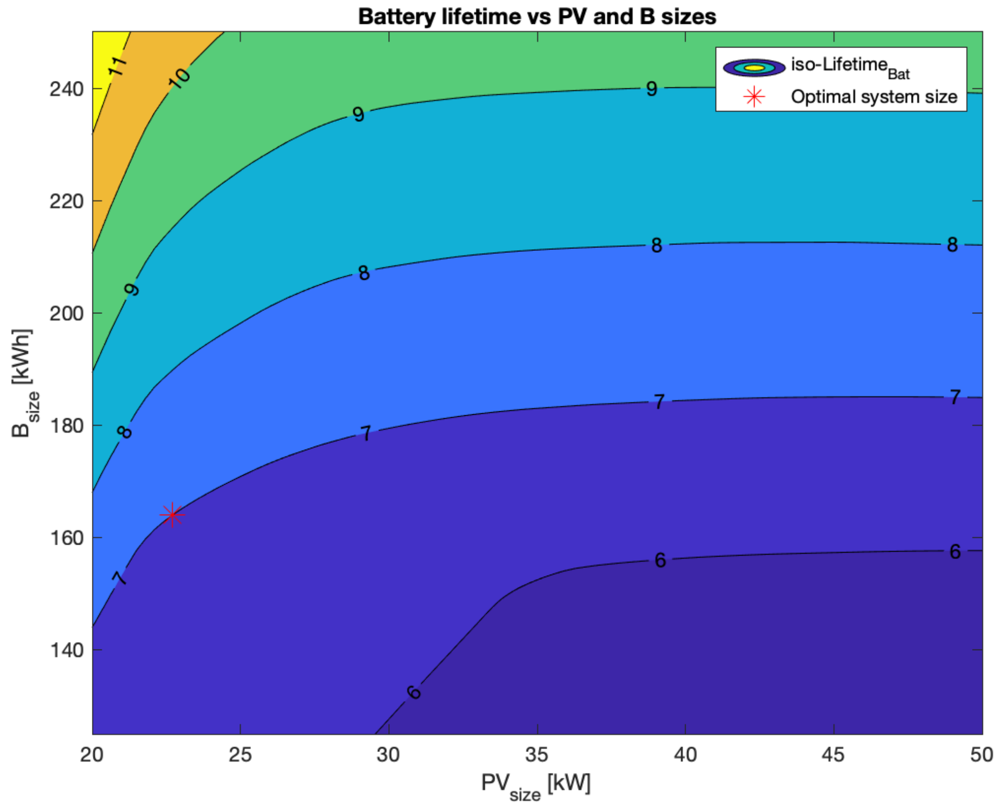

Figure 5.5: Simulation result for various batteries lifetimes

5.2 Economic assessment

With all the technical information analyzed, it is now necessary to look at the economic data of the system. Here a comparison between the prices of the so-called "Traditional" methodology and the modified methodology will be made in order to understand the benefits and disadvantages. As stated before, the traditional methodology tries to calculate the optimal system for a project using only economic tools (NPC and LCoE), while the modified methodology, presented in [7], already inserts into the equation the energy losses due to the lack of supply and, consequently, the additional costs that this might incur, always knowing in advance that when this happens the consumers will always switch to another energy source.

Analysing Figures (a) and (b) of Figure 5.6, it can be observed that for the simulated optimal system of 20 kW for PV size and 144 kWh for battery capacity, for this context and conditions, this system through the traditional methodology would have an NPC and LCoE of 184.724,29 € and 0,39 €/kWh, respectively. These figures only refer to the total value of the system over 20 years, not including the lack of electricity supply to consumers throughout these years. Furthermore, this system has a LPSP of 21%, something that cannot occur, due to the imposed limit of 20% minimum LPSP, meaning that almost one fifth of the required energy is not supplied.

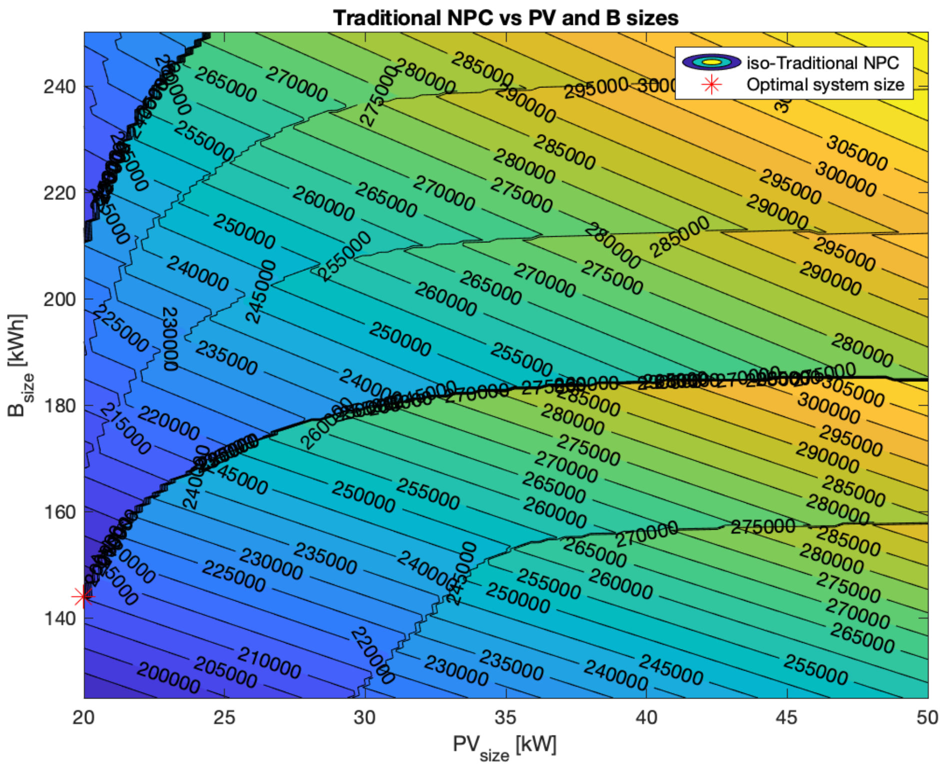

(a) Traditional NPC

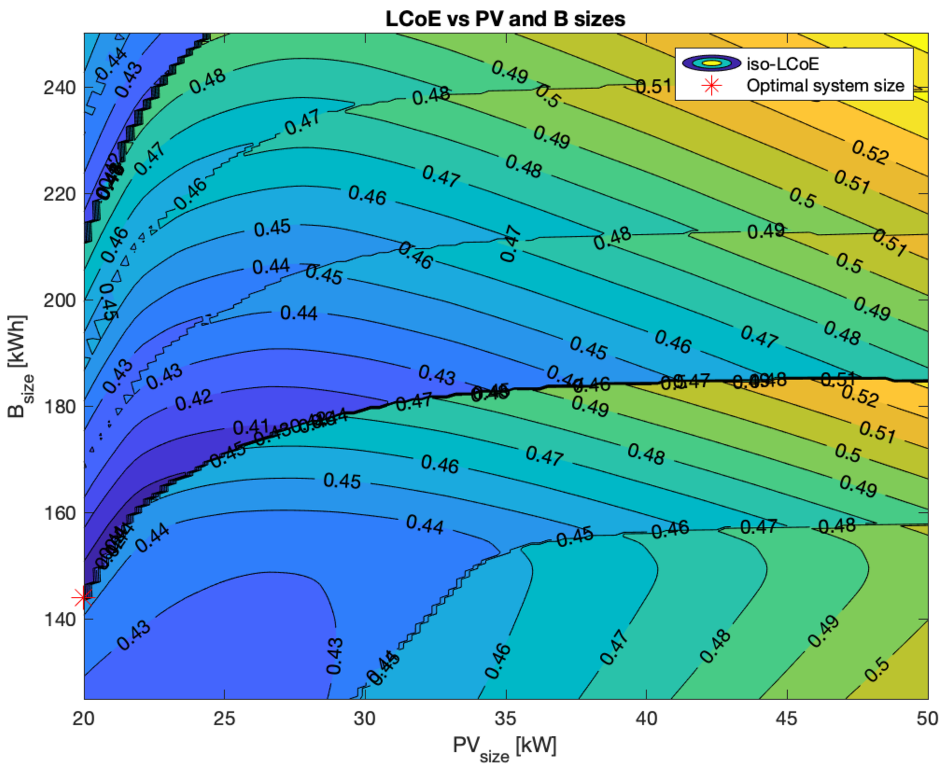

(b) Traditional LCoE

Figure 5.6: Results for the optimal system using Traditional Methodology

On the other hand, the sizing of the system using the modified methodology concluded that the optimum system size would be 22,7 kW for the total power of the solar panels and 164 kWh for the capacity of the batteries, concluding with a final value for the project of NPC* of 215.290,48 € over 20 years. In this sense, the final value of the electricity price for consumers, according to the final LCoSLE value, would be 0,41 €/kWh, as can be analysed in Figures 5.7 and 5.8. As can be observed, there is an increase in the total value of the system, over the 20 years, of about 14% and of 5% in the price that the kWh of electricity needs to be sold so that at the end of the 20 years the investment has some return.

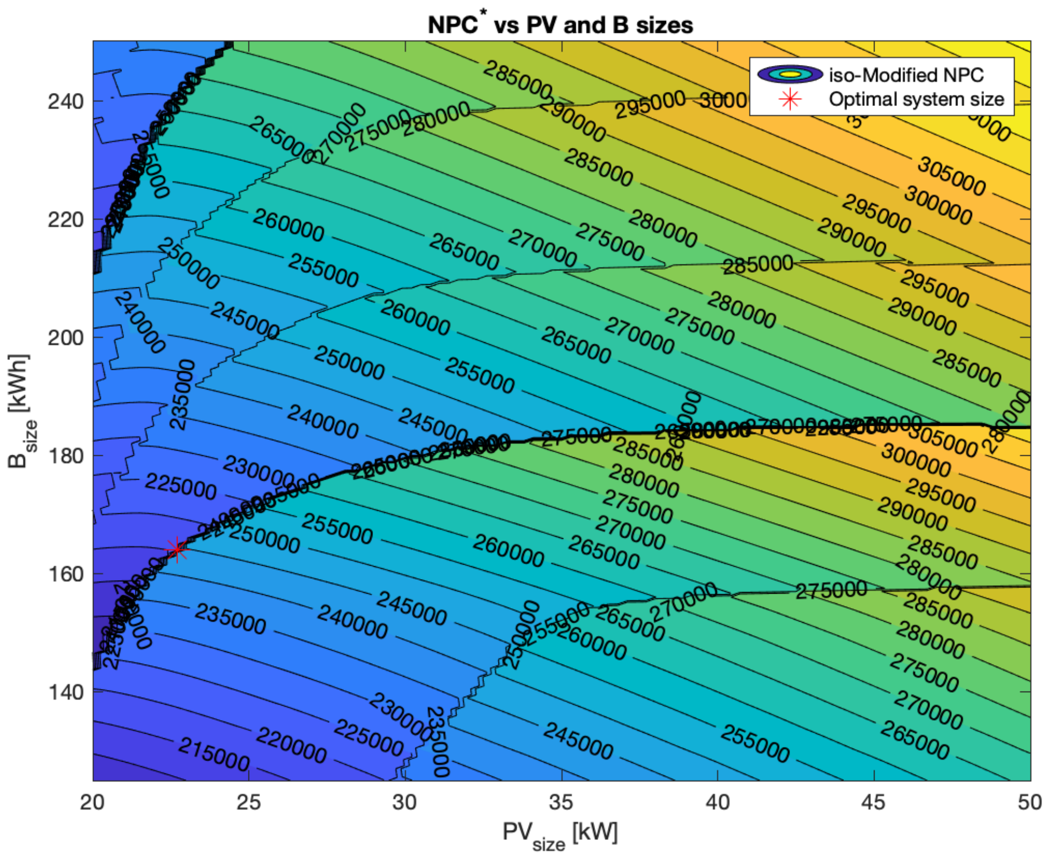

Figure 5.7: Simulation result for the Modified NPC for the optimal system

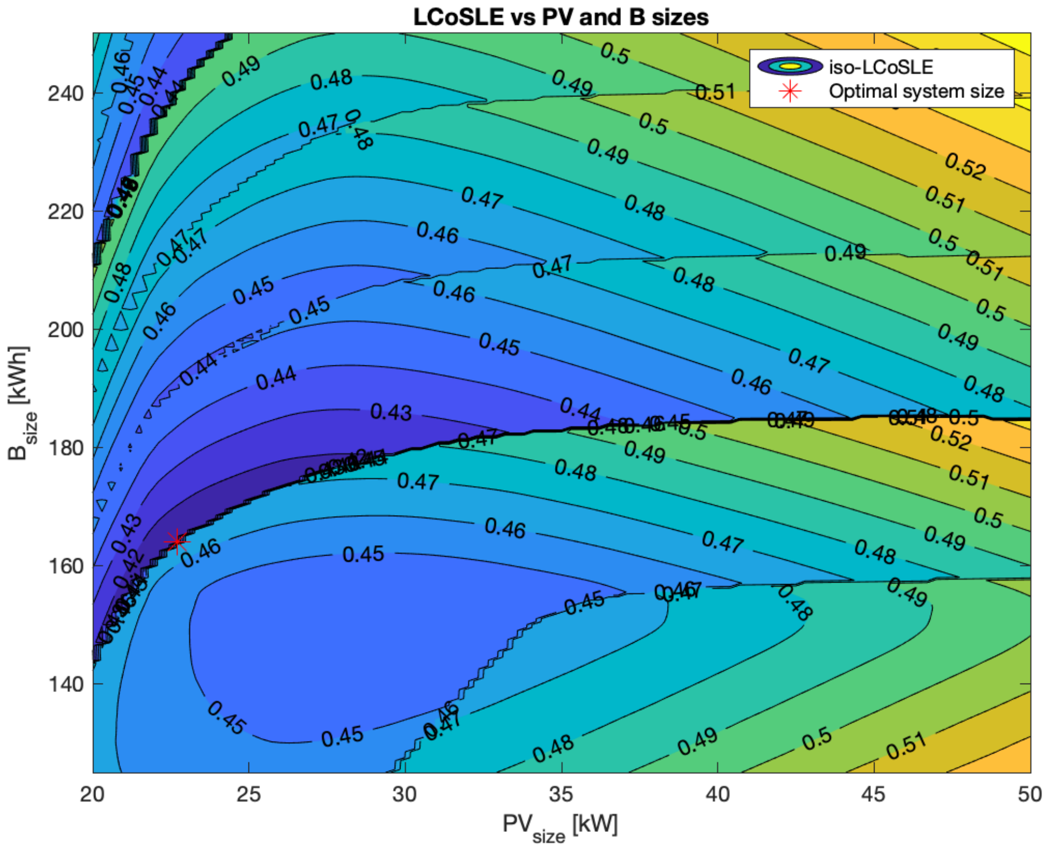

Figure 5.8: Simulation result for the LCoSLE for the optimal system

In addition, as can be seen in Figure 5.9, the LPSP value given by the simulation is 9,96%, which means that over its useful lifetime the plant will not provide 4,9 MW of the 49,85 MW per year of the energy needed to satisfy people's basic needs and will be lost. Furthermore, all the losses in the cables and in the energy conversions could also be included in the LPSP value, but because of their low value, they were not added to the algorithm. Knowing this value, one knows that people needed other forms of energy to sustain themselves, and these sources also have a cost, which is already calculated in the NPC* through VOLL.

That said, one can conclude that this 14% increase, or 30.566,20 €, in the total price of the PV system covers the 9,96% energy shortfall for consumers, despite the use of more basic and polluting forms of energy supply. But despite all this, by having this security, the consumers supplied by this mini grid will have 365 days of uninterrupted electricity, and approximately 91% of the energy required by the consumers can be supplied by the solar system. The other forms of energy, like diesel generators, kerosene lamps and mobile phone charging from kiosks and portable batteries, will be used as a last resort, and as it can seen from the technical analysis of the system, this will always happen at the deepest hours of the night when the batteries are fully discharged. Nevertheless, despite having an increase of almost 20% in the total price of the system, the final price of electricity ends up being only

5% higher, that for the case of these people in those conditions can end up being beneficial.

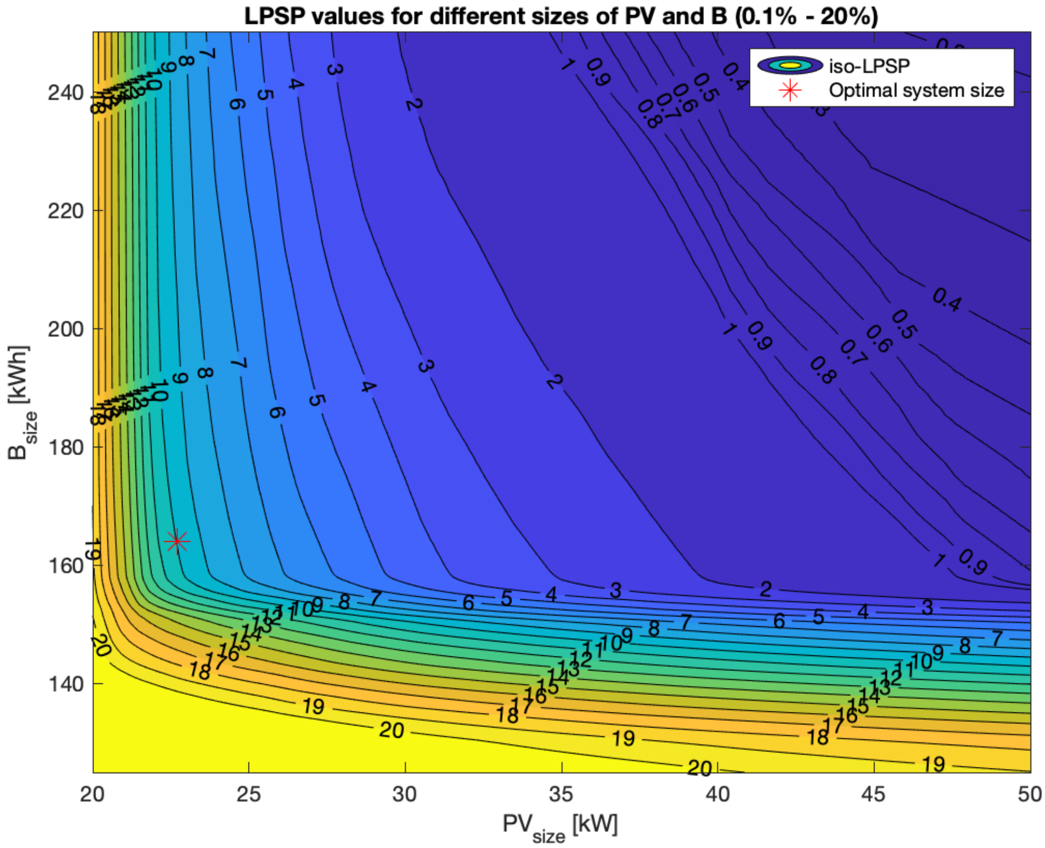

Figure 5.9: Lost of Power and Supply Probability between 0,1% and 20%

Furthermore, one can still observe, with the help of Figure 5.8, that the isoreability lines shown in the figure converge to 3 different zones, something that has never been seen in [7]. In the work studied, only one zone was presented, in which its center point of convergence was the optimal system. Here it manages to be a little different, since if one wants some projects that is in a range of, for example, 10% of the optimal LCoSLE (with a difference around 3 to 4 cents above the optimal system electricity cost) one can see that some of these systems are already in another isoreability zone. That is, if one uses Figure 5.8 and overlay it with the 4.2, one can conclude that the 3 different convergence zones have to do with the different years of battery changes of the different systems and its costs (see Figure 5.10), since there are systems that need 1, 2 or even 3 battery replacements. Due to the large capacity needed to ensure a good operation of such a project, this size was strictly necessary and since this work is using $LiFePO_4$ batteries, being their price higher than the lead acid ones, it is normal that the replacement of the batteries is one of the most important factors for the large price differences of the various systems.

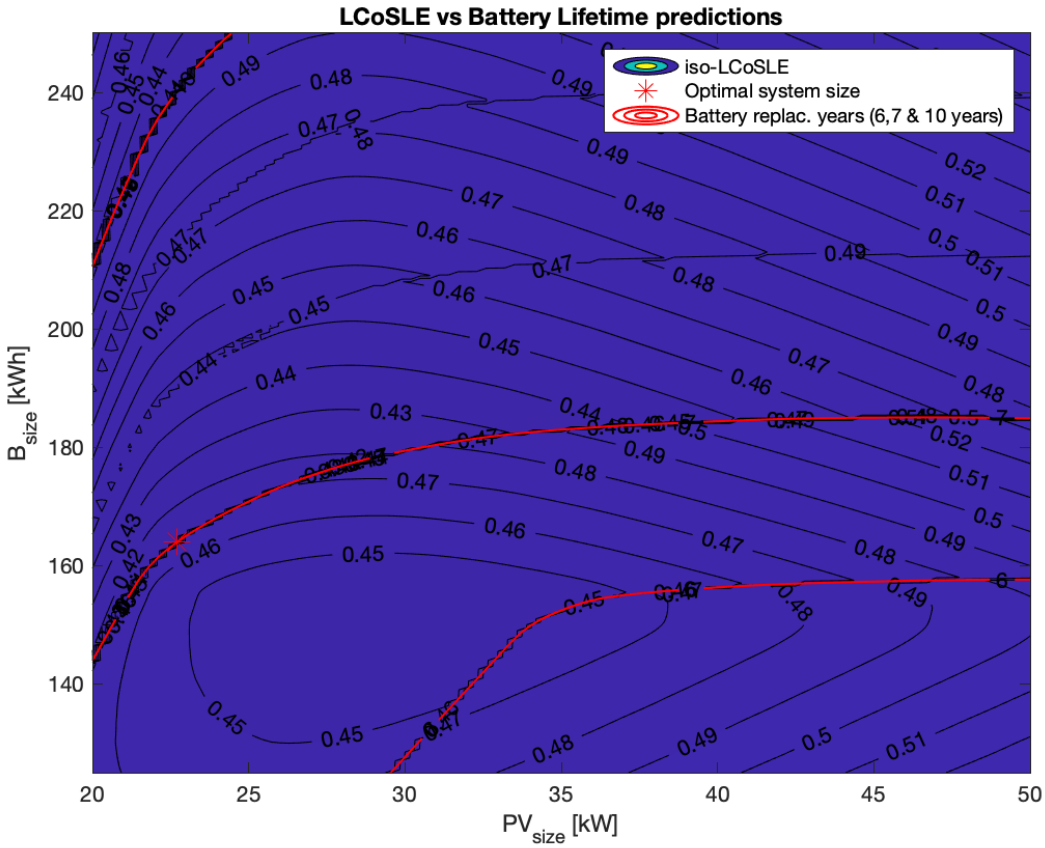

Figure 5.10: LCoSLE vs Battery replacement years

Since some assumptions have been made for this simulation, as can be seen in Chapter 3, it should be noted that this system, after a thorough study of the local conditions and consumers, may not be the best possible. Moreover, if its added the factor that there are 3 possible convergence zones for the electricity costs of the system, there is the possibility that the project investor may want something a bit oversized, according to their choices. If this happens, any of the systems present within the range of simulated systems, as in Figure 5.11, has the necessary capacities to provide good service, always presents values of LPSP below 20% and still, due to the 3 convergence zones, one can choose how often one will want to change the batteries. In this case, if the investor were to choose any of the simulated systems with the 10% value of LCoSLE above the optimal value, he could choose between 3 different systems all with similar LCoSLE but completely different sizes and prices. For example, if one wanted a larger project width or an oversized project, one could choose a LCoSLE value of for example 0,43 €/kWh and with this value, using the isoreliability map of all simulated systems, one can observe that a system for this value exists in any of the 3 convergence zones, meaning that there are 3 or more different systems that can be used for these exact conditions but with completely different prices, capacities and conditions of maintenance.

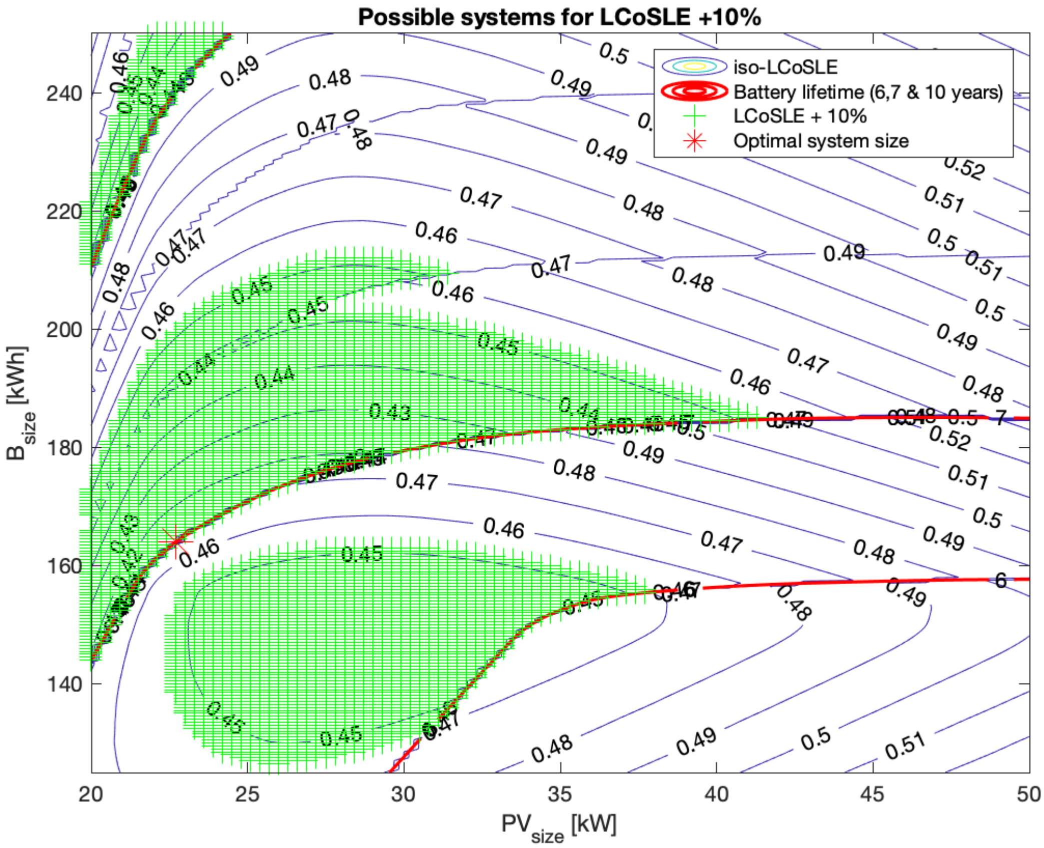

Figure 5.11: Possible optimal systems for LCoSLE +10%

More can be added by mentioning that if ones looks closely at the Figure 5.10, one can still see that there seems to be a little convergence to the set of systems that need a change at the end of 8 or 9 years. Since this change in terms of number of replacements makes no difference over the 20 year period that exists for the project, one can conclude that these "flaws" in the graph have more to do with the numerical way the LCoSLE and the NPC* were calculated. As a way of proving this, the isoreability graph below (see Figure 5.12), shows all the simulated systems and their Investment values. As described in Chapter 3, the investment of the project has to do with the number of panels needed according to the power needed for the entire project and its market values; the capacity of the battery system and its market values; the power needed for the inverter and its market price; and finally, with the other values, called "soft costs" which correspond to 25% of the total cost of the three parameters mentioned above. Having said this, observing the Figure 5.12,one can confirm that the different convergence zones due to the replacement of systems every 7 years and 10 years, exist due to the large discrepancy of costs in the replacement of the batteries. It can also be noted that this image does not show the distinction for the systems that need to be changed every 6 years due to the fact that the capacity of the batteries used in these systems is not as high to make such a difference, as in the other systems analyzed.

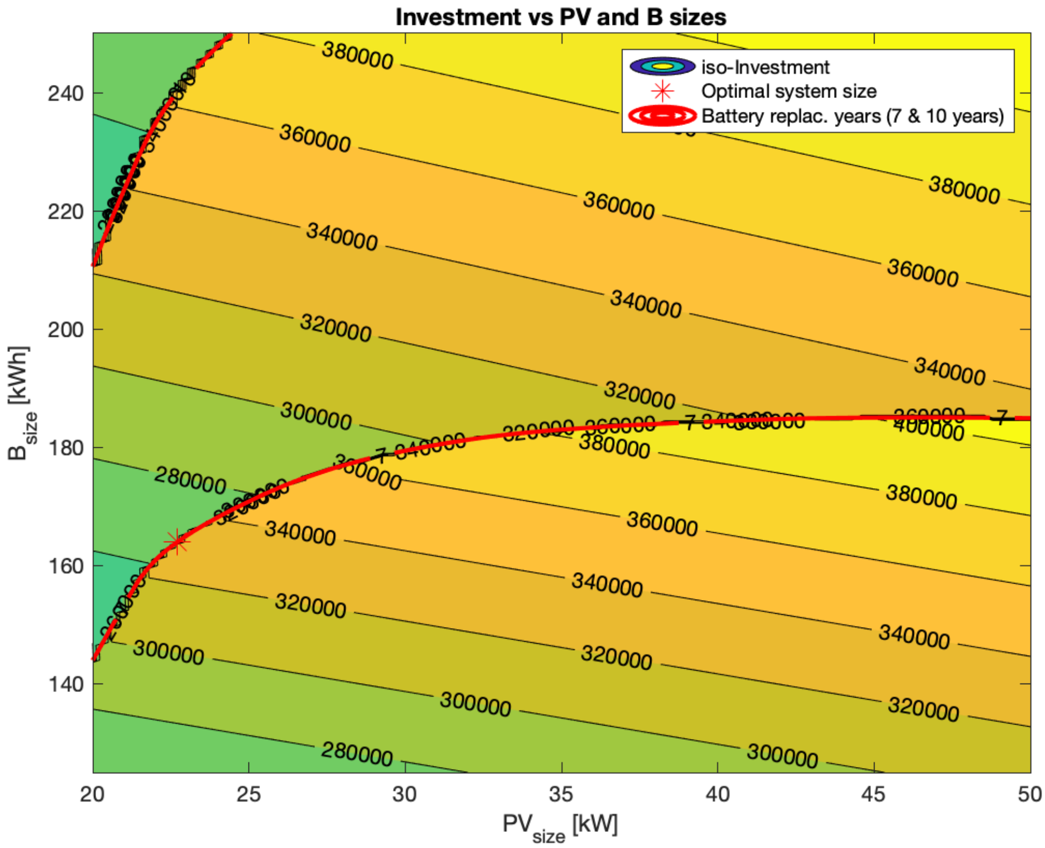

Figure 5.12: Investment and PV/Bat sizes

5.3 Social evaluation

Another important issue is the average price of electricity already in force in Angola, which is one of the countries with the lowest average cost of electricity in the world. As can be seen in various sites, such as on [110], the average price of electricity in Angola is approximately 0,02 €/kWh, this being a major factor for the lack of quality of the Angolan electricity systems, due to the large economic deficit that created in the company ENDE *(Empresa Nacional de Distribuição de Electricidade)*. Starting in 2019, a decree of law was signed for tariffs to be increased to 0,06 €/kWh, in order to combat the further impoverishment of Angola's energy utilities, despite the fact that hydroelectric and diesel generated power generation costs are 0,01 €/kWh and 0,08 €/kWh, respectively. If one makes a comparison between the electricity prices now in effect and the new price given by the system's LCoSLE, it can be seen that there is a huge discrepancy between values.

If this simulated system were now built under the economic conditions that the Angolan electricity system faces, there would be a difference of 0,35 €/kWh which would need to be subsidized by the state or by some other identity. Another disadvantage that does not help this situation is the minimum wage in Angola. As can be seen in Table 4.2, from Chapter 4, the minimum wage in Angola is currently

21.454,10 Kz per month, which, at the time of writing this dissertation, is equivalent to 27,29 €. Now analyzing this value, and looking at a monthly load based on a user of the $Family_2$ class of this work (93 kWh/month), with price per kWh at 0,06 €, one can calculate that of his salary, this type of user uses 20,44% of this value for his energy needs, which seen this way presents an extremely high value, since it is practically one fifth of the salary. If one wants to compare this situation with Portugal, for example, where the price of electricity per kWh is around 0,18 € and the minimum wage is 665 €, one can calculate that the Portuguese spend on average (if one uses the same load as above) 2,51% of their salary on electricity. Now looking at all these figures, one can confirm that the big problem comes from the wages practiced there, because although the value of electricity is very low, the slice that takes away from the wages of Angolan families is higher percentage than electricity in Portugal, one of the countries with the highest price of electricity per kWh in the world.

Knowing all this, one can conclude that with the value of electricity given by the simulated LCoSLE it would be impossible to set up such a system in Huambo, unless its consumers are highly subsidized by the state or other entity. Using $Family_2$'s energy consumption as an example again, with the price of electricity at 0,41 €/kWh, this would mean a monthly electricity bill of 38,13 €, which these days is impossible for an Angolan to pay due to the minimum wages in the country. If salaries stay the same, the only way to set up a system like this is to subsidize about 75% of the price per kWh of electricity, which would make the price be around 0,10 €/kWh. With this value, the price paid for electricity would already be similar to today's price, with an increase of 67%. Seeing that last time the price rose 6 times more than the price charged in 2016, one can conclude that it is a small cost to pay to have a cleaner and renewable energy. At this price, about 34% of their salaries would go on their electricity bill, an increase of 14% compared to electricity priced at 0,06 €/kWh. In addition, another important comparison can be made. For an Angolan to spend the same portion of their salary on electricity as a Portuguese at the end of the month (2,51%), their bill at the end of the month could only be 0,68€ using $Family_2$'s load. Knowing that over a month, with this solar system, the bill of $Family_2$ would be 37,20 €, it is known that the Angolan government would have to subsidize about 98% of the electricity bills of all consumers of this photovoltaic system.

Despite these high costs, one cannot forget the advantages that this project would have for communities that do not even have access to electricity or are completely isolated. For these areas it would be a way to bring a clean form of energy, with fewer emissions into the environment, less noise and possibly fewer outages than they are used to. It is necessary to understand that the price difference for the system between the traditional and modified methodology is not that big in monetary terms, but for these people who may never try to have a stable electricity service it can make all the difference. With this PV system, all the supply required during the day is assured, while the night supply is partially assured, looking at the value of only 9,96% that LPSP presents. In addition, some assumptions have been made in this work, which may have led to the price of electricity going up this much.

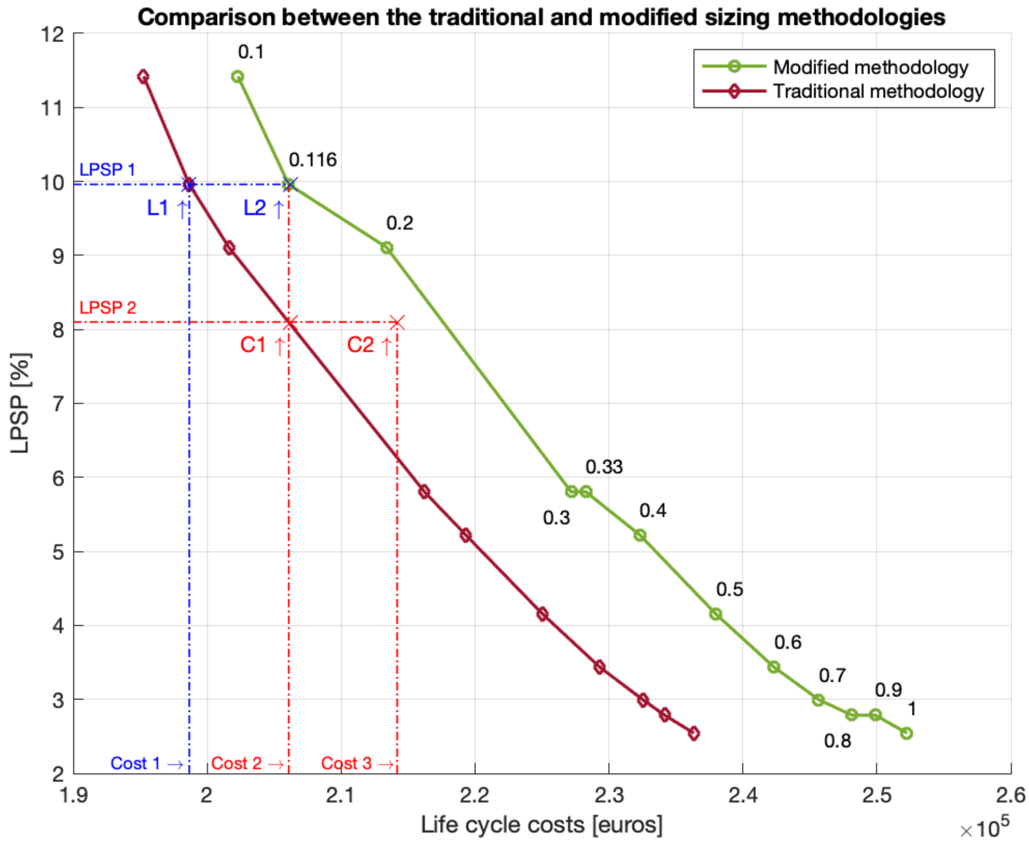

Figure 5.13: Comparison between the traditional and modified sizing methodologies

One way to analyze the difference that this modified methodology makes in contrast to the traditional methodology is to observe Figure 5.13, which shows the various optimal systems, for the Huambo zone, for various values of VOLL. Firstly, if one analyzes the line of *LPSP 1* present in the figure, one can conclude that a system for the same LPSP, in this case of 9,96%, for this zone would have two completely different cost values (points L1 and L2 of Figure 5.13). The difference in this cost is the costs associated with the use of more traditional sources of electricity (e.g. kerosene lamps, diesel generators), which would not be included in the traditional methodology (point L1). In other words, if one wanted a system with the same amount of losses, it would have an increase of about 7000 euros (point L2) but would have all expenses for the next 20 years of energy coming from other sources completely guaranteed. On the other hand, if one wanted a system with this cost (point L2) but with lower losses, or lower LPSP, one could take advantage and invest in a larger system, as shown with the system in point C1. The problem in this situation was what this thesis always wanted to avoid, that people using a system sized by the traditional methodology would end up having several energy losses during the nights. That's because it has already been seen in the technical analysis that this system will always end up, at least during the night, not being able to provide solar energy to the consumers and they will have to turn to other ways in order to have their basic needs satisfied. This, when it happens, will end up creating an even greater cost (point C3) than the other two points mentioned above, concluding that for this type of off-grid systems, this methodology ends up having good results, because it will always end up finding the most reliable system, with the cheapest price, thus always guaranteeing an almost uninterrupted supply throughout the year, with about 90% of this energy being completely clean.

5.4 Carbon emission value

These days, it is a fact that renewable energies are gaining more and more ground when it comes to being one of the main sources of clean energy around the world. This is largely due to the fact that the production of electricity in these systems does not pollute the atmosphere with Greenhouse Gases (GHG), making them a substitute for the many diesel generators or other fossil fuels present in many generation points around the world. The higher a country's portion of renewable energy sources in the fuel mix, the lower the CO_2 emissions. If for example, one feeds power into the public grid via a PV system, one makes a contribution to reducing the CO_2 emissions of the country. The amount of CO_2 avoided as a result of using a PV system, for example, depends on the fuel used (gas, heating oil, coal) and respectively the conventional energy used (electricity, district heating) by a country.

As a way of encouraging the construction or improvement of renewable energy production systems, an environmental subsidy was created. This subsidy is designed to reward renewable energy systems for helping to create clean electricity so as not to pollute the environment, as can be analysed in [110]. In this aspect and if it were possible to allocate this subsidy to this type of projects, it can be of great help to the project discussed in this thesis, since one of the main objectives is to try to reduce as much as possible the supply made by diesel generators or other more traditional but more polluting forms of energy, and at the same time make it as cheap as possible. To do this it will first be necessary to calculate the amount of CO_2 that the photovoltaic system will avoid emitting into the atmosphere. For this calculation, the following equation utilized by SMA Solar Technology, a well-know German solar energy equipment supplier, will be used:

$$\text{Generated electricity in } kWh \cdot \text{factor for CO}_2 \text{ avoidance in } kg/kWh = \text{avoided CO}_2 \text{ in } kg \qquad (5.1)$$

The factor for CO_2 avoidance (kg/kWh) indicates how much CO_2 is produced for every one kilowatt hour of electricity generated in the country. Depending on the technology used and the efficiency, the CO_2 factor can vary between the different energy supply companies in the region. According to [111], the value of the CO_2 avoidance factor for electricity produced by diesel (the fuel most commonly used in generators) is 0,3 kg/kWh. In addition, accordingly to [110], in World Bank's 2017 Guidance Note on Shadow Price of Carbon in Economic Analysis it is noted that there are two types of carbon emissions and the way they are assessed, being separated into "high" and low", each with its own value, as can be seen in Table 5.1.

Carbon emission value

Types of emission	2020	2030
"Low"	40 $/ton (33 €/ton)	50 $/ton (41 €/ton)
"High"	80 $/ton (66 €/ton)	100 $/ton (82 €/ton)

Table 5.1: Value per ton referring to CO_2 avoided to the atmosphere

In order to have only one value, an average was made and the value of 65 €/ton will be used. With all the above information and by adding the equation 5.1 in the optimization algorithm it is possible to arrive at a new optimal value for the PV system. For this new optimization, a system with 25,4 kW of solar panels and 172 kWh of battery capacity was found. It will have an LPSP of 6,97 %, managing to drop a little from the 9,96 % of the normal optimization using only the modified NPC*. Furthermore, even though the system is larger, its price, much thanks to the CO_2 avoidance subsidy, has caused its NPC* to drop further to 201.356,34 € and, consequently, its LCoSLE to drop to 0,37 €/kWh, as can be analysed in Table 5.2.

Traditional methodology		**Modified Methodology + CO2 avoidance**							
NPC	LCoE	VOLL	PV$_{size}$	B$_{size}$	LPSP	NPC*	LCoSLE	CO_2 avoided	Subsidy cost
184.724,29	0,39	0,116	25,4	172	6,97	201.356,34	0,37	439,20	23.995,40
€	€/kWh	€/kWh$_{LL}$	kW	kWh	%	€	€/kWh	ton	€

Table 5.2: Comparison values between the traditional methodology and the modified methodology with the added CO_2 subsidy

Chapter 6

Conclusions

This chapter takes the final conclusions of the work and gives some topics for a future work related to sizing of solar systems.

6.1 Conclusions

Right now, on the African continent, several countries are facing a major challenge of how to bring more electricity to people in isolated places in order to improve their quality of life. Unfortunately, due to the very weak economies that these countries have, this task has become increasingly difficult. Angola is one of the countries where this situation stands out the most, despite being one of the countries where electricity has a very low value (before 2019 it was 0,01 €/kWh and then went to 0,06 €/kWh). This value in the price of electricity is one of the main reasons for the fall in income of public utilities, which consequently leads to a lack of funding to improve public distribution networks, which could bring electricity to the most isolated areas.

Taking advantage of the big trend in renewable energies, in particular in photovoltaic energy generation systems, this thesis had the objective of helping in an effective way to discover the best framed systems for these isolated areas, in order to combat and help this situation. Using off-grid systems in isolated areas would make it possible to provide electricity in a clean way and it would not be necessary to wait for the installation of transmission and distribution lines to the area, something that could take several years. On the other hand, there is a problem that happens several times in these types of off-grid systems, which is the lack of power (or loss of load) at certain times of the day due to lack of produced or stored energy. This often happens because many systems are made to cost the least to the consumer and the investor, since for the systems to present a Lost of Power and Supply Probability of 0 they would have to have one of their components (solar panels or batteries) very oversized, something that cannot happen, especially in underdeveloped countries, where yields are extremely low. Given this situation, then, in addition to trying to arrive at a better way to size the solar system, this thesis, using the methodology presented in [7], incorporated the costs of the more traditional sources of energy that the people in these areas would use when there was a power outage, since there was already a notion that these consumers would not simply stop using these types of energy sources that they were already using immediately, even more so knowing that there is always the possibility of power failure.

A case study was then set up for the locality of Huambo, in a rural area, which has an average daily irradiance of 5,4 kW/m^2, with consumers presenting an average daily consumption of 136 kWh of electricity. Since the intention of this thesis was to come up with the cheapest and most reliable system possible, an algorithm was assembled in MATLAB with the help of the [7] methodology, so that this system, besides the referred conditions, has incorporated in its costs the values referring to the expenses spent when there is a lack of solar electric energy supply (VOLL - Value of Lost Load). With the incorporation of this value, the final LCoSLE will already have all the extra costs associated with the extra expenses throughout the useful life of the project.

That said, the optimal simulated solar system for the Humbo area, with the load, irradiance and economic conditions mentioned, would have to have a solar panel power of 22,7 kW, with a battery pack capacity of about 164 kWh. This system over the 20 years would present a LPSP of 9,96%, an NPC* of 215.299,48 € and a LCoSLE of 0,41 €/kWh. In addition, this system would be equipped with $LiFePO_4$ batteries capable of lasting twice as long as normal lead-acid batteries. With this system, over the 20 years, about 90% of the energy supplied would be totally renewable, with good production all winter long and an uninterrupted supply during sunny hours, with all the costs associated with the loss of load during some nights already built into the equation. Although the price difference for a traditionally sized system would be almost 20%, the amount payable per kWh of energy would only differ by 0,02 €/kWh, a small price to pay for uninterrupted energy supply throughout the years. In addition, it should be noted that the value referring to the expenses during the loss of load present a much lower value when compared to the case study in [7], much due to the fact that the price of a liter of diesel in Angola is extremely low.

Unfortunately, with these values and the incomes received by the people of Angola, it would be impossible for these consumers to pay an electricity bill of this value, so about 75% of the value of this system would have to be subsidized by the local government or other entities, so that the amount to be paid for electricity would be a reasonable value. On the other hand, as was seen in the previous chapter, for an Angolan to spend the same part of his salary on his electricity bill as a Portuguese pays, the Angolan government would have to subsidize about 98% of the users' final electricity bill. In addition, due to the increased attention to renewable energy and the growth of subsidies for switching from fossil to renewable energy, it would be possible to decrease the cost of this system by about 15% with the help of CO_2 avoidance subsidies. Unfortunately, the possibility of receiving these subsidies is not yet possible for all projects nor all countries.

6.2 Future Work

The sizing of solar systems is something that is widely studied in the literature today. Anyone wants to pay as little as possible for a system that is as reliable as possible, speaking of developed and underdeveloped countries alike.

One of the important points at this moment, and that could well be a follow-up to the work done in this thesis, would be the training of the neural network with all the data from the simulations carried out so that when it receives the irradiance, temperature, load and economic details, it would already know which would be the best solar system for the area in question without having to go through thousands of interpolations. The more results from different simulations the neural network is trained, the better prepared it is to choose the best system for a given area or type of consumer.

Bibliography

[1] I. E. Agency. World's Renewable Energies. `https://www.iea.org/fuels-and-technologies/renewables`, 2020. [Online; accessed 18-January-2021].

[2] M. Welsch, M. Bazilian, M. Howells, D. Divan, D. Elzinga, G. Strbac, L. Jones, A. Keane, D. Gielen, V. S. Balijepalli, A. Brew-Hammond, and K. Yumkella. Smart and just grids for sub-saharan africa: Exploring options. *Renewable and Sustainable Energy Reviews*, 20:336–352, 2013. ISSN 13640321. doi: 10.1016/j.rser.2012.11.004.

[3] J. A. Cherni, I. Dyner, F. Henao, P. Jaramillo, R. Smith, and R. O. Font. Energy supply for sustainable rural livelihoods. a multi-criteria decision-support system. *Energy Policy*, 35:1493–1504, 3 2007. ISSN 03014215. doi: 10.1016/j.enpol.2006.03.026.

[4] A. Mellit, G. M. Tina, and S. A. Kalogirou. Fault detection and diagnosis methods for photovoltaic systems: A review. *Renewable and Sustainable Energy Reviews*, 91:1–17, 8 2018. ISSN 18790690. doi: 10.1016/j.rser.2018.03.062.

[5] P. Shield. Angola Electric Power Generation. `https://www.privacyshield.gov/article?id=Angola-Electric-Power-Generation`, 2018. [Online; accessed 15-December-2020].

[6] I. E. Agency. Energies in Angola. `https://www.iea.org/countries/angola`, 2020. [Online; accessed 12-January-2021].

[7] S. Mandelli, C. Brivio, E. Colombo, and M. Merlo. A sizing methodology based on levelized cost of supplied and lost energy for off-grid rural electrification systems. *Renewable Energy*, 89:475–488, 4 2016. ISSN 18790682. doi: 10.1016/j.renene.2015.12.032.

[8] L. L. Bucciarelli. Estimating loss-of-power probabilities of stand-alone photovoltaic solar energy systems. *Solar Energy*, 2:5–299, 1984.

[9] M. Egido and E. Lorenzo. The sizing of stand alone pv-systems: a review and a proposed new method. *Solar Energy Materials and Solar Cells*, 26:51–69, 1992.

[10] S. A. Klein and W. A. Beckman. Loss-of-load probabilities for stand-alone photovoltaic systems. *Solar Energy*, 39:499–512, 1987.

[11] N. D. Kaushika, N. K. Gautam, and K. Kaushik. Simulation model for sizing of stand-alone solar pv system with interconnected array. *Solar Energy Materials and Solar Cells*, 85:499–519, 2 2005. ISSN 09270248. doi: 10.1016/j.solmat.2004.05.024.

[12] M. Benghanem. An optimal sizing method for stand-alone photovoltaic system for algeria. Master's thesis, Algeria: USTHB, 2000.

[13] A. M. Q. Morgado. Study and experimental characterization of a photovoltaic-wind standalone system with batteries for residential consumers. Master's thesis, Instituto Superior Técnico, 11 2017.

[14] F. M. Cornelio. Energy-poverty and its impacts on peri-urban zones of huambo city, angola. Master's thesis, Lund University, 2006.

[15] T. W. B. Group. Global Solar Atlas. `https://globalsolaratlas.info/`, 2021. [Online; accessed 15-January-2021].

[16] Weather and Climate. `https://weather-and-climate.com/average-monthly-Rainfall-Temperature-Sunshine,Huambo,Angola`, 2021. [Online; accessed 16-January-2021].

[17] MINEA. Angola power sector long term vision - angola energy 2025. Technical report, Ministério da Energia e Águas, 2016.

[18] J. M. Takouleu. ANGOLA: Government wants to produce 600 MW from solar off grid. `https://www.afrik21.africa/en/angola-government-wants-to-produce-600-mw-from-solar-off-grid/`, 2019. [Online; accessed 15-December-2020].

[19] Afrik21. Amendments to the General Law of Electricity create opportunities for renewables. `https://www.aler-renovaveis.org/en/communication/news/fundo-nacional-de-electrificacao-rural/`, 2019. [Online; accessed 15-December-2020].

[20] Krismadinata, N. A. Rahim, H. W. Ping, and J. Selvaraj. Photovoltaic module modeling using simulink/matlab. *Procedia Environmental Sciences*, 17:537–546, 2013. ISSN 18780296. doi: 10.1016/j.proenv.2013.02.069.

[21] R. Rawat, S. C. Kaushik, and R. Lamba. A review on modeling, design methodology and size optimization of photovoltaic based water pumping, standalone and grid connected system. *Renewable and Sustainable Energy Reviews*, 57:1506–1519, 5 2016. ISSN 18790690. doi: 10.1016/j.rser.2015.12.228.

[22] G. K. Singh. Solar power generation by pv (photovoltaic) technology: A review. *Energy*, 53:1–13, 5 2013. ISSN 03605442. doi: 10.1016/j.energy.2013.02.057.

[23] T. M. Razykov, C. S. Ferekides, D. Morel, E. Stefanakos, H. S. Ullal, and H. M. Upadhyaya. Solar photovoltaic electricity: Current status and future prospects. *Solar Energy*, 85:1580–1608, 8 2011. ISSN 0038092X. doi: 10.1016/j.solener.2010.12.002.

[24] X. Vallvi and J. Serrasolsest. Design and operation of a 50 kwp pv rural electrification project for remote sites in spain. *Solar Energy*, 59:119, 1997.

[25] T. M. Masaud, K. Lee, and P. K. Sen. An overview of enrgy storage technologies in electric power systems: What is the future? Technical report, Colorado School of Mines, Division of Engineering, 2010.

[26] W. E. C. (WEC). World Energy Ressources. `https://www.worldenergy.org/data/resources/resource/solar/`, 2020. [Online; accessed 14-January-2021].

[27] A. J. Perea-Moreno, Q. Hernandez-Escobedo, J. Garrido, and J. D. Verdugo-Diaz. Stand-alone photovoltaic system assessment in warmer urban areas in mexico. *Energies*, 11, 2 2018. ISSN 19961073. doi: 10.3390/en11020284.

[28] V. Svoboda, H. Wenzl, R. Kaiser, A. Jossen, I. Baring-Gould, J. Manwell, P. Lundsager, H. Bindner, T. Cronin, P. Nørgård, A. Ruddell, A. Perujo, K. Douglas, C. Rodrigues, A. Joyce, S. Tselepis, N. van der Borg, F. Nieuwenhout, N. Wilmot, F. Mattera, and D. U. Sauer. Operating conditions of batteries in off-grid renewable energy systems. *Solar Energy*, 81:1409–1425, 11 2007. ISSN 0038092X. doi: 10.1016/j.solener.2006.12.009.

[29] A. Jossen, J. Garche, and D. U. Sauer. Operation conditions of batteries in pv applications. *Solar Energy*, 76:759–769, 6 2004. ISSN 0038092X. doi: 10.1016/j.solener.2003.12.013.

[30] D. P. Jenkins, J. Fletcher, and D. Kane. Model for evaluating impact of battery storage on microgeneration systems in dwellings. *Energy Conversion and Management*, 49:2413–2424, 8 2008. ISSN 01968904. doi: 10.1016/j.enconman.2008.01.011.

[31] M. Sidrach-De-Cardona and L. M. Lo´pezlo´pez. A simple model for sizing stand alone photovoltaic systems. *Solar Energy Materials and Solar Cells*, 55:199–214, 1998.

[32] P. H. Tsalides and A. Thanailakis. Loss-of-load probability and related parameters in optimum computer-aided design of stand-alone photovoltaic systems. *Solar Ceils*, 18:115–127, 1986.

[33] B. Bartoli, V. Cuomo, F. Fontana, C. Serio, and V. Silvestrini. The design of photovoitaic plants: An optimization procedure. *Applied Energ)*, 18:37–47, 1984.

[34] T. Ishikawa. Grid-connected photovoltaic power systems: Survey of inverter and related protection equipments. Technical report, International Energy Agency Photovoltaic Power Systems Programme (IEA-PVPS), 12 2002. URL `http://www.iea-pvps.org`.

[35] M. A. Eltawil and Z. Zhao. Grid-connected photovoltaic power systems: Technical and potential problems-a review. *Renewable and Sustainable Energy Reviews*, 14:112–129, 1 2010. ISSN 13640321. doi: 10.1016/j.rser.2009.07.015.

[36] C. Bordin, H. O. Anuta, A. Crossland, I. L. Gutierrez, C. J. Dent, and D. Vigo. A linear programming approach for battery degradation analysis and optimization in offgrid power systems with solar energy integration. *Renewable Energy*, 101:417–430, 2 2017. ISSN 18790682. doi: 10.1016/j.renene.2016.08.066.

[37] M. Ashari and C. V. Nayar. An optimum dispatch strategy using set points for a photovoltaic (pv)-diesel-battery hybrid power system †. *Solar Energy*, 66:1–9, 1999. URL `www.elsevier.com/locate/solener`.

[38] V. Khare, S. Nema, and P. Baredar. Solar-wind hybrid renewable energy system: A review. *Renewable and Sustainable Energy Reviews*, 58:23–33, 5 2016. ISSN 18790690. doi: 10.1016/j.rser.2015.12.223.

[39] P. C. Saha. Sustainable energy development: a challenge for asia and the pacific region in the 21st century. *Energy Policy*, 31:1051–1059, 2003.

[40] O. D. C. S. Leone, M. C. Mozambique, E. K. Kenya, J. N. Zimbabwe, and K. Potgieter. Sustainable energy in sub-saharan africa. Technical report, International Council of Science, 2007.

[41] M. A. Rosen. Energy sustainability: A pragmatic approach and illustrations. *Sustainability*, 1: 55–80, 3 2009. ISSN 20711050. doi: 10.3390/su1010055.

[42] B. Mainali, S. Pachauri, N. D. Rao, and S. Silveira. Assessing rural energy sustainability in developing countries. *Energy for Sustainable Development*, 19:15–28, 2014. ISSN 09730826. doi: 10.1016/j.esd.2014.01.008.

[43] J. L. Bernal-Agustín and R. Dufo-López. Simulation and optimization of stand-alone hybrid renewable energy systems. *Renewable and Sustainable Energy Reviews*, 13:2111–2118, 10 2009. ISSN 13640321. doi: 10.1016/j.rser.2009.01.010.

[44] A. Q. Jakhrani, A. K. Othman, A. R. H. Rigit, S. R. Samo, and S. A. Kamboh. A novel analytical model for optimal sizing of standalone photovoltaic systems. *Energy*, 46:675–682, 2012. ISSN 03605442. doi: 10.1016/j.energy.2012.05.020.

[45] A. Fragaki and T. Markvart. Does climate change affect the design of stand-alone pv systems? *Progress in Photovoltaics: Research and Applications*, 13:635–639, 11 2005. ISSN 10627995. doi: 10.1002/pip.617.

[46] W. X. Shen. Optimally sizing of solar array and battery in a standalone photovoltaic system in malaysia. *Renewable Energy*, 34:348–352, 1 2009. ISSN 09601481. doi: 10.1016/j.renene.2008.03.015.

[47] S. Semaoui, A. H. Arab, S. Bacha, and B. Azoui. Optimal sizing of a stand-alone photovoltaic system with energy management in isolated areas. *Energy Procedia*, 36:358–368, 2013. ISSN 18766102. doi: 10.1016/j.egypro.2013.07.041.

[48] B. S. Borowy and Z. M. Salameh. Methodology for optimally sizing the combination of a battery bank and pv array in a wind/pv hybrid system. *IEEE Transactions on Energy Conversion*, 11, 1996.

[49] J. K. Kaldellis. Optimum technoeconomic energy autonomous photovoltaic solution for remote consumers throughout greece. *Energy Conversion and Management*, 45:2745–2760, 10 2004. ISSN 01968904. doi: 10.1016/j.enconman.2003.12.007.

[50] R. Baños, F. Manzano-Agugliaro, F. G. Montoya, C. Gil, A. Alcayde, and J. Gómez. Optimization methods applied to renewable and sustainable energy: A review. *Renewable and Sustainable Energy Reviews*, 15:1753–1766, 5 2011. ISSN 13640321. doi: 10.1016/j.rser.2010.12.008.

[51] N. Sharma, Varun, and Siddhartha. Stochastic techniques used for optimization in solar systems: A review. *Renewable and Sustainable Energy Reviews*, 16:1399–1411, 4 2012. ISSN 13640321. doi: 10.1016/j.rser.2011.11.019.

[52] A. Mellit, S. A. Kalogirou, L. Hontoria, and S. Shaari. Artificial intelligence techniques for sizing photovoltaic systems: A review. *Renewable and Sustainable Energy Reviews*, 13:406–419, 2 2009. ISSN 13640321. doi: 10.1016/j.rser.2008.01.006.

[53] T. Morgan. The performance and optimisation of autonomous renewable energy systems. Master's thesis, University of Wales, 1996.

[54] B. S. Borowy and Z. M. Salameh. Optimum photovoltaic array size for a hybrid wind/pv system. *IEEE Transactions on Energy Conversion*, 9, 1994.

[55] E. Koutroulis, D. Kolokotsa, A. Potirakis, and K. Kalaitzakis. Methodology for optimal sizing of stand-alone photovoltaic/wind-generator systems using genetic algorithms. *Solar Energy*, 80: 1072–1088, 9 2006. ISSN 0038092X. doi: 10.1016/j.solener.2005.11.002.

[56] V. K. Sharma, A. Colangelo, and G. Spagna. Photovoltaic technology: Basic concepts, sizing of a stand alone photovoltaic system for domestic applications and preliminary economic analysis. *Pergamon Energy Convers. Mgmt*, 36:161–174, 1995.

[57] T. Khatib, A. Mohamed, K. Sopian, and M. Mahmoud. Optimal sizing of building integrated hybrid pv/diesel generator system for zero load rejection for malaysia. *Energy and Buildings*, 43:3430–3435, 12 2011. ISSN 03787788. doi: 10.1016/j.enbuild.2011.09.008.

[58] J. Samimi, E. A. Soleimani, M. S. Zabihi, and R. Perez. Optimal sizing of photovoltaic systems in varied climates. *Solar Energy*, 60:97–107, 1997.

[59] G. E. Ahmad. Photovoltaic-powered rural zone family house in egypt. *Renewable Energy*, 26: 379–390, 2002. URL `www.elsevier.com/locate/renene`.

[60] M. M. H. Bhuiyan and M. A. Asgar. Sizing of a stand-alone photovoltaic power system at dhaka. *Renewable Energy*, 28:929–938, 2003. URL `www.elsevier.com/locate/renene`.

[61] R. N. Chapman. Development of sizing nomograms for stand-alone photovoltaic/storage systems*. *Solar Energy*, 43:71–76, 1989.

[62] G. Notton, M. Muselli, P. Poggi, and A. Louche. Autonomous photovoltaic systems- influences of some parameters on the sizing- simulation time step, input and output power profile. *Renewable Energy*, pages 353–369, 1996.

[63] O. Elsammani and E. Ibrahim. Sizing stand-alone photovoltaic systems for various locations in sudan. *Applied Energy*, 52:133–140, 1995.

[64] T. Khatib, A. Mohamed, K. Sopian, and M. Mahmoud. A new approach for optimal sizing of standalone photovoltaic systems. *International Journal of Photoenergy*, 2012, 2012. ISSN 1110662X. doi: 10.1155/2012/391213.

[65] T. Markvart, A. Fragaki, and J. N. Ross. Pv system sizing using observed time series of solar radiation. *Solar Energy*, 80:46–50, 1 2006. ISSN 0038092X. doi: 10.1016/j.solener.2005.08.011.

[66] N. N. Aeronautics and S. Administration. Surface Meteorology and Solar Energy website. `https://power.larc.nasa.gov/`, 2021. [Online; accessed 14-December-2020].

[67] M. Iqbal. *An Introduction To Solar Radiation*. Academic Press, 1st edition, 9 1983. ISBN 9780323151818.

[68] J. F. E. Carriço. Technical and economic assessment of a 500w autonomous photovoltaic system with lifepo 4 battery storage electrical and computer engineering examination committee. Master's thesis, Instituto Superior Técnico, 2015.

[69] J. D. Mondol, Y. G. Yohanis, and B. Norton. The impact of array inclination and orientation on the performance of a grid-connected photovoltaic system. *Renewable Energy*, 32:118–140, 1 2007. ISSN 09601481. doi: 10.1016/j.renene.2006.05.006.

[70] J. Duffie and W. Beckman. *Solar Engineering of Thermal Processes*. John Wiley and Sons: New York, 2nd edition, 1991.

[71] K. Ulgen. Optimum tilt angle for solar collectors. *Energy Sources, Part A: Recovery, Utilization and Environmental Effects*, 28:1171–1180, 9 2006. ISSN 15567036. doi: 10.1080/00908310600584524.

[72] B. Liu and R. Jordan. Daily insolation on surfaces tilted towards equator. *ASHRAE J.*, 10, 10 1961.

[73] C. Oancea and V. Badescu. A new kind of cloudy sky model to compute instantaneous values of diffuse and global solar irradiance. *Theor. Appl. Climatol*, 72:127–136, 2002.

[74] Y. Q. Tian, R. J. Davies-Colley, P. Gong, and B. W. Thorrold. Estimating solar radiation on slopes of arbitrary aspect. *Agricultural and Forest Meteorology*, 109:67–74, 2001.

[75] R. Castro. *Uma Introdução às energias Renováveis: Eólica, Fotovoltaica e Mini-hídrica*. IST Press, 1st edition, 2011.

[76] PV Education. http://www.pveducation.org/pvcdrom/properties-of-sunlight/solar-radiation-on-tilted-surface, 2021. [Online; accessed 20-January-2021].

[77] G. Yaciuk. Solar crop drying. *Solar Energy Conversion II*, 1981. doi: 10.1016/B978-0-08-025388-6.50049-0.

[78] C. O. Okoye and O. Solyalı. Optimal sizing of stand-alone photovoltaic systems in residential buildings. *Energy*, 126:573–584, 2017. ISSN 03605442. doi: 10.1016/j.energy.2017.03.032.

[79] Özge Ayvazoğluyüksel and Ümmühan Başaran Filik. Estimation of monthly average hourly global solar radiation from the daily value in Çanakkale, turkey. *Journal of Clean Energy Technologies*, 5:389–393, 9 2017. ISSN 1793821X. doi: 10.18178/JOCET.2017.5.5.403. URL http://www.jocet.org/index.php?m=content&c=index&a=show&catid=58&id=735.

[80] B. Y. H. Liu and R. C. Jordan. The interrelationship and of direct, diffuse and characteristic distribution total solar radiation*, 1960.

[81] M. Collares-Pereira and A. Rabl. The average distribution of solar radiation-correlations between diffuse and hemispherical and between daily and hourly insolation valuest. *Solar Energy*, 22:155–164, 1978.

[82] C. Gueymardt. Mean daily averages of beam radiation received by tilted surfaces as affected by the atmosphere. *Solar Energy*, 37:261–267, 1986.

[83] V. A. Graham, K. G. T. Hollands, and T. E. Unn. A time series model for kt with application to global synthetic weather generation. *Solar Energy*, 40:83–92, 1988.

[84] V. A. Graham and K. G. T. Hollands. A method to generate synthetic hourly solar radiation globally. *Solar Energy*, 44:333–341, 1990.

[85] W. Yao, Z. Li, T. Xiu, Y. Lu, and X. Li. New decomposition models to estimate hourly global solar radiation from the daily value. *Solar Energy*, 120:87–99, 10 2015. ISSN 0038092X. doi: 10.1016/j.solener.2015.05.038.

[86] D. Wit. *Simulation of assimilation, respiration and transpiration of crops*. Wiley, 1978.

[87] D. C. Reicosky, L. J. Winkelman, J. M. Baker, and D. G. Baker. Accuracy of hourly air temperatures calculated from daily minima and maxima*. *Agricultural and Forest Meteorology*, 46:193–209, 1989.

[88] H. Energy. PV Temperature Coefficient of Power. https://www.homerenergy.com/products/pro/docs/latest/pv_temperature_coefficient_of_power.html, 2021. [Online; accessed 11-March-2021].

[89] M. Dakkak, K. Hatori, and T. Ise. The concept of distribution flexible network pv system. *Renewable Energy*, 31:1916–1933, 10 2006. ISSN 09601481. doi: 10.1016/j.renene.2005.09.022.

[90] A. H. M. Nordin and A. M. Omar. Modeling and simulation of photovoltaic (pv) array and maximum power point tracker (mppt) for grid-connected pv system. In *2011 3rd International Symposium and Exhibition in Sustainable Energy and Environment*. IEEE, 2011. ISBN 9781457703423.

[91] E. Power. LiFePO4 Battery Series. `https://www.expertpower.us/collections/lifepo4-batteries`, 2019. [Online; accessed 10-February-2021].

[92] Y. Riffonneau, S. Bacha, F. Barruel, and S. Ploix. Optimal power flow management for grid connected pv systems with batteries. *IEEE Transactions on Sustainable Energy*, 2:309–320, 7 2011. ISSN 19493029. doi: 10.1109/TSTE.2011.2114901.

[93] T. S. Guys. How Long Do Solar Inverters Last? `https://thosesolarguys.com/how-long-do-solar-inverters-last/`, 2020. [Online; accessed 11-March-2021].

[94] A. A. Husain, W. Z. W. Hasan, S. Shafie, M. N. Hamidon, and S. S. Pandey. A review of transparent solar photovoltaic technologies. *Renewable and Sustainable Energy Reviews*, 94:779–791, 10 2018. ISSN 18790690. doi: 10.1016/j.rser.2018.06.031.

[95] R. E. Advisors. WHAT IS GRID PARITY? `https://web.archive.org/web/20170715051113/http://www.renewable-energy-advisors.com/learn-more-2/what-is-grid-parity/`, 2020. [Online; accessed 11-March-2021].

[96] I. R. E. Agency. Solar pv in africa: Costs and markets. Technical report, International Renewable Energy Agency (IRENA), 2016. URL `www.irena.org`.

[97] R. K. Akikur, R. Saidur, H. W. Ping, and K. R. Ullah. Comparative study of stand-alone and hybrid solar energy systems suitable for off-grid rural electrification: A review. *Renewable and Sustainable Energy Reviews*, 27:738–752, 2013. ISSN 13640321. doi: 10.1016/j.rser.2013.06.043.

[98] C. Oko, O. Diemuodeke, N. Omunakwe, and E. Nnamdi. Design and economic analysis of a photovoltaic system: A case study. *International Journal of Renewable Energy Development*, 1: 65–73, 08 2012. doi: 10.14710/ijred.1.3.65-73.

[99] A. Paul, B. K. Dey, N. Mandal, and A. Bhattacharjee. Matlab/simulink model of stand-alone solar pv system with mppt enabled optimized power conditioning unit. *7th IEEE Annual Information Technology, Electronics and Mobile Communication Conference, IEEE IEMCON 2016*, 11 2016. doi: 10.1109/IEMCON.2016.7746319.

[100] M. R. Patel. *Wind and solar energy*. CRC Press LLC, 1999.

[101] T. G. solar energy society. *Planning and installing photovoltaic*. Earthscan Publications Ltd., 2005.

[102] S. D. Downing and D. F. Socie. Simple rainflow counting algorithms, 1982.

[103] R. Dufo-López and J. L. Bernal-Agustín. Techno-economic analysis of grid-connected battery storage. *Energy Conversion and Management*, 91:394–404, 2015. ISSN 01968904. doi: 10.1016/j.enconman.2014.12.038.

[104] K. G. Willis and G. D. Garrod. Electricity supply reliability estimating the value of lost load. *Energy Policy*, 25:9–103, 1997.

[105] E. Leahy and R. S. Tol. An estimate of the value of lost load for ireland. *Energy Policy*, 39:1514–1520, 3 2011. ISSN 03014215. doi: 10.1016/j.enpol.2010.12.025.

[106] G. petrol Prices. Angola Diesel prices, liter, 01-Mar-2021. https://www.globalpetrolprices.com/Angola/diesel_prices/, 2021. [Online; accessed 07-March-2021].

[107] K. R. Wheeler and S. C. Southward. Efficient operation of diesel generator sets in remote environments. Master's thesis, Virginia Polytechnic Institute and State University, 2017.

[108] S. Fabrizio, K. Dybczak, V. Flamini, and J. Kapsoli. Angola fuel price subsidy reform: The way forward. Technical report, International Monetary Fund, 2014.

[109] E. Martinez-Laserna, V. I. Herrera, I. Gandiaga, A. Milo, E. Sarasketa-Zabala, and H. Gaztañaga. Li-ion battery lifetime model's influence on the economic assessment of a hybrid electric bus's operation. *World Electric Vehicle Journal*, 9, 8 2018. ISSN 20326653. doi: 10.3390/wevj9020028.

[110] I. B. F. RECONSTRUCTION and DEVELOPMENT. Electricity sector improvement and access project - angola. Technical report, International Bank for Reconstrution and Development, 2021.

[111] W. M. Office. Emission factors in kg CO2-equivalent per unit. https://www.winnipeg.ca/finance/findata/matmgt/documents/2012/682-2012/682-2012_Appendix_H-WSTP_South_End_Plant_Process_Selection_Report/Appendix%207.pdf, 2020. [Online; accessed 23-May-2021].